INTERNATIONAL WORKSHOP

ON

ADVANCES IN INORGANIC FIBRE TECHNOLOGY

13-14 August 1992
Clunies Ross House, 191 Royal Parade, Parkville
Melbourne, Australia

EXTENDED ABSTRACTS

Jointly Organised by

Sydney University Centre for Advanced Materials Technology
CSIRO Division of Materials Science and Technology
DSTO Materials Research Laboratory
Australian Ceramic Society

Supported by

US Army Research Office (LABCOM) - Far East
Defence Advanced Research Projects Agency/DSO
Department of Industry, Technology and Commerce (DITAC)

DISCLAIMER NOTICE

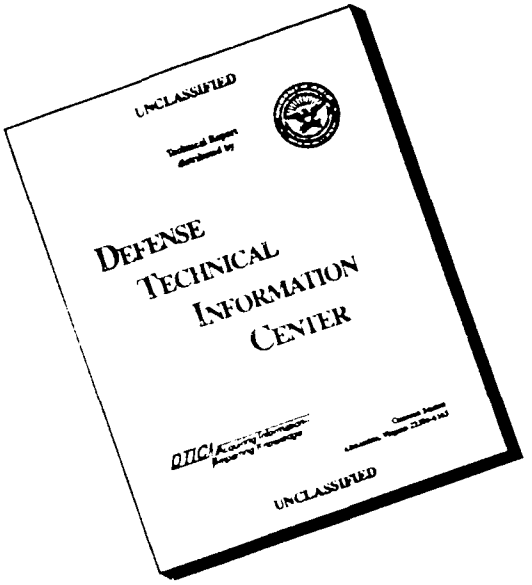

THIS DOCUMENT IS BEST QUALITY AVAILABLE. THE COPY FURNISHED TO DTIC CONTAINED A SIGNIFICANT NUMBER OF PAGES WHICH DO NOT REPRODUCE LEGIBLY.

MASTER COPY KEEP THIS COPY FOR REPRODUCTION PURPOSES

REPORT DOCUMENTATION PAGE

Form Approved
OMB No 0704-0188

1. AGENCY USE ONLY (Leave blank)	2. REPORT DATE	3. REPORT TYPE AND DATES COVERED
	Jul 92	Final 15 Jul 92-14 Jul 93

4. TITLE AND SUBTITLE
International Workshop on Advances in Inorganic Fibre Technology

5. FUNDING NUMBERS
DAAL03-92-G-0371

6. AUTHOR(S)
Yiu-Wing Mai principal investigator)

7. PERFORMING ORGANIZATION NAME(S) AND ADDRESS(ES)
University of Sidney
Sidney, Australia

8. PERFORMING ORGANIZATION REPORT NUMBER

9. SPONSORING / MONITORING AGENCY NAME(S) AND ADDRESS(ES)
U. S. Army Research Office
P. O. Box 12211
Research Triangle Park, NC 27709-2211

10. SPONSORING / MONITORING AGENCY REPORT NUMBER
ARO 30744.1-MS-CF

11. SUPPLEMENTARY NOTES
The view, opinions and/or findings contained in this report are those of the author(s) and should not be construed as an official Department of the Army position, policy, or decision, unless so designated by other documentation.

12a DISTRIBUTION / AVAILABILITY STATEMENT
Approved for public release; distribution unlimited.

12b. DISTRIBUTION CODE

13. ABSTRACT *(Maximum 200 words)*

The workshop was held as scheduled and extended abstracts of the presentations have been published.

14. SUBJECT TERMS
Glass Fibers, workshop, Inorganic Fiber Technology, Fiber Technology, Silicon Carbide Fibers, Ceramic Matrix Composites, Carbon Fibers,

15. NUMBER OF PAGES
95

16. PRICE CODE

17. SECURITY CLASSIFICATION OF REPORT	18. SECURITY CLASSIFICATION OF THIS PAGE	19. SECURITY CLASSIFICATION OF ABSTRACT	20. LIMITATION OF ABSTRACT
UNCLASSIFIED	UNCLASSIFIED	UNCLASSIFIED	UL

EXTENDED ABSTRACTS OF THE INTERNATIONAL WORKSHOP

ON

ADVANCES IN INORGANIC FIBRE TECHNOLOGY

Edited by

Yiu-Wing Mai
Centre for Advanced Materials Technology
University of Sydney

July 1992

Organising Committee

Professor Yiu-Wing Mai, Sydney University - Chairman
Dr John Bannister, CSIRO Division of Materials Science & Technology, Clayton
Dr Janis Cocking, DSTO Materials Research Laboratory, Maribyrnong

PROGRAM

Thursday, 13 August (Contd.)

1210 - 1250	New curing method for polycarbosilane with unsaturated hydrocarbons and application to thermally stable SiC fibre (Y. Hasegawa, Japan)	22
1250 - 1400	*Lunch*	

Session 2 — *Fibre-Matrix Interface Micromechanics and Ceramic Matrix Composites*

Chairpersons: Professor Yiu-Wing Mai (University of Sydney); Dr. Sri Lathabai (CSIRO Division of Materials Science & Technology)

1400 - 1440	Interfacial control and macroscopic failure in inorganic composites (T.W. Clyne and A.J. Phillipps, UK)	30
1440 - 1510	The role of fibre/matrix interface in the first matrix cracking of fibre-reinforced brittle matrix composites (T. Suzuki and M. Sakai, Japan)	37
1510 - 1550	Issues in the control of fibre-matrix interface properties in ceramic composites (R.J. Kerans, USA)	42
1550 - 1620	*Coffee and Tea Break*	
1620 - 1700	Recent progress in the design of advanced high temperature composites (J. Economy, USA)	44
1700 - 1740	Pressureless sintering of silicon nitride composites (T. Yonezawa, S. Saitoh, M. Minamizawa and T. Matsuda, Japan)	46

WORKSHOP DINNER

Friday, 14 August 1992

Session 3 — *Advances in Inorganic Fibres Technology II*

Chairpersons: Dr. Alan Baker (DSTO Aeronautical Research Laboratory); Dr. Besim Ben-Nissan (University of Technology, Sydney)

Session 4 — *Advances in Inorganic Fibres Technology III - Carbon and Glass Fibres*

Chairpersons: Dr. Caroline Baillie (University of Sydney); Dr. S. Bandyopadhyay (University of New South Wales)

"Recent Development on SiC fibers 'NICALON' and Their Composites - Including Properties of SiC Fibers 'HI-NICALON' for Ultrahigh Temperature"

Toshikatsu Ishikawa
NIPPON CARBON CO., LTD.
2 - 6 - 1, Hatcho-bori, Chuo-ku, Tokyo, 104, Japan.

SiC fibers NICALON, produced by NIPPON CARBON CO., LTD., has been placed a high value on excellent properties as a heat resistant material and reinforcements for polymer matrix composites, metal matrix composites and ceramic matrix composites. NICALON has growing uses as an advanced material.

NICALON has materialized one of my fundamental ideologies for . ology, that is. "from Organic to Inorganic".

Fig.1 shows the fabrication process on NICALON.

NICALON has been made from dimethyldichlorosilane of a raw material for silicone resin. Dimethyldichlorosilane has been changed to polydimethylsilane and then synthesized polycarbosilane having basic Si-C skeleton of an organic silicone compound. Polycarbosilane has been spun, cured and pyrolized. SiC fibers "NICALON" has ben fabricated by processing above.

The fundamental technology has been invented by Prof. S. Yajima et al. in 1975. We, NIPPON CARBON, have made the contract on the patent license immediately and started to industrialization based on my decision making, because the SiC fibers have fitted to my ideology.

In case of industrialization, the most difficulty was in spinning and curing for polycarbosilane of the precursor. Polycarbosilane is belonged to oligomer having 1,000 ~ 2,000 in mean molecular weight, against raw materials of synthetic fibers such as polymers of Nylon and polyester etc. having 40,000 ~ 50,000 in mean moiecular weight. Consequently, spun fiber had very low tensile strength of 5 MPa and broke easily at a touch with the hand. Long fiber could not obtain by the heat treatment system of carbon fiber and Prof. S. Yajima also obtained only single filament having less than 1 m in length.

NIPPON CARBON has developed the new method without a touch on spinning, drawing out, curing and pyrolizing for the oligomer.

In addition, we have established the know-how for below-mentioned and developed the industrial technology on mass-production for high-performance continuous fibers having more than 1,000m in length.

① Designs on optimum quality for polycarbosilane and fabrication condition;

② Technologies on spinning, drawing out, handling for the brittle green fiber;

③ Technologies on heat-treatment and surface treatment for the brittle green fiber.

Thus, the fibers made from the oligomer, have been commercialized first in the world. At present, NICALON has been fabricated by the facility having capability of 1 ton per month.

Table 1 shows the properties of commercialized NICALON now.

We have researched and developed also on various composites using NICALON in parallel with improving on NICALON.

Polymer matrix composite(PMC) has been developed on the micro wave absorber and the transmitter having light weight and high tensile strength(NICALON/epoxy resin composite).

Metal matrix composite(MMC) has been developed on the composite wire using NICALON as the reinforcement and aluminum as the matrix(NICALON/Al composite wire).

Ceramic matrix composite(CMC) has been developed on the composite, called "NICALOCERAM™", using NICALON and SiC made from polycarbosilane by polymer impregnation pyrolysis method(NICALON/SiC composite). NICALOCERAM™ has been put to practical use on rollers working in molten zinc for galvanized sheet iron. Ceramic matrix composite reinforced with NICALON has higher fracture toughness as compared to monolithic ceramics. The higher facture toughness has been verified on both NICALON/glass ceramic composite and NICALON/SiC(CVI) composite which are expected the practical use for light weight and heat resistant structural material at more than 1,100℃, because even super heat resistant alloy is useless at that temperature.

In addition, we have developed and commercialized NICALON fiber coated with carbon (NL-607) for CMC. NL-607 has been placed a high value on excellent effectiveness as a reinforcement.

NICALON has excellent properties, especially heat resistance of maximum working temperature at 1,200℃, however the heat resistance has not satisfied still the demands from materials for an advanced airframe, an advanced engine and an advanced gas turbine.

NICALON has been consisted of Si-C-O ternary compound and contained 12%-wt. of oxygen. Oxygen in the fibers decompose and remove with form of CO gas at more than 1,300℃and tensile strength of the fibers decrease.

We have developed the new curing process using an electron beam irradiation in an oxygen-free atmosphere, jointly with Japan Atomic Energy Research Institute, for improving the heat resistance. Consequently, we have developed the SiC fibers "HI-NICALON" containing 0.5%-wt. of reduced oxygen content (refer to Fig.1 for the fabrication proces of SiC fibers).

Table 2 shows typical properties of HI-NICALON having low oxygen content. HI-NICALON has same tesile strength and higher tensile modulus as compared to customary NICALON.
HI-NICALON keeps more than 2 GPa in tensile strength after 10 hours exposure at 1,500℃ in argon atmosphere, however customary NICALON decreases sharply tensile strength after same heat treatment. HI-NICALON keeps still more fibrous form and flexibility after 1 hour exposure at 2,000℃ in argon atmosphere. Thus, HI-NICALON has excellent heat resistance highly which customary NICALON could not realize. HI-NICALON/SiC composite (NICAROCERAM™) has excellent heat resistance highly, because the composite has 300MPa in flexural strength after 1

hour heat treatment at 500°C in air. This also shows HI-NICALON has excellent compatibility with ceramic matrix.

At present, industrialization for HI-NICALON has been promoted and we plan to make mass-production and place on sale starting 1995.

We expect that HI-NICALON will contribute to early developing for space plane, high temperature gas turbine and nuclear fusion reactor etc., based on increased heat resistance of materials using HI-NICALON for high temperature.

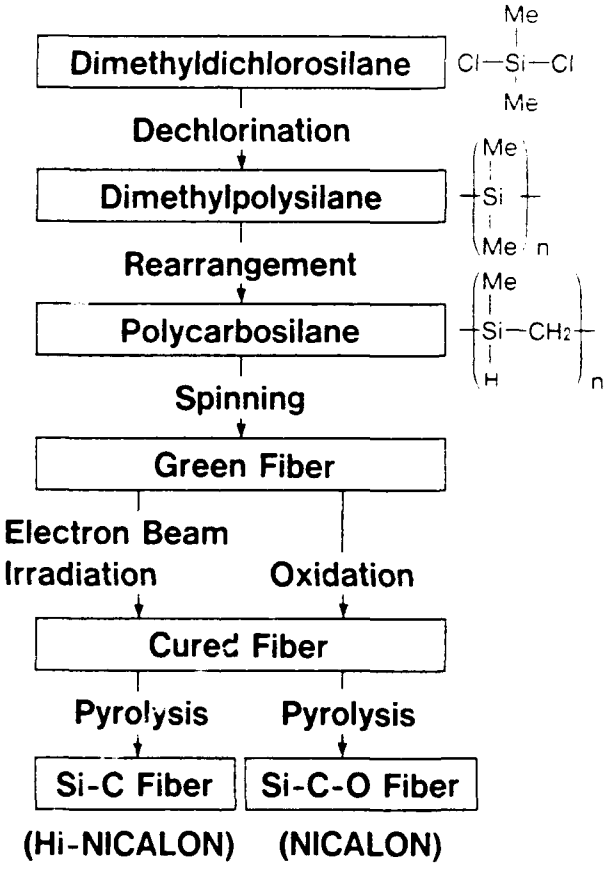

Fig. 1 FABRICATION PROCESS OF SiC FIBERS

Table 1 Typical properties and applications of NICALON

		Ceramic Grade NL-200	HVR Grade NL-400	LVR Grade NL-500	Carbon Coated NL-607
Diameter	(μm)	14/12	14	14	14
Numbers of filaments	(fil./yarn)	250/500	250/500	500	500
Tex	(g/1000m)	105/210	110/220	210	210
Tensile strength	(MPa)	3000	2800	3000	3000
Tensile modulus	(GPa)	200	180	220	220
Elongation	(%)	1.4	1.6	1.4	1.4
Density	(kg/m^3)	2550	2300	2500	2550
Specific resistivity	(ohm-cm)	10^3–10^4	10^6–10^7	0.5–5.0	0.8
Co-efficient of thermal expansion					
	(10^{-6}/K)	3.1	—	—	3.1
Specific heat	(J/(kg·K))	1140	—	—	1140
Thermal conductivity	(W/(m·K))	12	—	—	12
Dielectric constant	(at 10 GHz)	9	6.5	20–30	—
Applications		Heat resistant materials PMC, MMC, CMC	PMC	PMC	CMC

(Preliminary Data)

Table 2 Typical Properties of the Low Oxygen SiC Fiber "HI-NICALON"

				(NICALON Ceramic Grade)
Fiber diameter	(μm)		14	(14)
Numbers of filaments	(fil./yarn)		500	(500)
Tex	(g/1000m)		200	(210)
Tensile strength	(GPa)		2.8	(3.0)
Tensile modulus	(GPa)		270	(220)
Elongation	(%)		1.0	(1.4)
Density	(kg/m^3)		2.740	(2.550)
Specific resistivity	(ohm-cm)		1.4	(10^3–10^4)
Chemical composition				
	(wt. %)	Si	63.7	(58)
		C	35.8	(30)
		O	0.5	(12)

FINE DIAMETER POLYCRYSTALLINE SIC FIBERS

J. Lipowitz, T. Barnard, D. Bujalski, J. Rabe, G. Zank
Dow Corning Corporation
Midland, MI 48686
U.S.A.

A. Zangvil, Y. Xu
Materials Research Laboratory
University of Illinois
Urbana, IL 61801
U.S.A.

Introduction

Small diameter ceramic fibers, which are sufficiently flexible to permit weaving and knitting, provide many desirable properties for use in continuous-fiber ceramic matrix composites (CMC) intended for high temperature performance in oxidative and inert atmospheres (1). Such fibers are also useful in plastic and metal matrix composites. The fine diameter, non-oxide ceramic fibers have generally been prepared by polymer precursor routes. Products which have reached commercial status include NICALON™ ceramic fiber (2) a Si-C-O composition from Nippon Carbon Company, Japan; Tyranno ceramic fiber (3), a Si-C-O-Ti composition from Ube Industries, Ltd., Japan; and HPZ ceramic fiber (4), a Si-N-C-O composition from Dow Corning Corporation, USA. Typical properties for these fibers are shown in Table 1. The continuous phase in these fibers, which controls mechanical properties, is amorphous (5). NICALON and Tyranno fiber contains β-SiC crystallites dispersed in the amorphous phase. The elastic moduli are considerably lower than the fully dense polycrystalline values of 315 GPa for Si_3N_4 and 460 GPa for SiC. The fibers are thermochemically metastable and undergo gas loss (CO, some SiO, and N_2, if present) and crystallization at ~1300°C (NICALON and Tyranno ceramic fiber) or ~1450°C (HPZ fiber) in inert atmospheres. These fibers are useful up to 1200°C in oxidative atmospheres.

A crystalline SiC fiber is desired for high temperature CMC use because modulus, oxidation resistance and thermal stability would be improved compared to the primarily amorphous fibers. Furthermore, a SiC fiber would display desirable creep resistance and high thermal conductivity as found for SiC in bulk form.

Process

Polymer-derived ceramic fibers which contain sufficient excess carbon will convert to polycrystalline SiC on heating at ~1400°C or above in an inert atmosphere. Oxygen in these fibers is lost mainly as CO (some SiO may be lost) and nitrogen (if present) is lost as N_2, shown schematically in Equations 1 and 2.

$$SiC_aO_b \xrightarrow[\text{heat}]{} SiC + CO\ (+SiO) \qquad (1)$$

$$SiC_aO_bN_c \xrightarrow[\text{heat}]{} SiC + CO\ (+SiO) + N_2 \qquad (2)$$

On loss of these gases (thermal decomposition), a coarse granular SiC containing large voids between the grains is formed and no tensile strength is retained. Figure 1a shows a high temperature, thermally decomposed SiC fiber which had contained 4 wt% oxygen after pyrolysis to 1200°C. A similar fiber, which contained several wt% boron distributed throughout the fiber, undergoes loss of pyrolysis gases and crystallization to a dense, polycrystalline, smooth skinned fiber as shown in Figure 1b. These fibers retain their tensile strength after conversion from a Si-C-O composition to a polycrystalline SiC composition.

Polycrystalline SiC fibers have been prepared from polycarbosilane (6), polysiloxane (7) and polysilazane (8) polymer precursors. Polymers were synthesized to contain sufficient carbon to react with the silicon after high temperature loss of oxygen (as CO) and nitrogen (if present). Pyrolysis was generally performed in argon to a temperature above 1600°C.

The best fiber properties have been obtained using the polycarbosilane precursor. Polycarbosilane was melt-spun, oxidatively cured with NO_2 (9), doped with BCl_3 gas, and pyrolyzed to >1600°C in argon. Stoichiometric SiC fibers or fibers containing an excess of carbon (up to ~15 wt%) can be prepared from polycarbosilane by control of the level of oxygen introduced during the cure process. Polycarbosilane without oxygen pyrolyzes to SiC containing ~15 wt% excess carbon.

Properties and Structure

The microstructure of the SiC ceramic fiber formed from all of the polymeric precursors is very similar. X-ray diffraction shows a typical β-SiC pattern having an average crystallite size of 30-40 nm by line broadening measurements of the (111) diffraction peak. Up to several % of α-SiC structure is present and in some cases graphitic-like carbon was detected by a weak (0002) diffraction peak.

A SEM image of a high strength SiC fiber prepared from polycarbosilane is shown in Figure 2. Properties of SiC fibers prepared from polycarbosilane are listed in Table 2 and are as expected for a polycrystalline SiC fiber. The elastic modulus is approximately twice that obtained for the polymer-derived fibers shown in Table 1. Elastic modulus is reduced markedly by the presence of excess carbon, from ~450 GPa for stoichiometric SiC to ~300 GPa for fiber containing ~10 wt% excess carbon. Density is >97% theoretical for the stoichiometric SiC fiber. Fractography shows that weaker fibers generally fracture in tension at internal flaws or at kink sites.

Fiber retained 87% of the initial room temperature strength after exposure to argon at 1800°C for 12 hours. Strength retention after 1370°C exposure to air for 12 hours depends on the excess carbon content. Fiber which contained excess carbon retained only 35% of initial strength. Final strength after exposure was 0.6 GPa. SEM examination showed a ring of voids formed at the silica-fiber interface after oxidation. These ~1 μm diameter voids at the boundary of the ~1 μm thick silica layer appear to be the critical flaws which reduced strength. The stoichiometric SiC fiber retained 66% of initial strength after the same air exposure; final strength was 1.6 GPa. SEM imaging showed a ~1 μm thick silica layer with no voids present. Fractography showed tensile failure at regions of thick, bulbous silica growth.

Structure of the SiC fibers is described in Table 3. A thin (~50 nm) carbon-rich surface layer is seen on all fibers by scanning Auger depth profiling. The carbon-rich layer is believed to be formed by evaporation of silicon from the surface region during the pyrolysis process. By TEM techniques, the fiber interior contains β-SiC crystallites with numerous stacking faults. Small area electron diffraction (SAD) analysis shows twinning and stacking faults as is often found in β-SiC crystallites. Beneath the carbon-rich surface, fiber containing excess carbon has a 1-2 μm layer of equiaxed β-SiC crystallites of ~0.5 nm size. The interior consists of ~0.1 μm and smaller β-SiC crystallites in a graphitic-like continuous phase.

We are currently working to obtain continuous fiber in multifilament tow form.

Acknowledgement

We gratefully acknowledge the support and encouragement of the NASA-Lewis Research Center.

References

1. Fiber-Reinforced Ceramic Composites; Materials, Processing, and Technology. Edited by K. S. Mazdiyasni, Noyes Publications, Park Ridge, N.J., 1990.
2. A. R. Bunsell, G. Simon, Y. Abe and M. Akiyama, "Ceramic Fibers". Compos. Mater. Ser. (Fiber Reinf. Compos. Mater.), 2 [Chapt. 9], 446-78 (1988).
3. T. Yamamura, T. Ishikawa, M. Shibuya, T. Hisayuki and K. Okamura, "Development of a New Continuous Silicon-Titanium-Carbon-Oxygen Fiber Using an Organometallic Polymer Precursor", J. Mater. Sci., 23, 2589-94 (1988).
4. G. E. LeGrow, T. F. Lim, J. Lipowitz and R. S. Reaoch, "Ceramics from Hydridopolysilazane", Am. Ceram. Soc. Bull., 66, 363-67 (1987).
5. L. C. Sawyer, M. Jamieson, D. Brikowski, M. I. Haider and R. T. Chen, "Strength, Structure, and Fracture Properties of Ceramic Fibers Produced from Polymeric Precursors: I, Base-Line Studies", J. Am. Ceram. Soc., 70, 798-810 (1987).
6. D. C. DeLeeuw, J. Lipowitz and P. P. Lu, "Preparation of Substantially Polycrystalline Silicon Carbide Fibers form Polycarbosilane", U.S. Patent 5,071,600 (1991).
7. W. H. Atwell, D. R. Bujalski, E. J. Joffre, G. E. LeGrow, J. Lipowitz and J. A. Rabe, "Preparation of Substantially Polycrystalline Silicon Carbide Fibers from Polyorganosiloxanes", European Patent Appl. 0435065A1 (1991).
8. Unpublished data.
9. J. A. Rabe, J. Lipowitz and P. P. Lu, "Curing Preceramic Polymers by Exposure to Nitrogen Dioxide", U.S. Patent 5,051,215 (1991).

Table 2. Properties of SiC Fiber Prepared from Polycarbosilane

* Average tensile strength up to 2.6 GPa at 25 mm gauge length.
* Elastic modulus up to 450 GPa.
* Fiber diameter 8-9 μm.
* Density to >3100 kg/m^3 (>97% theoretical).
* Critical stress concentration factor (K_{Ic}) ~3 MPa $m^{1/2}$, based on strength/flaw size relationship.
* Coefficient of thermal expansion 5.1 ppm/K (300-1600 K).
* Fiber length ≤100 mm.
* 87% strength retention after 1800°C/12 hours aging in argon; no microstructural change after aging.
* 66% strength retention after 1370°C/12 hour aging in air.

Table 3. Structure of SiC Fiber Prepared from Polycarbosilane

* Composition is controllable from near-stoichiometric β-SiC to >10 wt% excess carbon.
* Oxygen and nitrogen content <0.1 wt%.
* β-SiC crystallite size by x-ray line broadening is 30-40 nm.
* All fibers have carbon-rich outer layer, ~50 nm thickness.
* Carbon-rich fiber has 3 layers:
  - outer ~50 nm is carbon-rich
  - next 1 to 2 μm is stoichiometric β-SiC (~0.5 μm crystallite size)
  - interior is carbon rich β-SiC (up to 0.1 μm crystallite size)
* β-SiC crystallites contain numerous twinning and stacking faults.
* Excess carbon between SiC grains is graphitic-like.

a.

b.

Figure 1. SEM images of silicon carbide fibers after final pyrolysis to high temperature in argon. Both fibers were prepared from the same polymer precursor, similarly cured with NO_2 and contained 4 wt% oxygen after pyrolysis to 1200°C in argon. Fiber (a) retained no tensile strength. Fiber (b) was doped with boron after cure. Tensile strength after pyrolysis was 1.7 GPa (250 ksi).

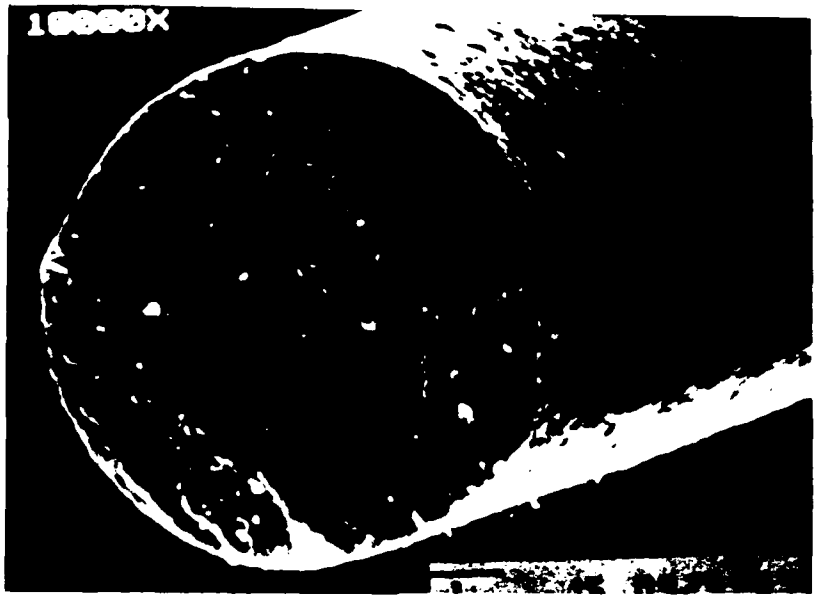

Figure 2. High strength (2.3 GPa), high modulus (400 GPa) SiC fiber derived from PCS.

"PYROLYTIC BEHAVIOR of POLYMER-DERIVED SiC FIBER"

Kiyohito Okamura, Junichi Nishida, and Toshio Shimoo,
Department of Metallurgical Engineering, College of Engineering,
University of Osaka Prefecture,
1-1 Gakuencho, Sakai, Osaka 593, Japan,

Tadao Seguchi
Takasaki Radiation Chemistry Research Establishment,
Japan Atomic Energy Research Institute,
Takasaki, Gunma 370-12, Japan,

Hiroshi Ichikawa
NIPPON CARBON CO., LTD., R & D Laboratory,
Yokohama, Kanagawa 221, Japan

1. Introduction

Polymer-derived SiC fibers[1] such as Nicalon[2] are applied to the reinforcements of glass matrix composite[3] or SiC matrix composite[4,5], and these composites have excellent mechanical properties. However, there is a problem that the tensile strength of the fibers decreases rapidly at high temperature. The fibers are amorphous and contain oxygen atoms invariably introduced during the fabrication process. The chemical composition of Nicalon is $SiC_{1.21}O_{0.37}$. The fiber pyrolyzes by the heat treatment above 1573K in an inert gas atmosphere[6,7], where the evolution of SiO and CO gas occurs. And the morphology of the fiber changes extremely, and the tensile strengtn rapidly decreases. However, the mechanisms in its pyrolysis are not fully understood at present. We have systematically studied the pyrolytic process of several kinds of polymer-derived SiC fibers at high temperatures in Ar gas atmosphere[8,9] or in ceramic matrix. Further, we have tried to decrease the oxygen in SiC fibers by applying radiation curing process instead of thermal oxidation in the process of Nicalon[10,11,12].

In this work, the pyrolytic behavior of Nicalon was studied at 1673-1973K in Ar in the fiber form, and in the form of fiber reinforced Si_3N_4 matrix in N_2 at 1873-1973K. It becomes clear that it is necessary to reduce the oxygen content for the promis-

ing fiber of ceramic matrix composites. On the basis of these researches, low-oxygen contained SiC fiber was produced using radiation curing process, and the tensile strength at high temperature was extremely improved.

2. Pyrolytic Mechanism of SiC Fibers in Ar

The mechanism of pyrolysis of amorphous SiC fiber (Nicalon NL200) was investigated. The rate of pyrolysis was measured with a thermobalance in Ar atmosphere at temperature of 1673-1973K. The formation of the pyrolytic product was examined by the chemical analysis, X-ray diffraction and TEM observation.

The fiber was pyrolyzed to form SiO and CO simultaneously by following reaction,

$$SiC_{1+x}O_y \longrightarrow \alpha\, SiC(s) + \beta SiO(g) + \gamma CO(g) \qquad (1)$$

where, α , β and γ are constants determined by the fiber type and pyrolytic temperature. The mass loss (Fig.1) measured was attributable to both SiO and CO gas evolved by the pyrolysis. $X=W_t/W_f$, X stands for the thermal-decomposed fraction, and W_t is the mass loss at time t, and W_f is the final weight loss. During pyrolysis, the three-dimensional growth of the crystallite of SiC was observed in the fiber by TEM. The amorphous fiber changed to the β-SiC crystallite. The rate of pyrolysis depended on temperature, and was described by the Avrami-Erofeev equation,

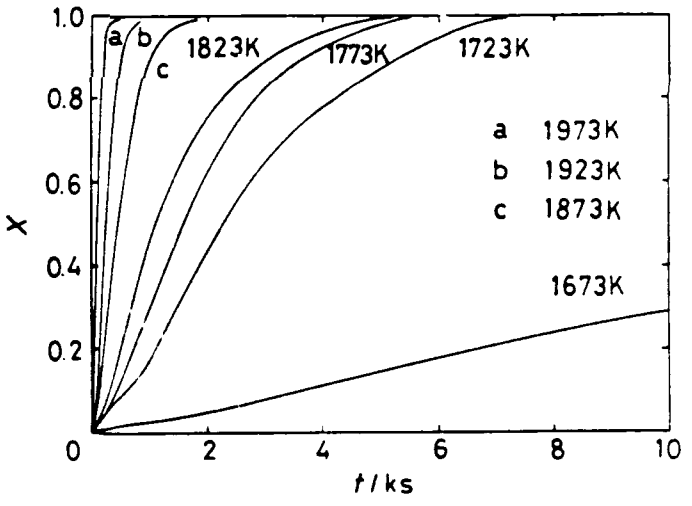

Fig.1 Thermal decomposition curves for SiC fiber(NL200).

$$-\ln(1-X) = k \cdot t^m \qquad (2)$$

where k and m are constants. The latter is strongly related to the grain growth mode, and ranges from 0.5 to 4, depending on the

growth mechanism, on the nucleus formation rate, and also on the grain shape. The mean value of m in this equation was 1.3. The k value varies with temperature, and has been assessed by an Arrhenius type relationship. The Arrhenius plots of the rate constants gave the apparent activation energy of 484 kJ/mol. These results show that the pyrolytic rate is determined by the diffusion-controlled nucleus formation and grain growth processes of SiC involving the diffusion of carbon in the fiber.

3. Pyrolytic Behavior of SiC Fibers in Si_3N_4 matrix

The pyrolytic behavior of SiC fibers in the sintered ceramic body is considered to be different from that of the fibers in an inert gas atmosphere. The variation of morphology of the fibers in Nicalon(NL200)/silicon nitride ceramics was investigated. Nicalon chopped fibers were blended with silicon nitride ceramics. The ceramics are Si_3N_4 fine powders (UBE SN E10) and the Si_3N_4 powders with 5 mass% Y_2O_3 and 5 mass% Al_2O_3 powders. They are referred as NL200/SiN(A) and NL200/SiN(B) respectively. The mass loss of Nicalon and those composites was measured by a thermobalance in N_2 atmosphere at temperature of 1873-1973K. The fiber in N_2 was pyrolyzed faster than the fiber in those composites at all temperatures tested. The pyrolysis of the fiber by equation (1) are suppressed in these composites. The morphology of fibers in the Si_3N_4 matrix does not changed much, and this is much different from that of the fibers heat-treated in N_2 atmosphere. The morphology of those fibers are shown in Fig. 2. The pyrolytic rate of the fibers is considered to be mixed-controlled by the diffusion of SiO and CO gases through the Si_3N_4 matrix, and the crystal growth of SiC in the fiber.

4. Preparation of High-Resistant SiC Fiber Using Radiation Curing

The decrease of the tensile strength at high temperatures by the thermal decomposition is due to the oxygen introduced in the thermal oxidation curing process. In order to improve its high-temperature strength, it is necessary to reduce the oxygen content of the fiber. We have studied an oxygen-free curing process using the electron beam irradiation.

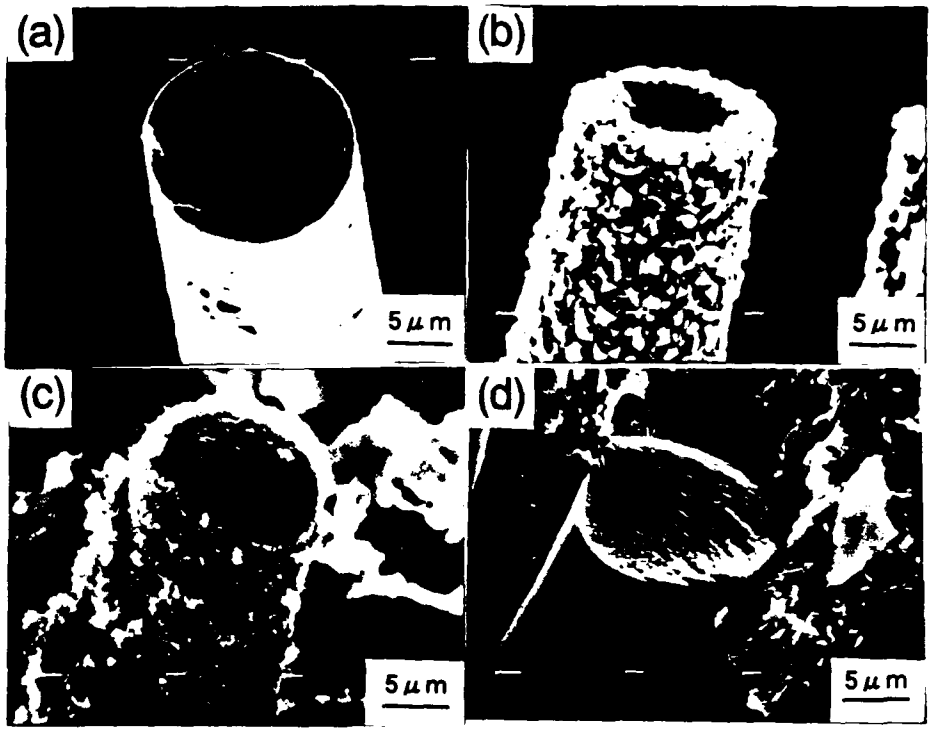

Fig.2 SEM micrographs of heat-treated SiC fiber(NL200).
(a):as received NL200,
(b):NL200 heat-treated at 1973K in N_2,
(c):NL200 heat-treated at 1973K in Si_3N_4 powder,
(d):NL200 heat-treated at 1973K in sintered Si_3N_4 matrix.

The synthesis process of SiC fiber with its curing is shown in Fig. 3. Polycarbosilane(PCS) fiber was irradiated by 2 MeV electrons under vacuum or in inert gas atmosphere, then the PCS fiber is crosslinked, and its curing is accomplished above about 10 MGy. The SiC fiber obtained by heating up to 1473K in Ar gas flow contained the oxygen less than 0.5%. As the original PCS fiber contains 0.3% or more, it means that there is no oxidation during the radiation curing. After 1773K heat treatment for 1h, the tensile strength kept 2.5 GPa at 1473K, and Young's modulus increased from 220 to 260 GPa. The tensile strength decreased gradually above 1993K, the morphology of the SiC fiber shows apparently no change after heat treatment at 2273K for 1 h by SEM observation.

The radiation curing of PCS fiber is found to be very useful for development of high-heat resistant SiC fiber. This research has been carried out by the fundamental and small scale experimental equipments. It is necessary to prepare a considerable amount of SiC fibers in order to apply to reinforcement fibers of composites. We designed and constructed the electron beam curing apparatus, which is composed of irradiation chamber, sample transfer, and heat-treatment vessel for the PCS fiber[13]. Using the apparatus, the PCS fibers of long strand (2km length and about 300g) composed of 500 filaments were cured, and the SiC fibers containing 0.4% oxygen were obtained.

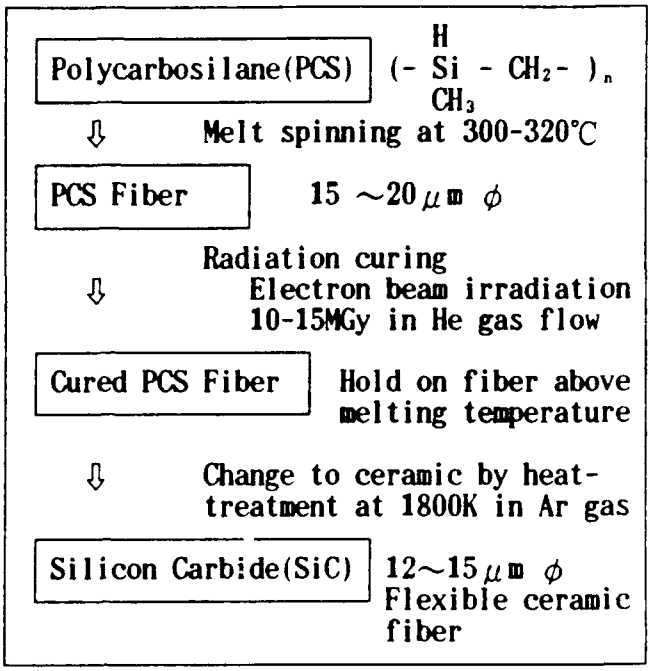

Fig.3 Process of SiC fiber synthesis by radiation curing of PCS fiber.

5. Conclusion

(a) The pyrolytic rate of Nicalon type SiC fiber in an inert gas atmosphere is determined by the diffusion-controlled nucleus formation and grain growth processes.

(b) The pyrolytic rate of the SiC fiber in Si_3N_4 matrix is mixed-controlled by the diffusion of SiO and CO gases through the Si_3N_4 matrix, and the crystal growth of SiC in the fiber.

(c) Heat-resistant SiC fiber is synthesized by the heat treatment of polycarbosilane fiber with electron beam irradiation curing. Applying this radiation curing technique, a consid-

erable amount of SiC fiber (about 200g) is synthesized.

References

1) S.Yajima, Am. Ceram. Soc. Bull., 62(1983)pp.893-98.
2) T.Ishikawa and T.Nagaoki, Recent Carbon Technology Including Carbon and SiC Fibers(1983), JEC Press Inc., p.348.
3) K.M.Prewo, J.J.Brennan and G.K.Layden, Am. Ceram. Soc. Bull., 65(1986)pp.305-13,322.
4) P.J.Lamicq, G.A.Bernhart, M.M.Dauchier, and J.G.Mace, ibid., 65(1986)pp.347-50.
5) D.P.Stinton, A.J.Caputo and R.A.Lowden, ibid.,65(1986) pp.336-38.
6) K.Okamura, M.Sato, T.Matsuzawa and Y.Hasegawa, Polym. Prepr., 25(1984)pp.6-7.
7) D.J.Pysher, K.C.Goretta, R.S.Hodder,Jr. and R.E.Tressler, J. Am. Ceram. Soc., 72(1989)pp.284-88.
8) T.Shimoo, M.Sugimoto and K.Okamura, J. Japan Inst. Metals, 54(1990)pp.802-08.
9) T.Shimoo, Y.Kakehi, M.Sugimoto and K.Okamura, J. Ceram. Soc. Japan, 99(1991)pp.401-06.
10) K.Okamura, M.Sato, T.Seguchi and S.Kawanishi, Proceedings of the 4th International Symposium on Science and Technology of Sintering held in Tokyo on 4-6 November, 1987, pp.102-7.
11) M.Takeda, Y.Imai, H.Ichikawa, T.Ishikawa, T.Seguchi and K.Okamura, Ceram. Eng. Sci. Proc., 12(1991)pp.1007-18.
12) K.Okamura and T.Seguchi, J. Inorganic and Organometallic Polymers, 2(1992)pp.171-179.
13) T.Seguchi, N.Kasai, and K.Okamura, Proceedings of the Internatinal Conference on Evolution in Beam Applications held in Takasaki, Japan, on November 5-8, 1991, pp.702-706.

POLYMER-DERIVED SILICON CARBIDE FIBERS WITH IMPROVED THERMOMECHANICAL STABILITY

Wm. Toreki, G.J. Choi, C.D. Batich, M.D. Sacks, and M. Saleem
Dept. of Materials Science and Engineering, University of Florida
Gainesville, FL 32611 U.S.A.

Introduction

Fiber-reinforced composites are of increasing importance in high temperature structural applications due to their excellent mechanical properties, such as high strength and high fracture toughness. However, the use of these composites is generally limited to temperatures below ~1200°C due to degradation of fiber mechanical properties at high temperatures. For example, Nicalon™ SiC fibers (which have been used to reinforce glass, glass-ceramic, and crystalline ceramic matrices[1,2]) may show significant decreases in tensile strength and elastic modulus after heat treatment at temperatures as low as 1000°C.[3,4] The poor thermomechanical stability is attributed to the presence of oxygen (~8-15 wt%) and excess carbon in the fibers which results in the formation of volatile reaction products (primarily CO and SiO) at relatively low temperatures.[5,6] Significant improvements in the high temperature mechanical properties of SiC fibers might be expected if the oxygen content can be reduced.

Nicalon™ fibers are prepared by melt spinning of a low-molecular-weight organosilicon polymer (i.e., polycarbosilane). As-spun fibers are then heated at low temperature (~150-200°C) in air in order to cure (cross-link) the polymer and to prevent fibers from melting during the subsequent pyrolysis step (in which the polymer is decomposed to a SiC-rich ceramic). In the present study, polycarbosilane-derived SiC fibers were prepared using processing conditions that allowed the oxidative cross-linking step to be eliminated. Therefore, the fibers produced after polymer pyrolysis and SiC crystallization had very low oxygen content (<2 wt%) compared to Nicalon.™

Experimental

The processing steps used to prepare SiC fibers with low oxygen content are summarized in Fig. 1. Polycarbosilane (PC) was synthesized by pressure pyrolysis of polydimethylsilane. Fibers were spun using intermediate-molecular-weight PC's (~5,000-10,000) which remained highly soluble in appropriate solvents, but did not melt during subsequent heat treatment. Polymer solutions were extruded through stainless steel spinnerets (~70 or ~120 μm diameter orifices) under nitrogen pressure. Continuous "green" fibers were collected by winding on a rotating drum and pyrolysis was subsequently carried out at temperatures in the range of 750-1000°C (1 h hold) under flowing nitrogen. Fibers with diameters in the range ~10-50 μm were produced.

Thermal gravimetric analysis (TGA), X-ray diffraction (XRD), scanning and transmission electron microscopy (SEM and TEM), and elemental analysis were used to characterize the fibers. Fiber tensile strengths were determined at room temperature according to ASTM procedure D-3379. Fibers were tested after pyrolysis at 1000°C and after additional heat treatments in argon at temperatures in the range 1200-1700°C.

CONTINUOUS SILICON CARBIDE FIBERS

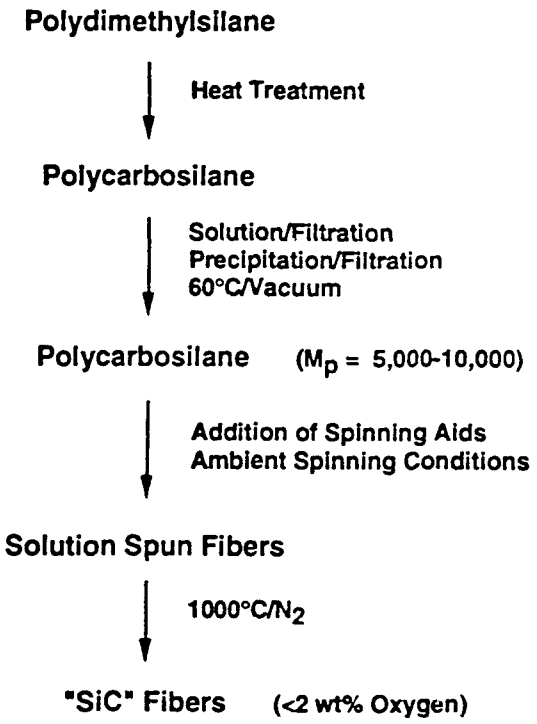

FIG. 1. Processing steps for preparation of SiC fibers with low oxygen content.

Results

TGA results on as-spun fibers show that pyrolysis reactions are mostly completed below ~900°C. The total weight loss is relatively low (~20 wt%), especially compared to losses (~40 wt%) reported for low-molecular-weight PC's (such as used in melt spinning of Nicalon fibers).[7] In fact, the ceramic yield is comparable to yields reported for *oxygen-cured* PC fibers.[6,7]

Pyrolyzed fibers (750-1000°C) had a visual appearance similar to Nicalon™ (i.e., black color). SEM observations showed that outer surfaces and fracture surfaces were smooth. XRD analysis indicated that 1000°C-pyrolyzed fibers were substantially amorphous, although very broad peaks associated with SiC were evident. These peaks progressively narrowed and increased in intensity for samples subjected to further heat treatment (to 1600°C in nitrogen or argon atmospheres), indicating that growth of SiC crystallites occurs with increasing temperature. The same trends were revealed by TEM.

Figure 2 shows a comparison of TGA data for Nicalon™ fibers and pyrolyzed (750°C, 1h) fibers prepared in this study ("UF fibers"). Weight loss was monitored as the fibers were heated in argon at 10°C/min to 1550°C and then held for 1 hour at temperature. The UF fiber lost only ~3 wt% during this treatment, while the Nicalon™ fiber lost ~25 wt% The relatively low weight loss observed for the UF fibers can be attributed to the low oxygen content. Neutron activation analysis (NAA) of three different UF fiber batches (pyrolyzed at 1000°C) revealed oxygen contents in the range ~1.5-1.8 wt%, while Nicalon™ fibers showed 15 wt% oxygen by NAA.

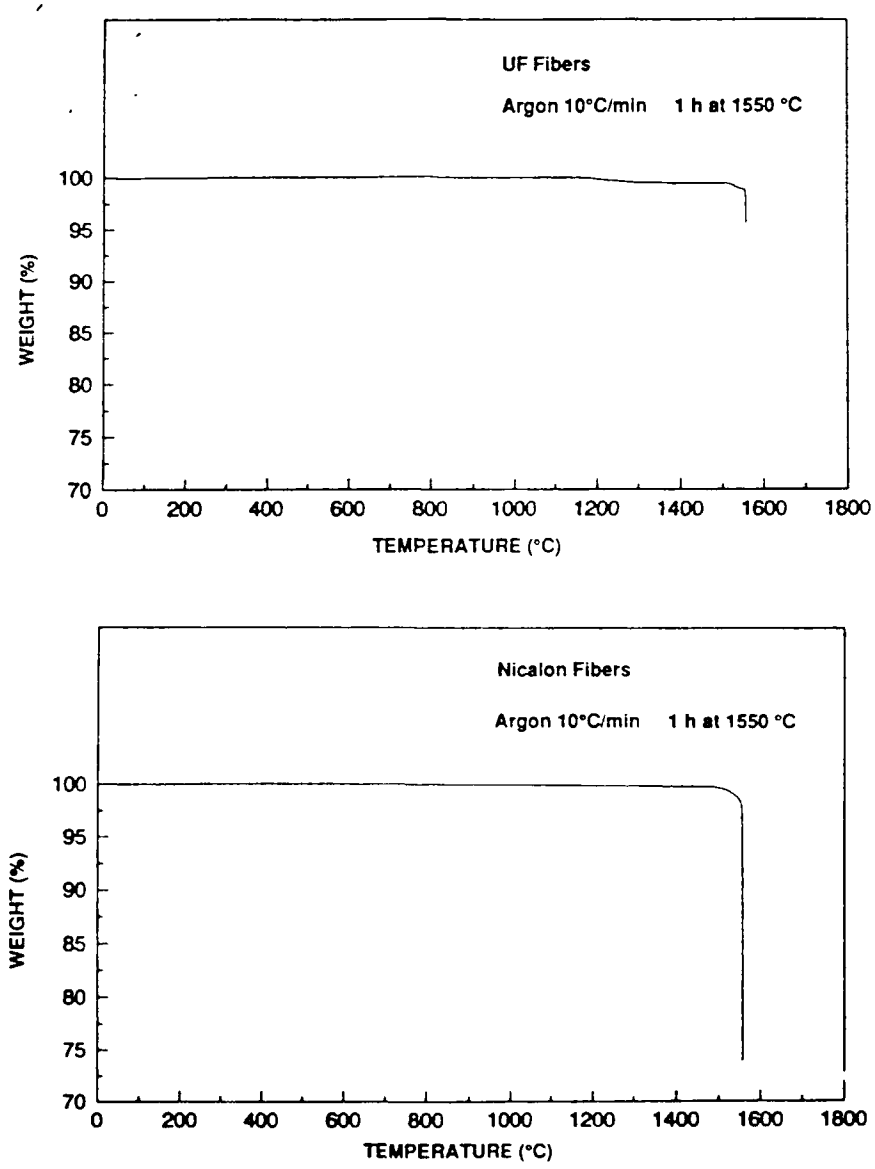

FIG. 2. Weight loss behavior for UF fibers (top) and Nicalon™ fibers (bottom) heated in argon to 1550°C at 10°C/min and then held for 1 hour at temperature.

Figure 3 shows average tensile strengths for UF and Nicalon™ fibers after heat treatment at various temperatures in an argon atmosphere. It is evident that UF fibers show much greater retention of strength after heat treatment. The strengths reported in Fig. 3 were obtained from a single batch of UF fibers. Although the data is considered representative, it should be noted that higher strengths have been observed in some other batches. For example, *average* strengths as high as ~3 GPa have been observed for as-pyrolyzed batches (10-15 μm fiber diameters) and ~1.9 GPa in some batches heat treated at 1400°C (for 1 h). Thus, it may be possible to produce fibers with consistently higher strength levels than reported in Fig. 3 if processing conditions are more rigorously controlled.

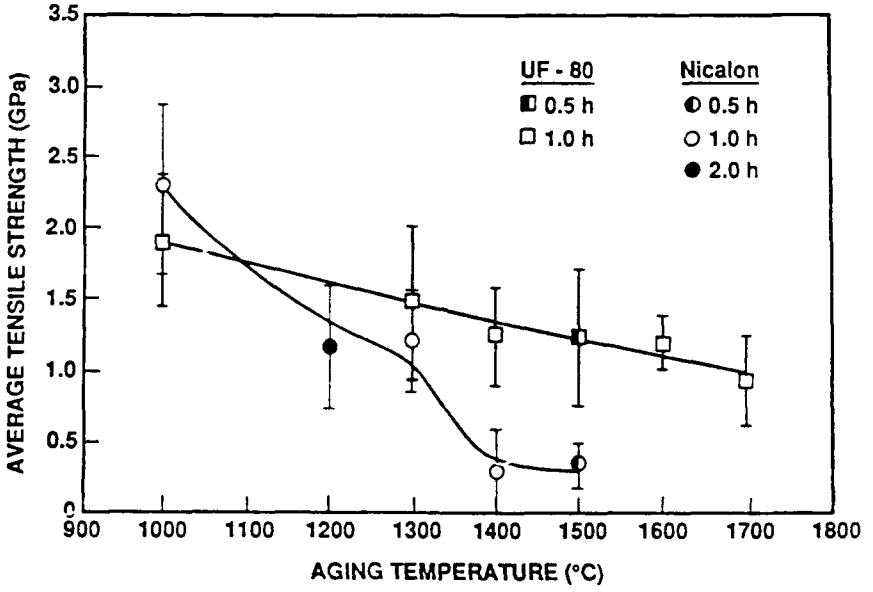

FIG. 3. Plots of average tensile strength vs. heat treatment temperature for UF fibers and Nicalon™ fibers.

Conclusion

Continuous silicon carbide fibers with low oxygen content (< 2 wt%) were prepared in a range of diameters (~10-50 μm) by dry spinning of polycarbosilane solutions and subsequent pyrolysis of the polymer fibers. Average tensile strengths approaching 3 GPa were obtained for some batches with fiber diameters in the range ~10-15 μm. These fibers showed excellent thermomechanical stability compared to commercially-available Nicalon™ fibers, i.e., significantly lower weight loss and higher tensile strength were observed after heat treatment in argon at elevated temperatures (1200-1700°C).

Acknowledgement

This work was supported by the Defense Advanced Research Projects Agency under Contract Nos. MDA 972-88-J-1006 and N00014-91-J-4075.

References

1. K.M. Prewo, J.J. Brennan, and G.K. Layden, Am. Ceram. Soc. Bull., 65 [2] 305-313, 322 (1986).
2. P.J. Lamicq, G.A. Bernhart, M.M. Dauchier, and J.G. Mace, Am. Ceram. Soc. Bull., 65 [2] 336-338 (1986).
3. M.H. Jaskowiak and J.A. DiCarlo, J. Am. Ceram. Soc., 72 [2] 192-197 (1989).
4. D.J. Pysher, K.C. Goretta, R.S. Hodder, Jr., and R.E. Tressler, J. Am. Ceram. Soc., 72 [2] 284-288 (1989).
5. S.M. Johnson, R.D. Brittain, R.H. Lamoreaux, and D.J. Rowcliffe, Comm. Am. Ceram. Soc., 71 [3] C-132 -C-135 (1988).
6. Y. Hasegawa, J. Mater. Sci., 24 1177-1190 (1989).
7. S. Yajima, Y. Hasegawa, and M. Iimura, J. Mater. Sci., 15 720-728 (1980).

New Curing Method for Polycarbosilane with Unsaturated Hydrocarbons and the Application to Thermally Stable Si-C Fibre

YOSHIO HASEGAWA
The Research Institute for Special Inorganic Materials,
Asahi-mura, Kashima-gun, Ibarai 311-14, JAPAN

Introduction

Continuous SiC fibres synthesized from polycarbosilane (PC) precursor are already in industrial production as NICALON fiber and TYRANNO fibre, which are used as reinforcements for composites. However, for the purpose of utilizing SiC fibre as reinforcement in many ceramic matrix composites, development of oxygen-free Si-C fibre, having high thermal stability and oxidation resistance, is necessary.

Recently, Si-C-O fibre with a small amount of oxygen was prepared from PC fibre cured by electron beam irradiatoion [1]. It was shown that this fibre had improved thermal stability. And then, the auther found that PC was cured by heating in halogenated hydrocarbon or unsaturated hydrocarbon vapor [2]. This method, hereafter, is referred to as chemical vapor curing (CVC) method. In comparison with the electron beam method, this new method is assumed to be more ecomomical. In the previous report [2], by CVC method, the fibre heat-treated at 1500°C in a nitrogen gas flow had tensile strengths more than 2GPa. On the other hand, in an argon gas flow, the strength

decreased rapidly above 1400°C. It was assumed that the nitrogen atoms introduced into the fibre depressed cristallization of β-SiC.

In the present research, the fibre with high thermal stability has been synthesized by CVC method and heat-treatment in an argon gas flow.

Fibre Synthesis

The number average molecular weight of PC is 2060. PC was melt-spun at about 370°C. The resulting fibre bundle was cured by heating in a tubular furnace up to a specific temperature in an argon gas flow containing unsaturated hydrocarbon vapor. Cyclohexene, 1-hexyne or 1-octyne was used as unsaturated hydrocarbon. A schematic diagram of the curing apparatus is shown in Fig.1.

The cured fibre was then heat-treated in a tubular furnace up to a specific temperature at a rate of $100°C \cdot h^{-1}$ in an argon gas flow.

Argon gas was dried by passing through columns packed with successive, silica gel, magnesium perchlorate and phosphorus pentoxide.

Mechanical properties of fibres were measured at room temperature with a 25-mm gauge length for 30 filaments, the average values being taken.

Results and discussion

Tensile strength and Young's modulus of Si-C fibres are

shown in Fig.2 as a function of the heat-treatment temperature, in comparison with those of Si-C-O fibres obtained by thermal-oxidation curing. It appears that the properties of the fibres obtained by CVC method are higher than tose of Si-C-O fibres.

The IR spectra of Si-C fibres showed no absorption at 1000 ∿ 1100cm^{-1} due to Si-O stretching. If oxygen atoms are present in the fibres, carbothermal reduction or thermal degradation take place above 1300°C with weight loss and β-SiC crystal growth. Consequently, the strength of the fibre decreases. In the fibre obtained by CVC, these high-temperature reaction should not occur.

In Fig.3, β-SiC crystalline size (L_{111}) are shown as a function of the heat-treatment temperature. It is clear that rapid crystal growth did not take place, while L_{111} gradually increased with increasing heat-treatment temperature. This increse of L_{111} may decrease the strength of Si-C fibre as shown in Fig.2. The relation between the tensile strength and L_{111} is shown in Fig.4 which supports the decrease of the strength due to the crystal growth.

The thermal stability of Si-C fibre obtained by CVC method with 1-hexyne is shown in Fig.5. The fibre was heated at 1500°C for 0 ∿ 8h. These results show that the thermal stability of Si-C fibre by CVC method is superior to Si-C-O fibre in non-oxidizing atmosphere.

The following subject to be studied will be improving the oxidation resistance of the fibre.

References

1. K.Okamura, M.Sato, T.Seguchi and S.Kawanishi, J. Japan Society of Powder and Powder Metallurgy, 35 (1988) 170.

2. Y.Hasegawa, J. Inorganic and Organometallic Polymers, 2 (1992) 161.

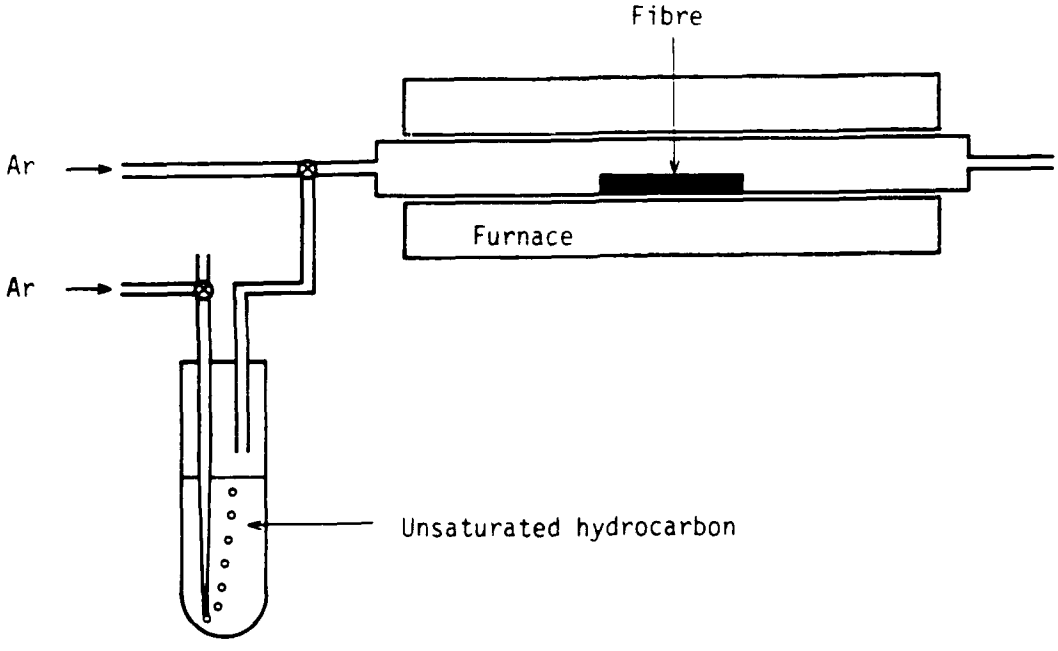

Fig.1 A schematic diagram of the curing apparatus.

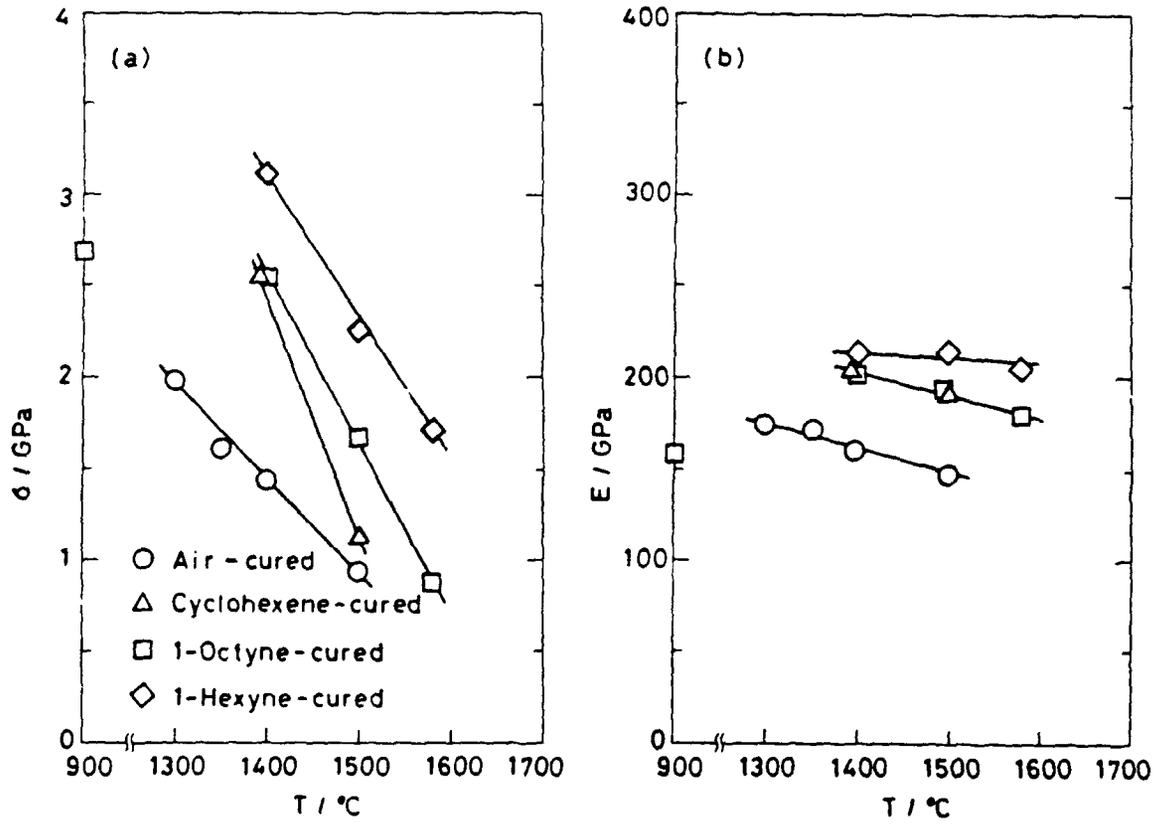

Fig.2 The relation between heat-treatment temperature and (a) tensile strength and (b) Young's modulus of Si-C and Si-C-O fibres.

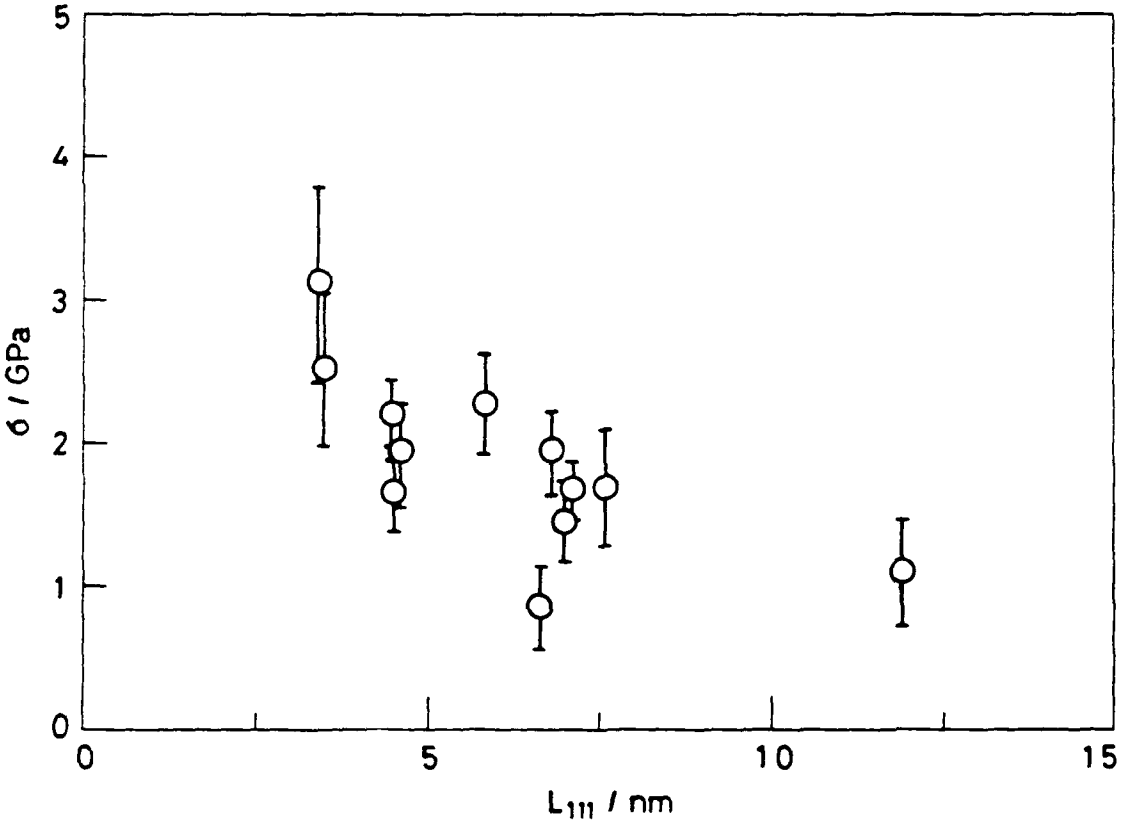

Fig.3 The relation between heat-treatment temperature and β-SiC crystalline size (L_{111}) in Si-C and Si-C-O fibres.

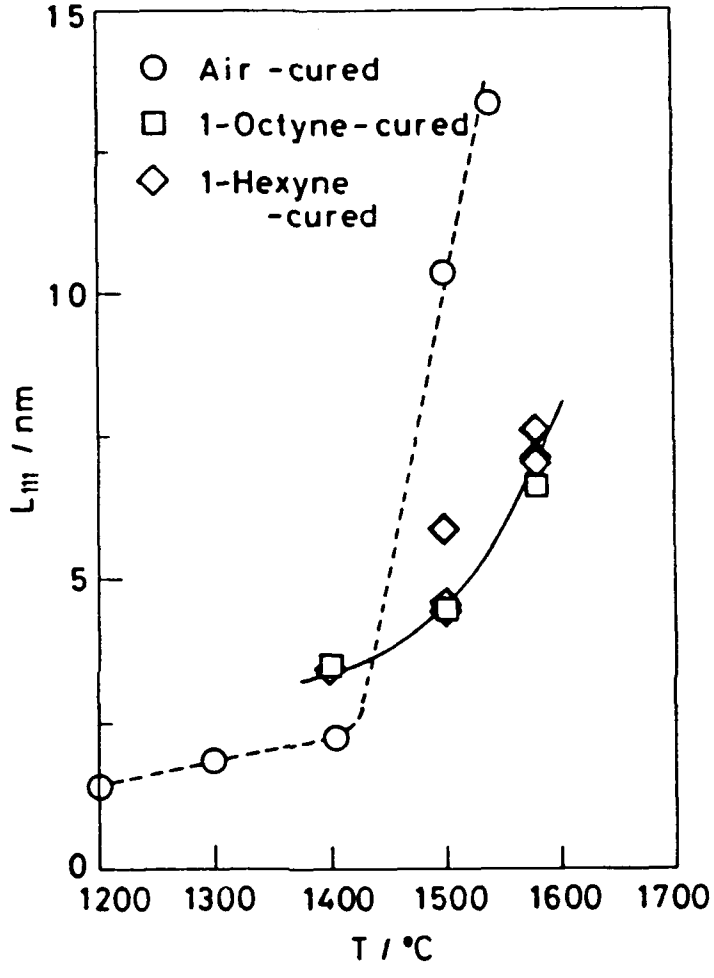

Fig.4 Tensile strength of Si-C fibre as a function of β-SiC crystalline size (L_{111}).

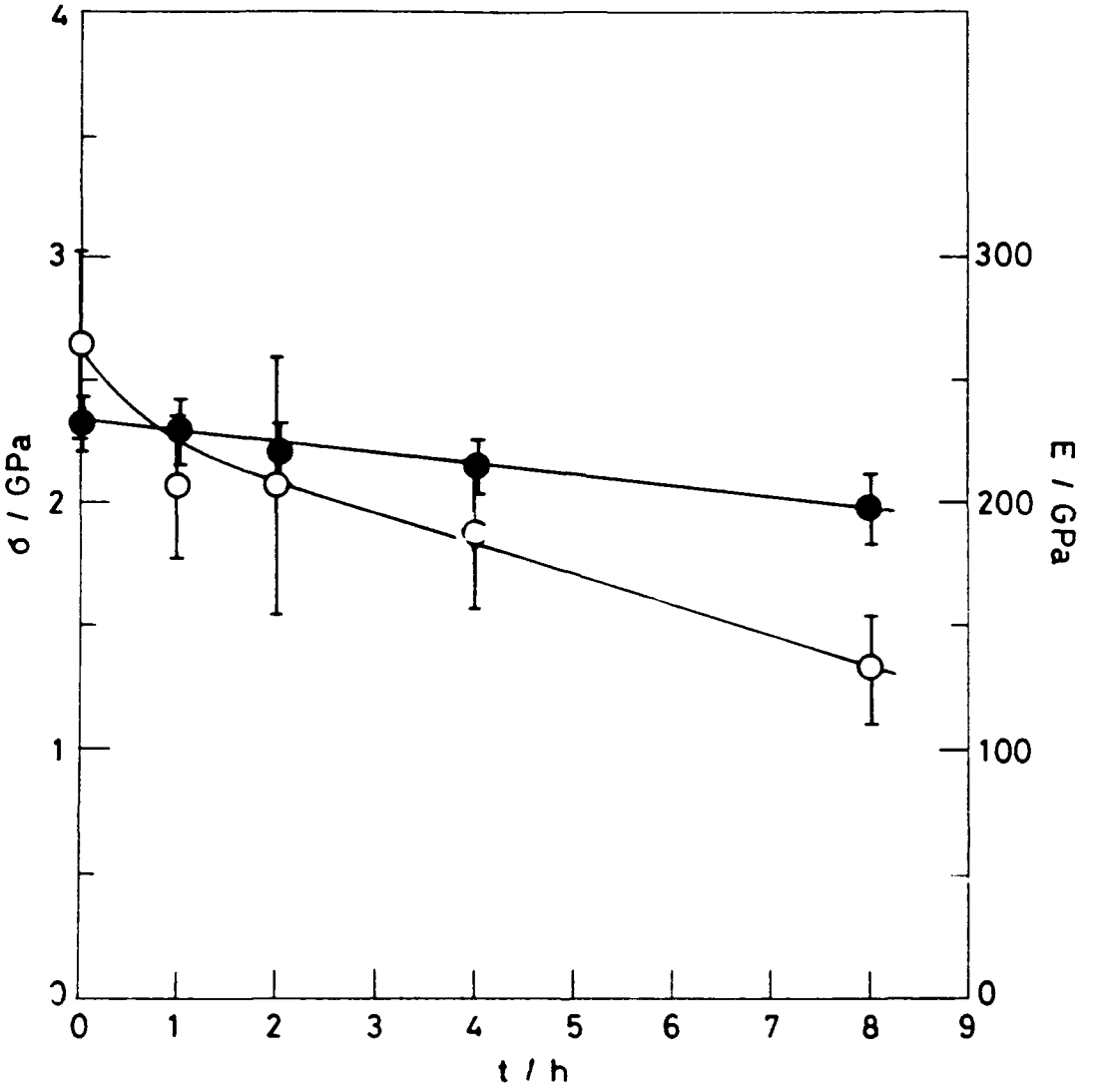

Fig.5 Tensile strength (O) and Young's modulus (●) of Si-C fibre obtained by 1-hexyne-curing as a function of heat-treatment time at 1500°C.

INTERFACIAL CONTROL AND MACROSCOPIC FAILURE IN INORGANIC COMPOSITES

T.W.Clyne and A.J.Phillipps

Department of Materials Science and Metallurgy
Pembroke Street, Cambridge CB2 3QZ, U.K.

tel 44-223-334332 fax 44-223-334567

Interfacial Processes

The nature of the interface has profound effects on the performance of all types of composite material. The central problem concerns inelastic processes at the interface which might be stimulated by the operative stress field. Some such processes (which might operate in metal- or ceramic-based composites) are shown schematically in Fig.1, together with a possible set of stresses in the vicinity of the interface. For ceramic matrix composites, there is a clear requirement that the interface be sufficiently "weak" to allow debonding, and the associated energy-absorbing processes, to be stimulated by the local stresses set up when the material is loaded[1]. Interfacial fracture is therefore the key process in such composites. There have been significant advances over recent years concerning interfacial fracture mechanics, particularly for bimaterial interfaces[2-6].

For metal matrix composites, the situation is somewhat less clear. Although the matrix has an enormous potential for energy absorption via dislocation motion, this will in general be much more difficult to promote than in a monolithic metal because of the constraint to matrix plasticity offered by the reinforcement. Under these circumstances, there could in principle be scope for significant toughness enhancement in MMCs as a consequence of inelastic processes occurring at the interface. In practice, a strong bond is probably beneficial in most cases since it will delay the onset of failure. However, the interplay between microstructure, stress state and the nature of the inelastic processes can be highly complex and is further complicated in many MMCs by the scope for progressive interfacial chemical reaction[7], which can substantially alter the mechanical response characteristics of the interface.

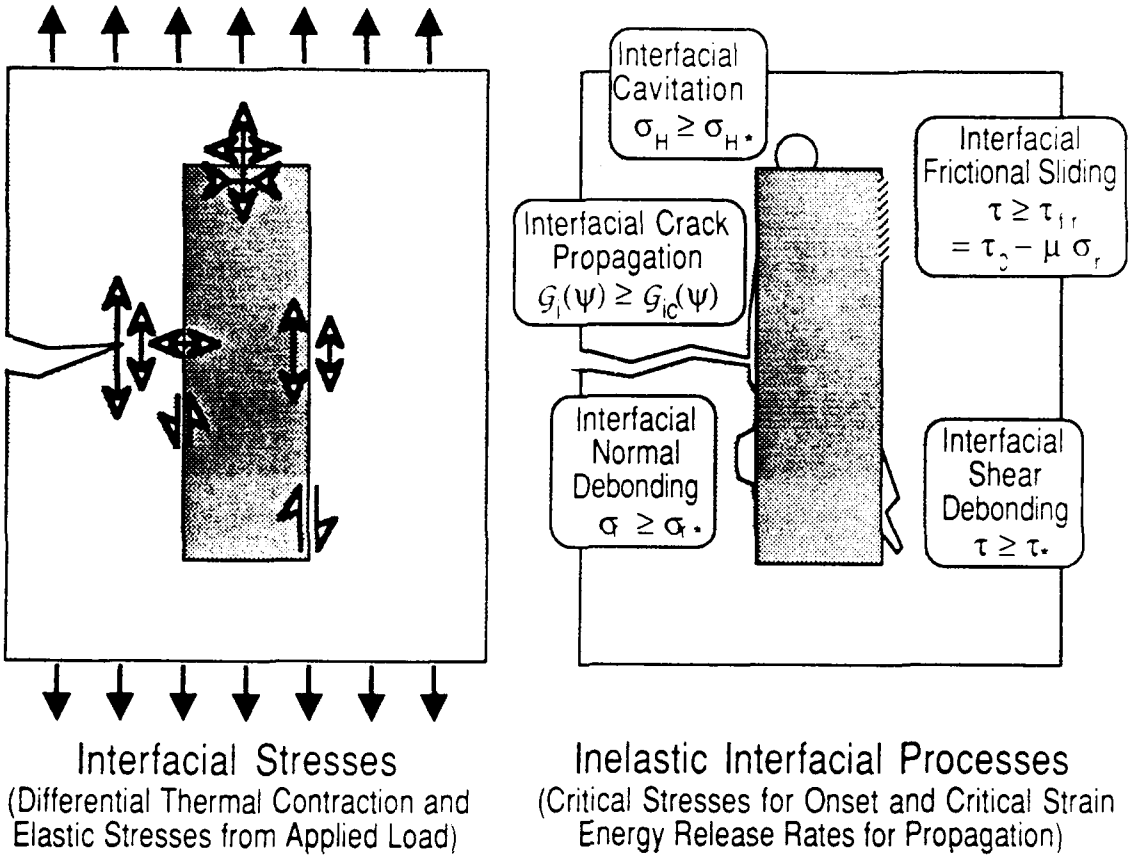

Fig.1 Schematic depiction of possible stress state variations in the vicinity of a fibre embedded in a matrix and some of the inelastic processes which can be stimulated at the interface by such stresses.

Interfacial Testing

A variety of tests have been developed to measure mechanical characteristics of the interface in composite materials. These involve situations ranging[8-11] from single fibre pullout and pushout tests to interfacial cracking during bending of laminates. There are, however, often difficulties in identifying precisely what mechanical property of the interface is being measured. An important point is that different tests cover a range of proportions of opening and shearing mode stress intensities at the crack tip. Parameters being measured, such as a critical shear stress for the onset of debonding or a critical value of the interfacial strain energy release rate, will vary with this proportion. An increasingly popular approach[12-14] to the characterisation of this mode mixity is to identify the so-called phase angle, ψ, ($=\tan^{-1}(K_{II}/K_I)$), although there are some difficulties with this approach - particularly when compressive

stresses are present. It can be seen from Fig.2 that measured values of interfacial parameters can vary quite sharply with mode mixity, which can range from pure opening (ψ=0°) to pure shear (ψ=90°); in general, resistance to crack propagation rises with predominance of shearing over opening mode, as frictional work in the wake of the crack tip increases.

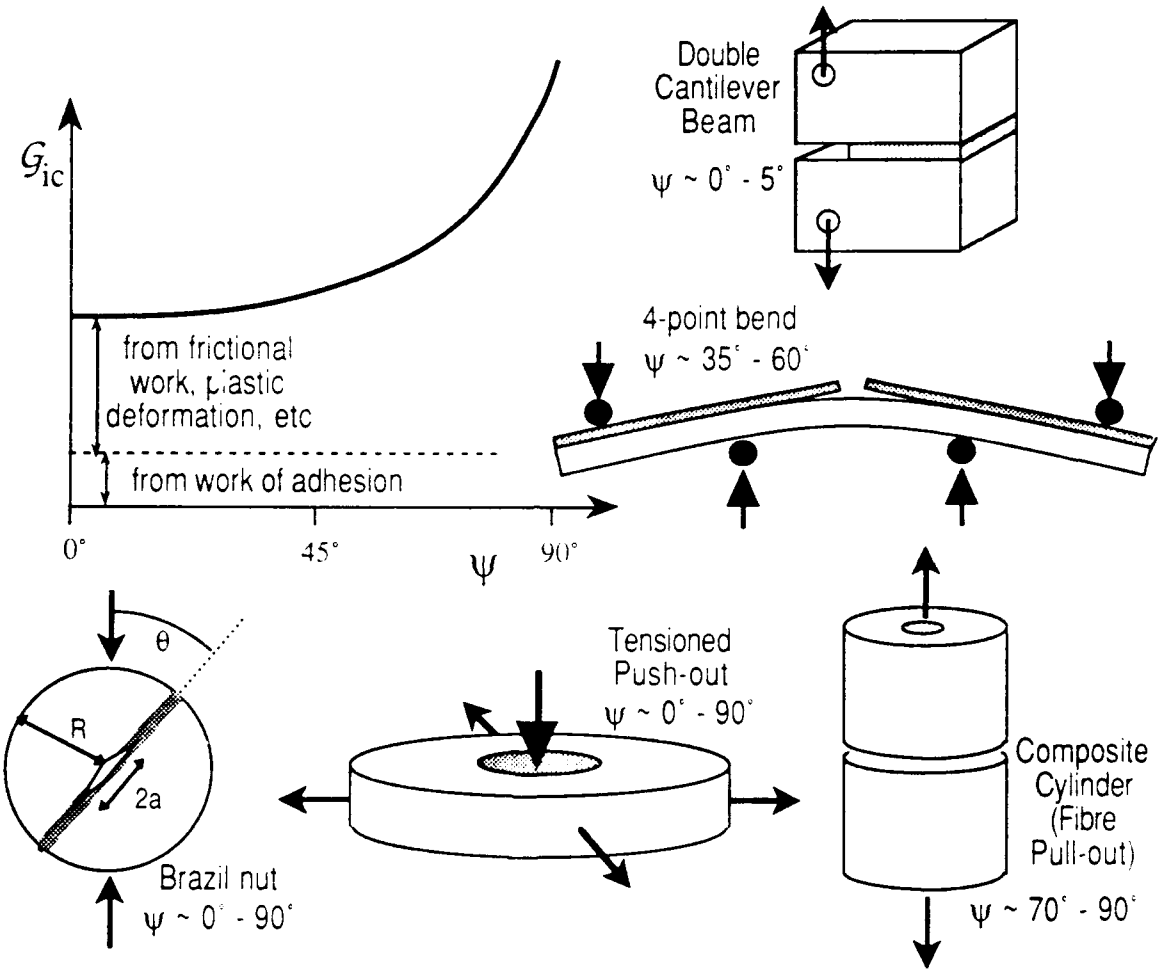

Fig.2 Schematic illustration of the dependence of the interfacial critical strain energy release rate, G_{ic}, on the phase angle of loading mode mixity, ψ. Different tests involve a wide range of ψ values.

Interfacial Modification

There are several ways in which useful modifications to interfacial features can be effected in inorganic composites. For example, careful control over the structure of graphitic interfaces in SiC laminates can ensure that the value of G_{ic} is sufficiently low,

relative to G_c for the bulk SiC, to ensure that transverse cracks are consistently deflected[15]. For MMCs, the concern is often more likely to be prevention of the formation of brittle interfacial reaction layers. For example, duplex C/TiB_2 coatings[16] have been deposited by CVD during fabrication of SiC fibres to be used in titanium composites. Studies have also been carried out on duplex yttrium/yttria coatings deposited onto SiC by sputtering[17]. This system is thermodynamically stable in Ti at high temperature and, since there is scope during the sputtering process for inducing high compressive stresses[18] in the coating by atomic peening - see Fig.3, the problems of deposit cracking as a result of differential thermal contraction stresses can be overcome.

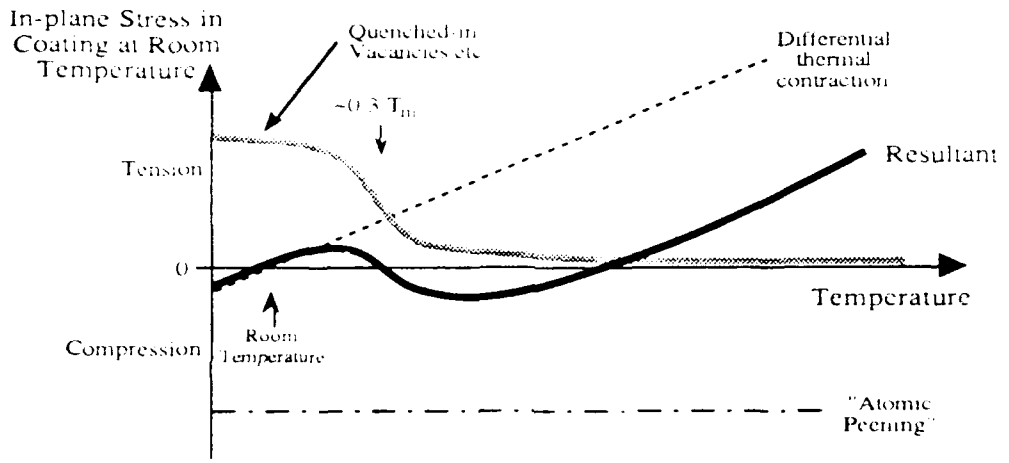

Fig.3 Schematic illustration of various contributions to the stress state at room temperature in a sputtered yttria layer on a SiC monofilament, as a function of the coating fabrication temperature.

Macroscopic Deformation and Failure

One of the major challenges in the development of advanced composites is to establish quantitative correlations between mechanical characteristics of the interface and composite properties - particularly those concerning plastic deformation and failure. The current situation varies sharply depending on the type of composite concerned. At one extreme, it is now possible to develop models completely describing the fracture behaviour under 3-point bending of laminates made up of brittle sheets joined by interfaces of specified toughness. For example, a comparison is shown in Fig.4 between measured and predicted load-displacement plots for such a laminate, with the series of peaks representing the onset of fracture of successive layers and subsequent crack deflection by the interfaces. It is acceptable to take a

constant value for G_{ic}, since the variation of ψ as the crack propagates along such a laminate is small. Agreement can be improved by the use of an appropriate Weibull modulus, m, in the modelling, although obviously the actual distribution of peak heights can only be predicted on a statistical basis.

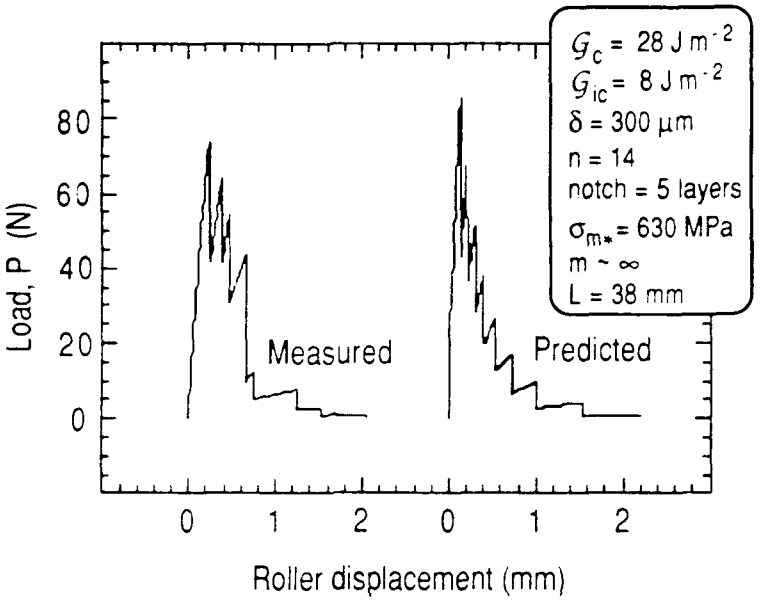

Fig.4 Experimental and predicted load-displacement plots for notched SiC laminates in 3-point bending.

The above situation is highly amenable to modelling because the matrix is brittle and the crack geometry is simple. Fibre composites are inevitably much more complex geometrically, with the mode mixity at an interfacial crack usually varying with position both around the fibre circumference and along its length. In addition, for metal matrix composites there is substantial scope for energy absorption and plastic deformation within the matrix and predictive modelling of this is difficult, even with recourse to numerical methods[19]. Nevertheless, some predictive capability relating interface characteristics to composite performance can be established. For example, it has been shown[20] that continuous monitoring of the Poisson's ratios during tensile loading of long fibre reinforced Ti can reveal whether matrix plasticity or interfacial debonding and damage are responsible for observed inelastic behaviour and this can be correlated with measured interfacial properties. There is also some scope for predicting whether interfacial energy absorption could be significant in different situations; in general, it would appear that this is only possible if very pronounced

fibre pull-out can be stimulated and even then the contribution is only likely to be really important in relatively brittle metals, such as zinc[21,22].

References

1. A.G. Evans, F.W. Zok and J. Davis, *The Role of Interfaces in Fiber-Reinforced Brittle Matrix Composites*, Comp. Sci & Tech., vol.**42**, (1991) p.3-24.
2. J.R. Rice, *Elastic Fracture Mechanics Concepts for Interfacial Cracks*, J.App. Mech. (Trans. ASME), vol.**55**, (1988) p.98-103.
3. M.S. Hu, M.D. Thouless and A.G. Evans, *The Decohesion of Thin Films from Brittle Substrates*, Acta Metall., vol.**36**, (1988) p.1301-1307.
4. M. Hu, *The Cracking and Decohesion of Thin Brittle Films*, Materials Research Society Symposium, vol.**130**, (1989) p.213-218.
5. A.G. Evans, M. Rühle, B.J. Dalgleish and P.G. Charalambides, *The Fracture Energy of Bimaterial Interfaces*, Mater. Sci. Eng., vol.**A126**, (1990) p.53-64.
6. Z. Suo and J.W. Hutchinson, *Interface Crack Between Two Elastic Layers*, Int. J. Fract., vol.**43**, (1990) p.1-18.
7. T.W. Clyne and M.C. Watson, *Interfacial Mechanics in Fibre-reinforced Metals*, Comp. Sci. Tech., vol.**42**, (1991) p.25-55.
8. P.S. Chua and M.R. Piggott, *The Glass Fibre-polymer Interface: I Theoretical Considerations for Single Fibre Pullout Tests*, Comp. Sci. Tech., vol.**22**, (1985) p.33-42.
9. P.G. Charalambides, H.C. Cao, J. Lund and A.G. Evans, *Development of a Test for Measuring the Mixed Mode Fracture Resistance of Bimaterial Interfaces*, Mech. Mater., vol.**8**, (1990) p.269-283.
10. M.C. Watson and T.W. Clyne, *The Use of Single Fibre Pushout Testing to Explore Interfacial Mechanics in SiC Monofilament-reinforced Ti. Part I : A Photoelastic Study of the Test*, Acta Metal et Mater, vol.**40**, (1992) p.135-140.
11. M.C. Watson and T.W. Clyne, *The Tensioned Push-Out Test for Measurement of Fibre/Matrix Interfacial Toughness under Mixed Mode Loading*, to be published in Scripta Met,(1992) .
12. B. Budiansky and J.W. Hutchinson, *Matrix Fracture in Fiber Reinforced Ceramics*, J. Mech. & Physics of Solids, vol.**34**, (1986) p.167-189.
13. J.W. Hutchinson and Z. Suo, *Mixed Mode Cracking in Layered Materials*, Adv. Appl. Mechs., vol.**28**, (1991)
14. J.W. Hutchinson. *Mixed Mode Fracture Mechanics of Interfaces*, Report, Harvard Technical Report, Mech-139, (1989), Division of Applied Sciences, Harvard University, Cambridge, Massachusetts, USA.

15. A.J. Phillipps, W.J. Clegg and T.W. Clyne, *The Effect of Processing Variables on the Interfacial and Macroscopic Toughness of SiC Laminates*, to be published in Composites, (1992) .

16. N.A. James, D.J. Lovett and C.M. Warwick, *Mechanical Behaviour of a Continuous Fibre Reinforced Titanium Matrix Composite*, in "Composites: Design, Manufacture and Application (ICCM8)", S.W. Tsai and G.S. Springer (eds.), Hawaii, USA, SAMPE, (1991) p.19I/1-19I/10.

17. R.R. Kieschke, R.E. Somehk and T.W. Clyne, *Sputter Deposited Barrier Coatings on SiC Monofilaments for Use in Reactive Metallic Matrices - Part I Optimization of Barrier Structure*, Acta Metall.et Mater., vol.**39**, (1991) p.427-436.

18. C.M. Warwick, R.R. Kieschke and T.W. Clyne, *Sputter Deposited Barrier Coatings on SiC Monofilaments for Use in Reactive Metallic Matrices - Part II System Stress State*, Acta Metall. Mater, vol.**39**, (1991) p.437-444.

19. J.R. Brockenbrough, S. Suresh and H.A. Wienecke, *Deformation of MMCs with continuous fibers: geometrical effects of fiber distribution and shape*, Acta Metall. Mater, vol.**39**, (1991) p.735-752.

20. M.C. Watson and T.W. Clyne, *Reaction-induced changes in Interfacial and Macroscopic Mechanical Properties of SiC Monofilament reinforced Titanium*, to be published in Composites, (1992)

21. F. Vescera, J.P. Keustermans, M.A. Dellis, B. Lips and F. Delannay, *Processing and Properties of Zn-Al Alloy Matrix Composites Reinforced by Bidirectional Carbon Tissues*, in "Metal Matrix Composites - Processing, Microstructure and Properties, 12th Risø Int. Symp. on Materials Sci.", N.Hansen, D.J. Jensen, T. Leffers, H. Lilholt, T. Lorentzen, A.S. Pedersen, O.B. Pedersen and B. Ralph (eds.), Roskilde, Denmark, (1991) p.719-724.

22. W. Chengfu, Y. Meifang and W. Zhangbao, *Analysis of Fracture Features of Carbon Fibre Reinforced Zinc base alloy Composite*, in "6th International Conference on Composite Materials", F.L. Matthews, N.C.R.Buskell, J.M. Hodgkinson and J. Morton (eds.), London, Elsevier, (1987) p.2.476-2.480.

The Role of Fiber/Matrix Interface in The First Matrix Cracking of Fiber-Reinforced Brittle Matrix Composites

Takayuki Suzuki and Mototsugu Sakai

Department of Materials Science
Toyohashi University of Technology
Tempaku-cho, Toyohashi 441, JAPAN

INTRODUCTION

In a brittle/brittle composite system, such as ceramic-fiber/ceramic-matrix system composed of reinforcing fibers and matrix with very similar values of the elastic moduli and the fracture toughness values, a propagating matrix crack is unlikely to "recognize" the fiber at the interface, if the interface bonding is perfect. The matrix crack will extend into and through the fiber without interface debonding, crack face bridging and subsequent fiber pullout along the fracture path. The composite failure is thus very brittle and catastrophic. Little or no property enhancement will be expected in this form of composite failure. In order to attain increased toughening in brittle/brittle composite systems, it is required for the interface to have a certain optimum bonding force which is strong enough for stress transfer, yet weak enough for considerable interface debonding, being a requisite for toughening brittle matrix composites through fiber bridging and subsequent fiber pullout processes. The stress-induced interface debonding may also be expected to have an important role in the first matrix cracking of brittle matrix composites. In this paper, the fracture toughness for first matrix cracking of unidirectionally reinforced carbon-fiber/carbon-matrix and carbon-fiber/Si_3N_4-matrix composites is studied in relation to the ratio of elastic moduli E_f/E_m between the fiber and the matrix as well as to the difference in the interface bonding nature.

EXPERIMENTAL

Test Samples

A carbon-matrix composite (C/C) (Nippon Steel Co., Ltd.) and an Si_3N_4-matrix composite (C/S) (Noritake Co., Ltd.), both of which are unidirectionally reinforced with carbon fibers, were used. In the C/C-composite, PAN-based carbon fibers (7 μm in diameter, tensile strength of 3 GPa for the gage length of 25 mm, Young's modulus of 230 GPa) with phenolic resin were heat-treated at 1000 $^{\circ}C$, followed by impregnation/carbonization

processes for four times and finally baked at 2000 $^{\circ}C$. The fiber content, bulk density, and the Young's modulus of the resultant composite were 56 vol%, 1.63 g/cm^3, and 200 GPa, respectively.

Mesophase pitch-based carbon fibers were used for the C/S-composite. The fiber strength (gage length of 25 mm) and the Young's modulus are 2 GPa and 500 GPa, respectively. The fibers were shaped with Si_3N_4-slurry by a filament winding method to make green bodies, and then heat-treated at temperatures from 400 to 700 $^{\circ}C$ to eliminate the organic binder, followed by hot-pressing at 1500 $^{\circ}C$. The fiber content of the resultant composite was 35 vol%. Some characteristic material properties include the bulk density of 2.55 g/cm^3, porosity of 5.70 %, and the thermal expansion coefficient and the Young's modulus along the direction of reinforcing fibers are 5.4×10^{-7}/deg and 310 GPa, respectively.

Fracture Toughness Test for First Matrix Cracking

Three-point flexural test specimens with different dimensions, the thickness B = 5.7, 12 mm, and the width W = 1.6, 1.2 mm, were machined. The tensile (or compressive) axis of the flexural specimen coincides with the reinforcing fiber axis. In order to introduce a controlled semi-elliptical surface flaw on the surface at a right angle to the tensile stress, a thin steel blade (ϕ 5mm) with the tip radius less than 5 μm was used. Since the conventional fracture mechanics test specimen geometry with a straight-through notch, such as the compact tension or the single edge-notched bend specimen, yields a plane-stress or plane-strain at the notch-tip, the crack does not extend across the unidirectionally reinforcing fibers, but instead propagates along the fiber direction by delamination cracking. However, because of the triaxial stress-strain state of the semi-elliptical surface flaw, the present flexural test specimen avoids such undesirable delamination cracking at the crack-tip, and results in an ideal matrix cracking, the crack plane passing through the composites at a right angle to the reinforcing fibers. The fracture toughness K_c for matrix cracking of these composite materials was examined by changing the size of the surface flaw ranging from 10 to 400 μm in the depth.

A special type of displacement-controlled test apparatus was designed for the present study for first matrix cracking. A precise determination of the onset critical load for first matrix cracking, which occurs at the bottom of the semi-elliptical surface flaw, was easily conducted through the *in-situ* optical observation of cracking at the bottom of the surface flaw during the flexural loading over the test span, S = 40 mm. The details of the flexural test apparatus have been reported in the literature.

RESULTS AND DISCUSSION

The interrelationships of the fracture toughness K_c for first matrix cracking and the depth b of the surface flaw are plotted in Fig. 1 for the C/C- and the C/S-composites. The K_c-values are nealy constant (7.0 $\pm$ 0.6 MPa$\sqrt{m}$ for the C/C- and 5.2 $\pm$ 0.5 MPa$\sqrt{m}$ for the C/S-composites) over a wide range of the surface notch depth. The normalized toughness improvement by fiber reinforcement (K_c/K_m) (the composite toughness K_c divided by the fracture toughness K_m of the unreinforced monolithic carbon or Si_3N_4 used for the matrix) is illustrated in Figs. 2(a) and 2(b). It is worthy of note that the toughness improvement of the C/C-composite ($K_c/K_m \approx 7.0$) is considerably higher than that of the C/S-composite ($K_c/K_m \approx 1.3$). Miyajima and Sakai have demonstrated that the toughness improvement can be expressed by

$$\frac{K_c}{K_m} = (SSC)_{db} \cdot (SSC)_{el} \tag{1}$$

where $(SSC)_{db}$ and $(SSC)_{el}$ stand for, respectively, the contributions of stress shielding by the fiber/matrix interface debonding processes in the frontal process zone and by the internal elastic stress partition between fiber and matrix due to the difference in their elastic modulus. The latter contribution ($(SSC)_{el}$) of the elastic shielding is given by

$$(SSC)_{el} = \sqrt{\frac{E_c}{E_m} \cdot v_m} \tag{2}$$

where E_c, E_m, and v_m are the elastic moduli of the composite and the matrix, and the volume fraction of the reinforcing fibers, respectively. The numerical relations of $(SSC)_{el}$ versus the volume fraction of matrix are shown in Fig. 2 by solid lines. The elastic stress shielding effect of the C/C-composite [$(SSC)_{el} \approx 3$] actually exceeds that of the C/S-composite [$(SSC)_{el} \approx 0.8$]. This difference in the elastic stress shielding effect mainly arises from the significant difference in the ratios of the elastic moduli E_c/E_m of the C/C-composite (≈ 20) and the C/S-composite (≈ 1.1), as easily expected from Eq. (2).

The finite discrepancies between the experimental results (circles with a vertical bar showing experimental variations) and the theoretical predictions ($(SSC)_{el}$-curves) in Figs. 2(a) and 2(b) can be accommodated to the stress shielding coefficient $(SSC)_{db}$ by substituting $(SSC)_{db} \approx 2.5$ for the C/C-composite, and ≈ 1.5 for the C/S-composite. The differences in the E_f/E_m-values as well as in the interface bonding nature between the C/C- and the C/S-composites may yield this important difference in the interface debonding stress shielding.

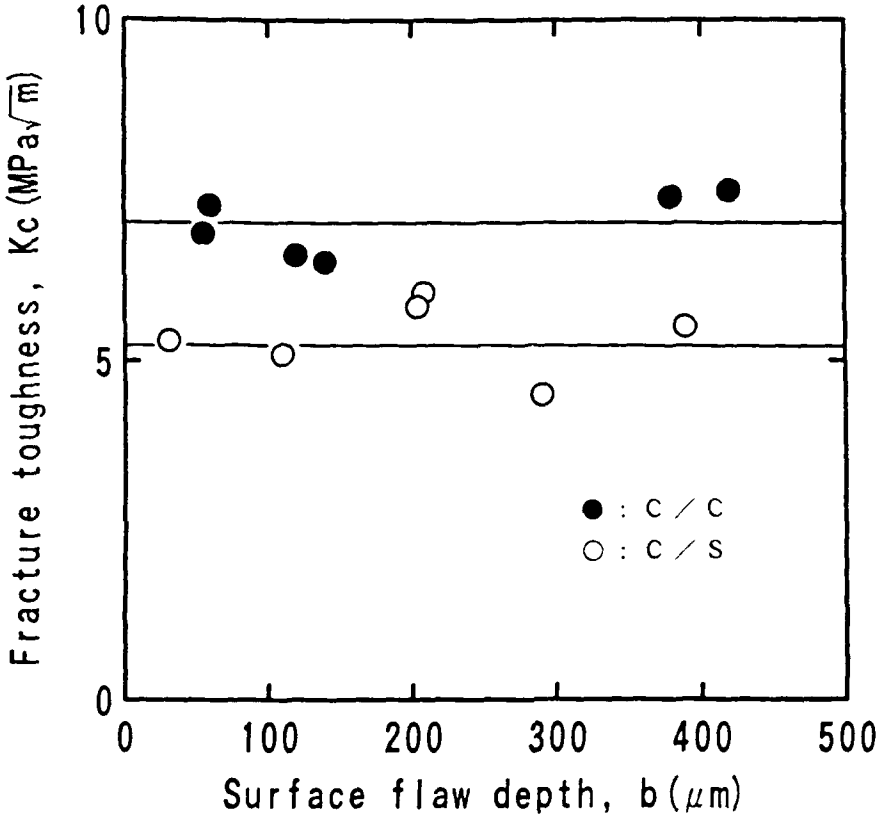

Fig. 1 Fracture toughness values for first matrix cracking of a carbon-fiber/carbon-matrix composite (C/C) and a carbon-fiber/Si_3N_4-matrix composite (C/S).

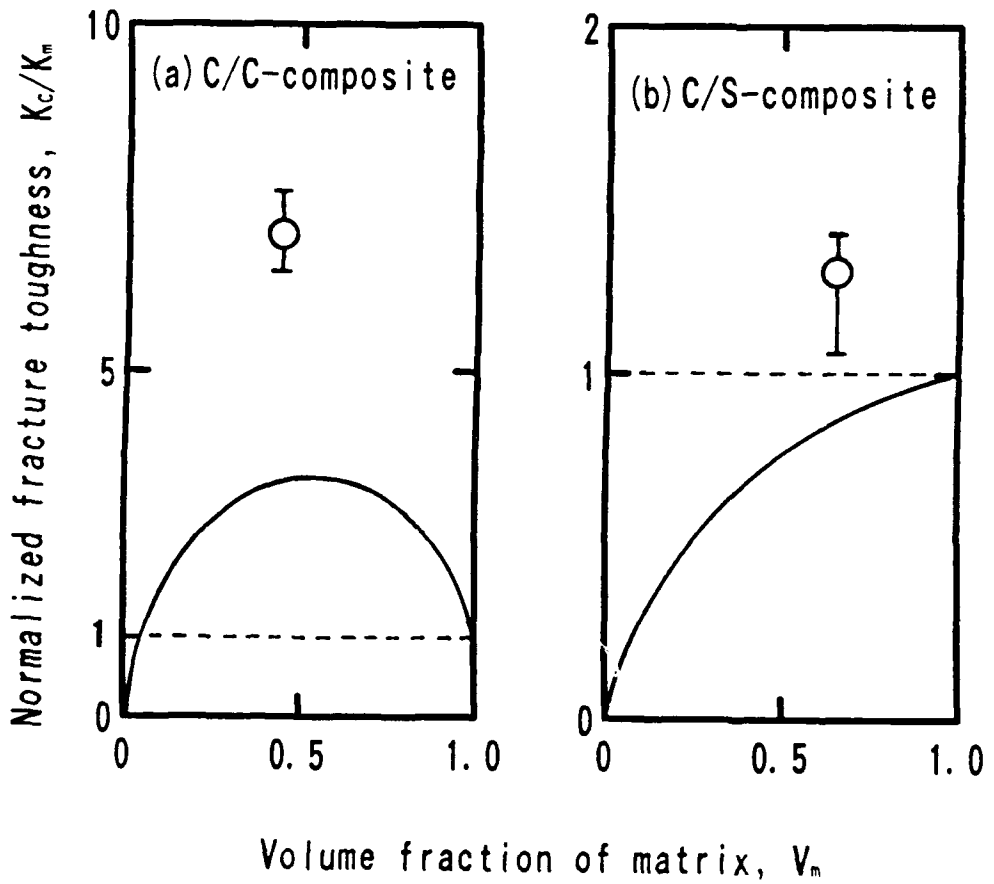

Fig. 2 Normalized fracture toughness values of the C/C- and the C/S-composites. Solid lines represent the theoretical predictions (Eq. (2)) for elastic stress shielding.

ISSUES IN THE CONTROL OF FIBER-MATRIX INTERFACE PROPERTIES IN CERAMIC COMPOSITES

Ronald J. Kerans
Wright Laboratory / Materials Directorate
Wright-Patterson AFB, Ohio 45433-6533, USA

ABSTRACT

The current interest in ceramic composites is a consequence of their potential for dramatically improved damage tolerance as compared to monolithic ceramics while delivering similar high temperature properties. This damage tolerance is accomplished through local accommodation of overstresses by microcracking. The existence of microcracks in a damaged composite has clear implications regarding environmental resistance. There has been much discussion about either using composites at stresses below matrix cracking or developing oxidation resistant interface treatments. However, careful consideration leads to the conclusion that the former is not viable and that oxidation resistant interface control is a necessity. Damage tolerance is not an occasional requirement, but a pervasive consequence of the lack of knowledge and control of the stress state in an actual part. This means that all parts will be at least locally microcracked. The consequence of this is that the most productive uses of ceramic composites in heat engines are dependant upon the development of oxidation resistant interface treatments; an area in which there has been relatively little progress.

It is evident that the fiber debonding and sliding that accompany the inception and propagation of cracks are important factors in determining the mechanical behavior of ceramic composites. They are also complicated processes dependant upon several variables. Numerous issues exist regarding measurement and interpretation of interface properties and elucidation of the roles of these variables. The development of viable approaches to interface control will be greatly aided by comprehensive understanding of these factors.

If a composite is to be toughened by the presence of the fibers, it is necessary that the fibers are bypassed by the matrix crack. If the toughness of the interface is too high, or if the frictional resistance to sliding of an unbonded

interface is too high, the fibers will fracture. Therefore, we expect both the interfacial toughness and friction to be important in determining if crack bridging can occur.

The magnitude of the frictional resistance to the sliding of the fiber determines how far the debonding crack propagates and the energy expended during pull-out after the fiber breaks. Since the friction will depend upon residual stresses, coefficient of friction, roughness of the fiber, and abrasion of the interface; these are all important factors. Furthermore, they are not all constants. Abrasion and roughness effects are functions of sliding distance. The effective coefficient of friction might also be expected to change with the accumulation of abrasion debris in the interface. It is expected then, that to fully understand and control interface behavior, it is necessary to measure and understand the roles and contributors to the interfacial toughness and interfacial friction, and the changes in these quantities with time and environmental exposure.

All of these factors will affect the design of interface control treatments. In addition, time dependent factors will further constrain the designs. Required coating thicknesses will depend in part on the fiber roughness and on the rate of microstructural evolution of both fiber and matrix. Composite lifetimes may depend strongly on the rate at which fiber or coating oxidation changes interface properties. A stable, oxidation resistant fiber is essential to the most dramatic impact of ceramic composites, but the fiber - matrix interface is a no less important link in composite performance. Without equally sophisticated interface control, the best composites will turn into expensive monoliths.

Recent Progress in the Design of Advanced High Temperature Composites

by
J. Economy
University of Illinois
Urbana, IL

In this paper recent progress in our group on new types of reinforcing agents and matrices is described with particular emphasis on systems with enhanced performance, ease of processing and potentially lower costs. Continuous multi-filament yarns under study include boron nitride (BN) and boron carbide (B_4C). Work on high aspect ratio, single crystal flakes of aluminum diboride (AlB_2) as a reinforcement for aluminum is summarized. In addition, recent studies on developing novel organic oligomers for use in a one step process for fabrication of carbon/carbon composites is described. A precursor to a BN matrix has been designed and successfully demonstrated.

Boron Nitride Fibers

BN fibers were successfully prepared in the 1960's by reacting boric oxide filament with ammonia in a batch process over the temperature range of 350° to 850°C. Stretching of the fibers at 2000°C (~17%) resulted in orientation of the layered structure to produce a high σ/E fiber similar in properties to carbon fibers. This earlier work is now being revisited with the goal of designing a continuous process for drawing, nitriding and stretching the filament yarn. If successful such a process could yield a low cost route to BN fibers since the fiber is formed in 70% yield from the reaction of relatively cheap starting materials; namely, $B_2O_3 + NH_3$. BN fibers display far better thermooxidative stability than carbon fibers i.e. 900°C vs 450°C and are resistant to many molten metals. In this paper recent progress on achieving the goal of a low cost continuous process is described along with a brief comparison of properties between BN and carbon fibers.

Boron Carbide Fibers

B_4C continuous filament yarn has been successfully prepared by reaction of a precursor carbon yarn with $BCl_3 + H_2$ at temperatures of 1800°C followed by tensioning at 2150°C. Such fibers display average tensile strengths of 350,000 p.s.i. and a modulus of 50,000,000 p.s.i. (carbon fiber is converted to ~ 70% B_4C). Since B_4C is known to retain most of its mechanical properties up to 1600-1700°C, it would be an excellent

candidate for design of ceramic composites for use at 1000-1300°C. To address the problem of limited oxidation resistance of B_4C above 1000°C, a program is being initiated to further convert the B_4C fibers to B_4Si fibers which hopefully will display oxidative resistance similar to SiC.

Aluminum Diboride Single Crystal Flakes

AlB_2 flakes have been prepared with high aspect ratio (200/1) and shown to provide outstanding planar reinforcement in epoxy composites (flexural/tensile/compressive moduli values range from 40-45,000,000 ps.i. at 65% loading). The flakes which are crystallized from molten aluminum are unfortunately isolated in the presence of a number of other cubic crystals such as AlB_{12}, $C_2Al_3B_{48}$,$MgAlB_{14}$ and C_4AlB_{24}. This of course necessitates an extensive separation procedure which negates their direct use as a reinforcement of aluminum. The program currently underway is designed to eliminate formation of the undesirable crystals permitting concentration and processing of the flakes in molten aluminum to yield the desired composite shape in one step.

Design of One Step Precursors to Carbon and Boron Nitride Matrices

Carbon/carbon composites have been available for over 25 years as a commercial product. Typically, the manufacturing process requires multiple reimpregnations with phenolic, pitch or furfural oligomers to build up the carbon yield, and this is usually followed by a CVD impregnation of carbon from methane. Total time of manufacture can run up to 5-6 months making for a rather unwieldy process. In our program we have designed a diacetylenic oligomer which carbonize in 95% yield at 800°C. This system has been used to fabricate carbon/carbon composites in one step in an overall reaction time of 30 minutes.

Similarly, borazene has been found to convert to BN in ~ 90% yield on heating from 70°C to 1000°C. In our program we have prepared carbon fiber (PAN based) reinforced BN matrix which displays outstanding mechanical properties e.g. ~ 15,000,000 flexural modulus and 130,000 p.s.i. flexural strength. The composite was annealed at 1200C for 30 minutes. Further work is being carried out to better characterize the nature of the BN at the carbon fiber interface and also to improve the degree of order in the BN structure (i.e. reduce the interlayer spacing to 3.40Å).

PRESSURELESS SINTERING OF SILICON NITRIDE COMPOSITE

T.Yonezawa, S.Saitoh, M.Minamizawa, T.Matsuda
Japan Metals & Chemicals Co., Ltd.
No.8-4, Koami-cho, Nihonbashi, Chuo-ku, Tokyo 103, Japan

ABSTRACT

Silicon nitride composites containing up to 20 wt% silicon carbide whiskers were slip casted to orient the whiskers two dimensionally, parallel to the plaster mold surfaces. The sintered body with 20 wt% whiskers showed 98% relative density, 950 MPa flexural strength and 7.0 MPa$\cdot m^{1/2}$ fracture toughness. Also the thermal shock resistance was found to be as high as 950 °C.

INTRODUCTION

Silicon nitride ceramics have a good balance of various properties such as strength, toughness, thermal shock resistance, oxidation resistance and the like. Wide applications of silicon nitride ceramics such as use for automobile parts are now being developed. Parallel with the development of such applications, further improvement of the properties of silicon nitride ceramics themselves is being promoted steadily.

Current studies of the composite ceramic materials are also now active in order to obtain remarkably improved properties. In particular, whisker reinforced ceramics (denoted as WRC) are attracting a great deal of attention.[1] However, there are very few reports describing the mechanical properties of pressureless sintered WRC[2-4] and the reported data are still unsatisfactory, because of the network of whiskers in the green body. The whisker does not shrink during pressurless sintering, and the whisker networks prevents the material movement. Then, the sintered composite has a lot of pores and low strength (shown as Fig.1-a).

Hot pressing method has been used conventionally for the production of a high dense WRC.[5-7] During hot pressing, the pressure destroys the whisker networks and rearranges whiskers oriented two dimensionally (shown as Fig.1-b). WRC can be densified perfectly using the hot pressing method, but the shapes of hot pressed products are limited to the simple ones, and the fabrication cost of the products are also expensive. In order to extend practical application of WRC, the densification by pressureless sintering (up to 1 MPa) must be performed.

If we would make a green compact in which the whiskers were oriented one or two dimensionally, the shrinkage toward the oriented direction could be hindered significantly, but the sufficient shrinkage could be possible toward the direction perpendicular to the oriented direction (shown as Fig.1-c).

From these points of view, we had compared and examined various compaction methods, and as a result, we believe that the slip casting method is the highest possible method in terms of orienting whiskers one or two dimensionally and also in terms of

industrial application. We had succeeded in densifying a WRC by pressureless sintering and manufactured some practical wares.[8-10]

EXPERIMENTAL PROCEDURE

The silicon nitride powder (grade: SNP-8S, Japan Metals & Chemicals Co., Japan), the silicon carbide whiskers (grade: TWS-100 and TWS-400, Tokai carbon Co., Japan), the sintering aids and the deionized water were mixed in an alumina ball mill for 46 hours with addition of the deflocculant. The average diameter and length of TWS-100 and TWS-400 are 0.4 μm and 30 μm, 1.3 μm and 50 μm, respectively. The amount of whisker was 0, 10, 15 and 20 wt%. The mixtures of yttria (99.99% pure, Shin-etsu Chemical Co., Japan), alumina (grade: AKP-30, Sumitomo Chemical Co., Japan) and Cordierite (grade: SS600, Marusu Yuyaku Co., Japan) were used as the sintering additives and those amount was 12 and 15 wt%. After adjusting the viscosity to about under 50 mPa•s by adding water, the slips were casted in molds of plaster of Paris. The solid content of the slips were about 70 wt%. The green compacts (50 by 50 by 6-10 mm) were dried and then sintered in the range of 1600 to 1750°C for 5 hours at 0.1 MPa of nitrogen or 1825°C for 2 to 6 hours at 1 MPa of nitrogen. The bulk density was measured by the Archimedean displacement method using toluen. The relative density was determined by dividing the bulk density by the true density calculated from the composition of the starting materials. The flexural strength was determined by three-points flexure on bars having the dimension of 3.0 by 4.0 by 40.0 mm, with polished tensile surface (JIS-R-1601). The fracuture toughness was obtained by Single Edge Precracked Beam method (JIS-R-1607). The thermal shock resistance was determined as follows. Inserting theflexure bars into a resistance heated tube furnace, soaking 10 to15 min at given temperature and then quenching into a water-bath (25 °C). The test bars were then broken in three-point flexure at room temperature and the flexural strengths were measured. The microstructure of the green and sintered bodies were studied by an optical and a scanning electron microscopy.

RESULT AND DISCUSSION

By controlling the properties of the slips, we got the green compact in which the whiskers were oriented two dimensionally. Seeing from the direction parallel to the mold surface with the optical microscope, the whiskers were alignment in the same direction, but seeing from the direction perpendicular to the mold surface, the whiskers were randomly distributed.

Figure 2 shows the anisotropic shrinkage and the relative density of the composite. As the whisker content increases, the anisotropic shrinkage increases and the relative density decreases. The shrinkage toward perpendicular direction is 1.5 to 2.3 times larger than the one toward parallel direction. The relative density increases as the sintering temperature increases. And the relative density of composite containing TWS-400 is higher than the one containing TWS-100. As the sintering time increases from 2 to 4 hours, the relative density of the composite with 20 wt% TWS-400 goes up to 98%.

Figure 3 shows the flexural strength and the fracture toughness of the composite with TWS-400 sintered at 1825°C. As the whisker content increases, the fracture toughness increases but the flexural strength reduced at 20 wt%, and it occurred from low relative density. The sintered body with 20 wt% TWS-400 sintered 4 hours showed 950 MPa flexural strength and 7.0 $MPa \cdot m^{1/2}$ fracture toughness.

The composite has a excellent thermal shock resistance. Monolithic silicon nitride sintered at 1750 °C exhibited 800 °C of a critical thermal shock temperature difference, on the other hand, the composite sintered at 1750 °C with 10 wt% of TWS-100 gets 950 °C of a critical thermal shock temperature difference which is 20% improvement.

APPLICATIONS

These new composite materials for which we named "KRYPTONITE" have superior thermal shock resistance to the conventional silicon nitride. So, the various applications in severe working conditions, where rapid or local heating is necessary, will be developed. For example, the heatertube, stokes, ladles, etc. used in an aluminum casting factories are expected as the specifid application. The ladles for 0.3 to 1.5 kg molten aluminum and the crucibles for 3 kg molten aluminum are manufactured

CONCLUSIONS

By orientating whiskers for two dimensionally in the silicon nitride matrix using the slip casting method, the high dense WRC are produced by pressureless sintering. The sintered composites have good mechanical properties especially excellent thermal shock resistance and been applied as ceramic parts for molten aluminum casting.

REFERENCES

(1)S.Yamada, ONRFE Sci. Bull. 12[4],17-44,(1987)
(2)N.Tamari, I.Kondoh, S.Kamioka, K.Ueno and Y.Toibana, Yogyo-kyokai-shi,94[11],1177-79,(1986)
(3)T.Kandori, S.Kobayashi, S.Wada and O.Kamigaito, J. Mater.Sci. Lett.,6[11],1356-58,(1987)
(4)M.J.Hoffman, A.Nagel, P.Greil and G.Petzow, J.Am.Ceram.Soc., 72[5],765-69,(1989)
(5)K.Ueno and Y.Toibana, Yogyokyokai-shi,91[11],491-97,(1983)
(6)R.Lundberg, L.Kahlman, R.Pompe, R.Carlsson and R.Warren, Am. Ceram.Soc.Bull.,66[2],330-33,(1987)
(7)S.T.Buljan, J.G.Baldoni and M.L.Huckabee, ibid.,66[2],342-52, (1987)
(8)S.Saitoh, M.Minamizawa, T.Yonezawa, T.Matsuda and C.Sakai, Synopsis of "The 27th Basic Foram of the Ceram. Soc. Japan", p.208,(1989)
(9)S.Saitoh, M.Minamizawa, T.Yonezawa, T.Matsuda, Synopsis of "The 2nd Autumn Symposium of the Ceram. Soc. Japan",508-09,(1989)
(10)T.Yonezawa, S.Saitoh, M.Minamizawa, T.Matsuda, Proceed. of the First International SAMPE Symposium & Exhibition, 1131-36, (1989)

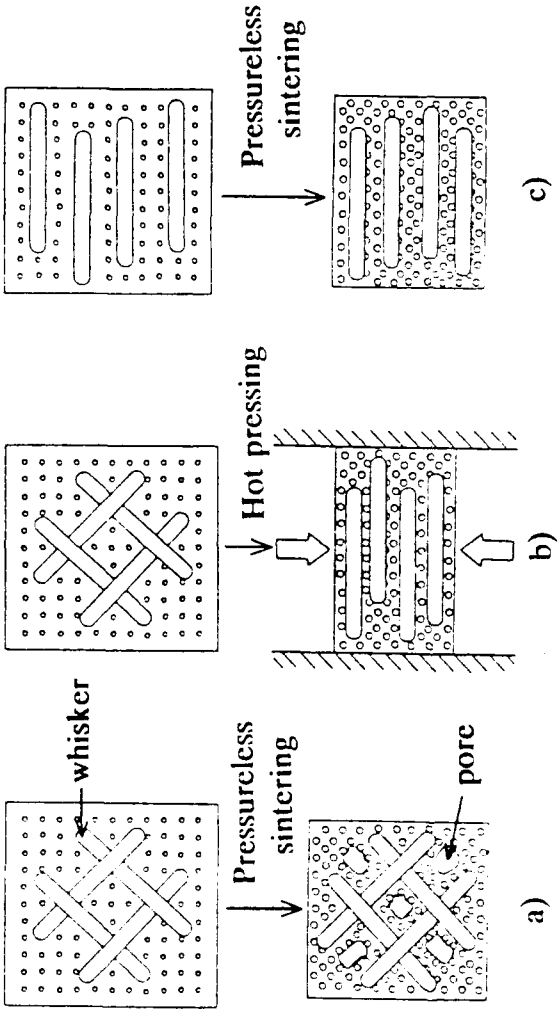

Fig.1 Shrinkage mechanism of whisker reinforced ceramics

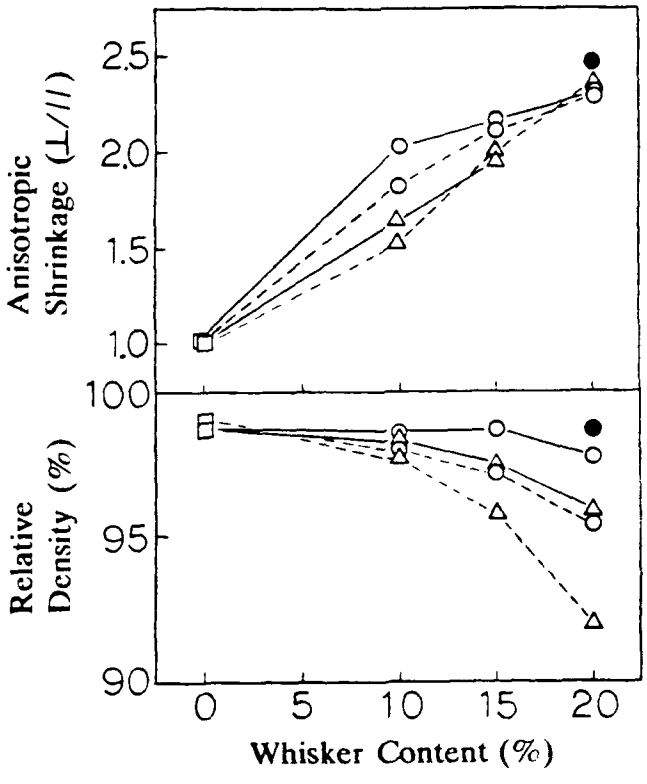

Fig.2 Effect of the whisker content on the anisotropic shrinkage and the relative density of the composite

△ TWS−100 − − − 1750 °C, 5h
○ TWS−400 —— 1825 °C, 2h
● TWS−400, 1825 °C, 4h

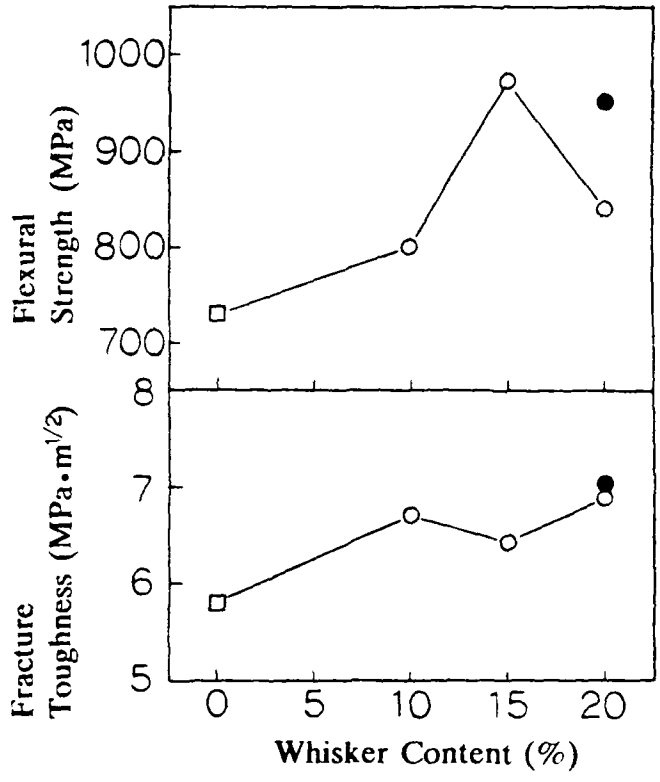

Fig.3 Effect of the whisker content on the flexural strength and the fracture toughness of the composite sintered at 1825 °C

○ TWS-400, 2h
● TWS-400, 4h

INORGANIC FIBRES FOR COMPOSITE MATERIALS

A.R. BUNSELL
Ecole Nationale Supérieure des Mines de Paris
Centre des Matériaux P.M. Fourt
B.P. 87
91003 EVRY CEDEX FRANCE

Ceramic fibres of potential interest for reinforcement may be divided into four very different types. Those made by chemical vapour deposition onto a substrate, those made by the conversion of a fine precursor fibre into a ceramic fibre, continuous mono crystalline filaments and ceramic whiskers. The first type of fibre has its origin in the early 1960's and is characterised by a large diameter, usually between 100 and 140 μm, good mechanical properties but inherent high cost. The boron and silicon carbide fibres made by the CVD process have been produced on both tungsten and pitch based carbon fibre cores and can be used to reinforce metals. Small diameter ceramic fibres began to appear in the later 1970's with the development of the α-alumina fibre FP from Du Pont. These fibres have diameters of around 20 μm. It was the development of fine diameter silicon silicon carbide based fibres by the pyrolysis of polycarbosilane precursor fibres however which stimulated research into reinforcing ceramics. These fibres have diameters generally between 10 and 20 μm and result from research begun in the 1970's . The Nicalon fibre produced by Nippon Carbon and which resulted from this research first became commercially available around 1982. There now exists several types of small diameter ceramic fibre which are candidates for reinforcing ceramic matrices and their number is likely to increase. The Tyranno fibre, produced several years after the launch of the Nicalon fibre by another Japanese company, Ube Chemicals, is produced by a similar route but a small amount of titanium in the structure gives it a slight temperature advantage as well as inhibiting crystallisation.

The Nicalon and Tyranno fibres represent the first generation of small diameter ceramic reinforcements which offered the possibility of reinforcing ceramics and glasses. Both Nippon Carbon and Ube Chemicals have retained the names of their fibres so that more recent fibres which represent a second

generation of reinforcements have the same names despite substantial changes to their compositions, notably a reduction in oxygen. The presence of oxygen in the fibres is due to a crosslinking stage in the production of the precursor filament which is usually achieved by heating in air. The latest versions of these fibres which are not yet available outside Japan, are made from precursors crosslinked by radiation.

An alternative route for the production of ceramic fibres has been adopted by a number of companies in Japan, U.S.A. and Europe. These fibres are made from polycarbosilazane precursors and produce fibres containing C, Si and N. The U.S. effort which was Federally funded brought together Dow Corning and Celanese which produced several fibres. The one which seems to be being produced commercially is the HPZ fibre made by Dow Corning. A similar fibre was to be made by Rhone Poulenc in France but this work has been discontinued. Hoechst has developed such a fibre but is at a laboratory stage. The only fibre which is said to possess an almost completely stochiometric structure however is made by Tonen.. It should be noted that the Tonen fibre is just becoming commercially available and it is claimed by the manufacturer that this silicon nitride fibre is stable in air up to 1400°C.

Some of the most stable materials when heated in air are oxides and since the production of the Fiber FP in the late seventies other fibres based on alumina have appeared. Du Pont produced PRD 166 which was an α -alumina fibre partially stabilised with 20% wt zirconia. This fibre, like its predecessor, had an average grain size of 0.5 μm, possessed a high Young's modulus and a small strain to failure (O.5 %). Alumina based fibres have also been produced by Sumimoto Chemicals but in this case the fibres were microcrystalline and contained 15 % of silica. The result was a drop in Young's modulus of nearly 50 % (200 GPa). The American company 3-M has produced a range of fibres based on mullite called Nextel. The latest α-alumina fibre to appear is the Almax 10 μm diameter fibre from Mitsui Mining.

All of the above mentioned alumina fibres are polycrystalline and are promoted as being potential reinforcements for light alloys. All seem to be restricted to temperatures below 1200°C. This is because all phases of alumina are converted to α-alumina at around this temperature or, in the presence of silica, mullite is produced. Grain growth due to grain boundary diffusion occurs at around 1200°C. and the fibres are seen to creep above 1000°C. None of these fibres retain sufficient strength above 1200°C to allow them to be used as

a reinforcement however the fibres may be able to be used as refractory insulation to higher temperatures (1600°C).

Most of the problems with the small diameter oxide fibres and for that matter to some extent with the other small diameter ceramic fibres are linked to grain boundaries. The production of single crystal filaments is clearly one way around the difficulty and this philosophy has a parallel in the development of monocrystal superalloys. Such alumina fibres have been produced in the U.S.A. for nearly twenty years under the name of Saphikon and renewed interest is being shown for them. The fibre retains its properties at high temperature in a way that the polycrystalline fibre do not however strength loss occurs at discreet temperatures due to the cleavage of the crystal structure.

Single crystal filaments are also found at the other extreme of fibre diameters in the form of whiskers. These filaments generally possess diameters of between 0.5 and 1.5 μm with lengths from 20 μm to 250 μm however greater lengths of several centimeters have been made in the USA and there are reports that whiskers having lengths of more than ten centimeters are available in the former USSR.

INORGANIC FIBERS DIRECTLY FROM THE VAPOR PHASE.

FREDERICK T. WALLENBERGER*
Du Pont Fibers, Experimental Station, P. O. Box 80302, Wilmington, Delaware 19880-0302

PAUL C. NORDINE
Containerless Processing Incorporated, 3453 Commercial Avenue, Northbrook, Illinois 60062

1. Introduction

We wish to report (1) a new generic process capable of making small diameter, strong substrate-free inorganic fibers including carbon, boron, silicon, silicon carbide and silicon nitride directly from the vapor phase (2) the effect of variables in this laser assisted chemical vapor deposition, or for short LCVD, process on the properties of the resulting fibers using boron fibers as the example of choice, and (3) early results with this LCVD process regarding other fibers.

2. Background

Several fiber-forming CVD processes are known. The best documented of these involves the deposition of refractory compounds onto a heated metal or carbon filament. A commercial bicomponent, boron/tungsten sheath/core fiber, for example, is made by this method for structural composites applications by reducing boron trichloride in the presence of hydrogen to form a deposit of boron on the heated tungsten wire. The fibers are continuous, but have large diameters.

Another fiber-forming CVD process, the metal catalyzed vapor-liquid-solid (VLS) process, affords single crystal silicon carbide fibers. A hot liquid droplet of a metal alloy is the site for vapor deposition and subsequent fiber growth. Fiber growth stops when the catalyst is exhausted. The process is very slow and discontinuous and only very short fibers (often erroneously called whiskers) result. These fibers are among the strongest materials known.

---

* Present Address: University of Illinois at Urbana-Champaign, Department of Materials Science and Engineering, 204 Ceramics Building, 105 South Goodwin Avenue, Urbana, Illinois 61801

Laser assisted fiber processes are also known. The best documented is the laser heated pedestal growth (LHPG) method. It uses a very large diameter, crystalline source rod and an annularly symmetric laser beam. A molten float zone is created in the in the source rod. A seed rod is introduced and slowly withdrawn to initiate the growth of single crystal fibers including sapphire and other optical non-silica oxide fibers. Growth is slow; very small diameters are not attainable.

3. LCVD Fiber Process

Growth of strong, substrate-free, small diameter, fibers including carbon, boron, silicon, silicon carbide and silicon nitride fibers, has now become possible by laser assisted chemical vapor deposition (LCVD) at substantially higher rates than any other fiber forming laser assisted and/or chemical vapor deposition process The LCVD process uses the focal point of a laser beam, rather than the surface of a hot tungsten wire, or a hot molten catalyst droplet as the heat source to decompose the gaseous reactants at above atmospheric pressures. The hot focal point of the laser (Figure 1) is continually adjusted to coincide with the tip of the continuously growing fiber.

The boron deposition process and the resulting boron fiber were selected as the example of choice to illustrate the new technology. The apparatus for growing the fibers consisted of an optical bench with a continuous 5-watt Nd-YAG laser, a small reaction chamber in an enclosed laboratory hood, a system for delivering the feed gases, a microscope attached to the reaction chamber to observe and/or record the growth of individual fibers, and a computer to drive the gas supply, deposition reaction, and fiber growth. A small reaction chamber was used as a research tool suitable for producing, side-by-side, up to ten individual 1.4 cm long, <10 to >30 μm diameter boron fiber specimens along the edge of a common substrate, e.g., a carbonized cardboard.

The small reaction chamber was found to facilitate an investigation where one process variable (e.g., pressure, feed rate, pulling rate) was being changed in a given set of experiments, while keeping all the others constant. An adaptation of this process made it possible to grow up to

2 meter long boron fiber specimens. In principle the process is capable of yielding endless fibers.

Specifically, pure boron fibers were grown from a gaseous mixture of 40% diborane and 60% hydrogen at temperatures ranging from 1000 to 1500K. The resultant fiber diameters ranged from 9 to 100 μm, but much smaller diameters are possible. The fiber diameters achieved in this process are approximately equal to the diffraction limited laser focal spot size. The size of laser focal spot is in turn dependent on the wavelength that the laser used.

4. LCVD Fiber Properties

The reactor pressure ranged from <100 to >1000 kPa, fiber growth rates from 0.1 to 1.0 mm/sec, and tensile strengths from < 3.0 to > 7.0 Gpa.. Tensile strength increased with increasing reactor pressure. Strong fibers (>2.5 GPa) were readily obtained with high growth rates (>0.6 mm/sec) over a wide range of pressures. Ultra-strong (7.6 GPa), small diameter boron fibers were obtained with growth rates of 0.5 to 0.6 mm/sec at the upper end of pressures used (1020 kPa).

The new boron fibers which were obtained by the LCVD process were x-ray amorphous and had a smooth, uniform fiber surface. According to their absolute and specific tensile properties (Table I) they are stronger and stiffer than the other major composite reinforcing fibers which can be made in the form of continuous fibers, i.e., boron/tungsten, IM carbon, and Nicalon* silicon carbide fibers. Reinforcing fibers and composite parts are often used in weight sensitive applications. To reflect their value in this regard, tensile strength and modulus are expressed in terms of specific strength and specific modulus (strength and modulus divided by weight density).

The LCVD boron fibers had >0.7x the average strength and modulus of single crystal VLS SiC whiskers and >96% of the specific properties, but no continuous process is available for the latter. As a result, they are among the strongest and stiffest inorganic fibers known. Early results show that other materials which can be formed into small diameter fibers by laser assisted chemical

vapor deposition include carbon, silicon, silicon nitride, silicon carbide, germanium, and others. The technology is expected to open up major new opportunities both in the non-silica optical fibers market and the specialty structural fibers market.

TABLE I.
Advanced Inorganic Fibers

Fiber Forming Processes and Fiber Tensile Properties	Pure Boron Fibers	Boron/W Fibers	IM Carbon Fibers	Nicalon*/SiC Fibers	S. Cryst. SiC Whiskers
Fiber Forming Process	LCVD	CVD	PAN	CARBOSILANE	VLS
Process Capability	continuous	continuous	continuous	continuous	discontinuous
Fiber Length, Demonstrated	long (>2 m)	endless	endless	endless	short (4-29 mm)
Fiber Diameter, mμ, Average	10	100	10	17	6
Tensile Strength, GPa	5.2	3.5	3.5	2.6	7.5 (28 mm)
Strength , GPa (Best Sample)	7.6	5.1	4.1	3.1	15.9 (4 mm)
Tensile Modulus, GPa	400.0	400.0	280.0	190.0	578.0
Density, g/cm^3	2.3	2.6	1.8	2.4	3.2
Specific Strength, km	228.3	135.9	196.4	109.4	236.7
Specific Modulus, 10^3 x km	17.6	15.5	15.7	8.0	18.2

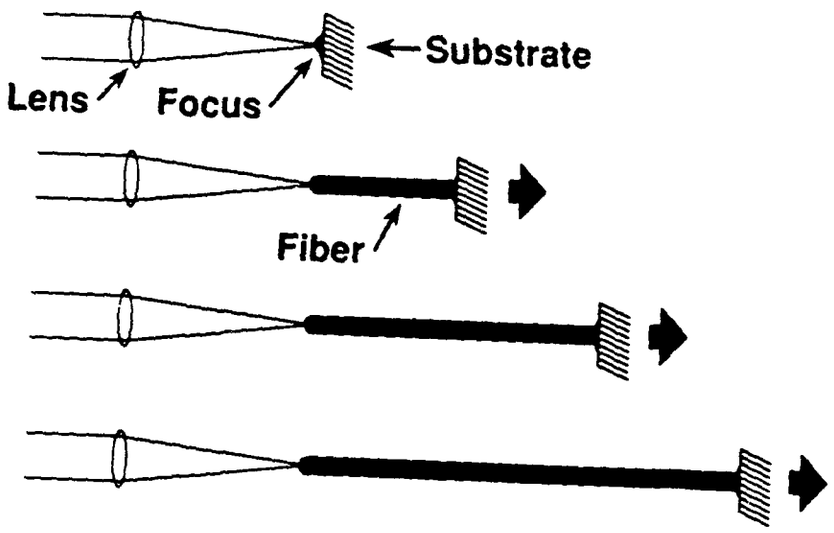

Figure 1. Laser Fiber Growth (Schematically)

HIGH-PERFORMANCE BORON NITRIDE FIBERS FROM POLY(BORAZINE) PRECERAMICS

Y. Kimura, Y. Kubo, and N. Hayashi

Department of Polymer Science and Engineering
Kyoto Institute of Technology, Matsugasaki, Kyoto 606, Japan

Abstract

Boron nitride (BN) fiber was fabricated by utilizing an organic preceramics which was obtained by thermal condensation of B,B,B-tri(methylamino)borazine (MAB) and 10 wt% of laurylamine (LA). The condensate, poly(aminoborazine), was melt-spun into thin fibers by an ordinary screw extruder. Its spinnability was excellent in spite of its low molecular weight (*ca.* 500), because the condensate consisted of planar borazine rings as the melt-spinnable carbon pitch is composed of fused aromatic rings. On spinning the fiber surface was hydrolyzed, and the fiber became infusible. The fiber was then pyrolyzed up to 1000°C in a flow of ammonia gas and was further sintered up to 1800°C in a nitrogen flow. The strength of the fiber was found to increase above 1400°C and to reach 1 GPa at 1800°C. It was therefore suggested that the BN fiber is free from the degradation above 1400°C where most ceramic fibers are known to lose their original strength.

1. INTRODUCTION

Much attention has recently been paid to hexagonal boron nitride (h-BN) because of its excellent thermal, mechanical and lubricating properties. One of the most striking characteristics of h-BN may be small specific gravity (2.26) and low reactivity with metals and ceramics relative to common ceramic materials. Therefore, h-BN can be utilized as a reinforcing fiber and a coating for other ceramic fibers in fabricating fiber-metal and fiber-ceramic composites.

For the processing of h-BN fiber, however, the conventional thermal processes cannot be utilized, because of its difficulty of melting and sintering. In early 1970s, Economy *et al.* invented a chemical conversion method to fabricate BN fiber in which boron oxide fiber was converted to BN by solid phase nitridation in an ammonia atmosphere[1]. In this process, however, the quality control of the precursor fiber and the process control of the nitridation were not easy. Therefore, a new process called preceramic method has been developed, in which processable polymer precursors made of the same elements with the desired ceramics are utilized. In this method the structure and properties of the precursor have close relation with the performance of the ceramics obtained. Paciorek[2], Paine[3], and Sneddon[4] designed various derivatives of poly(aminoborazines) as the BN precursors, although these precursors could not be utilized for fiber spinning. In this paper we describe a new derivative of poly(borazine) which can be used as the precursor for fabricating BN fiber. It was readily prepared by thermal condensation of B,B,B-tri(methylamino)borazine (MAB). Since it was thermoplastic, it was melt-spun into thin fiber by the conventional method. The fiber was then subjected to pyrolysis to obtain a high-performance BN fiber.

2. EXPERIMENTAL

2.1 Materials

Methylamine (MA) and laurylamine (LA) were purified by distillation. B-trichloroborazine (TCB) was prepared as reported previously[5]. TCB was reacted with an excess of MA in toluene at room temperature. MAB was isolated as white waxy material (90% yield): IR (nujol) 3460 (NH), 1410 cm^{-1} (B_3N_3 ring), *etc.*; ^{11}B NMR (C_6D_6) δ 26 ppm.

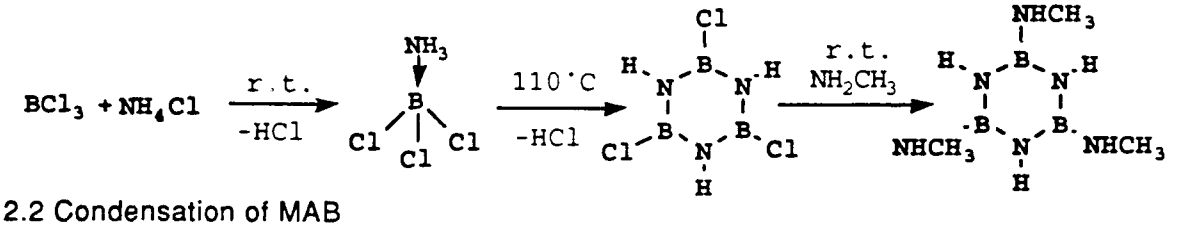

2.2 Condensation of MAB

About 20g of MAB and 10wt% of LA were placed in a 140ml tubular reactor fitted with a three-way stopcock. The reactor was heated to 200-260°C for 1h with the mixture vigorously stirred on a magnetic stirrer and with nitrogen gas introduced from one inlet of the three way cock. During the reaction MA gas evolved out of the system, and the condensation product became gradually viscous. After the reaction, the product was thoroughly dried *in vacuo* and analyzed by spectroscopies. ^1H NMR (C_6D_6) δ 1.1 (t, CH_3-C), 1.45 (s, C-CH_2-C), 2.5 (m, CH_3-N), 2.2-3.0 (broad, NH); ^{11}B NMR (C_6D_6) δ 26 ppm.

2.3 Melt-spinning

Using a micro screw extruder with a nozzle of 500μm in diameter, the condensate was melt-spun at 160-170°C. The extrudate from the spinneret was taken up by a winder to give a continuous filament of about 50μm in diameter.

2.4 Pyrolysis

Several pieces of the above filament (or powders) were placed on an alumina boat and were immediately transferred to an electric tube furnace. The temperature of the furnace was then raised to 600-1000°C at a rate of 100°C/hr in a flow of ammonia gas (30ml/min), held at the predetermined temperature for an hour, and cooled down to room temperature. The pyrolysates obtained were transferred to an alumina crucible and were further sintered at 1400 and 1800°C in a nitrogen flow. Their chemical and physical properties were characterized by diffuse-reflectance IR, WAXS, and density measurements.

3. RESULTS AND DISCUSSION

3.1 Condensation of MAB

Table I shows some results of the thermal condensation of MAB in the presence of 10wt% LA. We had found before that the thermal condensation of MAB without additives gave infusible products with poor spinnability because of the easy formation of crosslinks[6]. In the presence of LA the degree of condensation was successfully controlled, and colorless thermoplastic products were formed after weight losses of 10-20wt% due to the elimination of MA.

Table I Thermal condensation of MAB

Run No.	LA Content (wt%)	Temp. (°C)	Time (hr)	Total Weight Loss (%)	Mn*	Spinnability
1	10	200	1	10.1	—	△
2	10	220	1	13.4	—	△
3	10	240	1	17.1	470	○
4	10	260	1	18.6	—	×

* Mw/Mn=1.75

The average molecular weight of the soluble condensates were in the range of 500-800 as determined by GPC, which corresponds to that of the pentamer or the hexamer of MAB. The ^{11}B NMR spectrum of the condensates exhibited a single peak at δ 26 ppm, which was identical with that of MAB. It suggested that the borazine rings of MAB were preserved in the condensates. Therefore, their structure is postulated as 1, in which LA units are introduced as alkylimino chains or pendant alkylamino groups, by which the intermolecular crosslink can be controlled to maintain the thermoplasticity of the product.

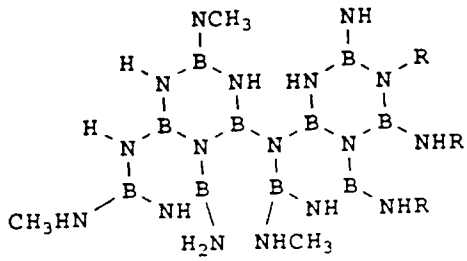

1

3.2 Thermal analyses of the MAB condensates

Fig. 1 shows the typical DTA and TGA curves. The broad endothermic peak around 85°C is due to the melting. The exothermic peak ranging from 200 to 430°C is ascribed to the further decomposition of the condensate because it is accompanied by the weight loss in TGA. At 900°C, the weight loss became 38%, and a black residue was obtained by carbonization of the organic groups.

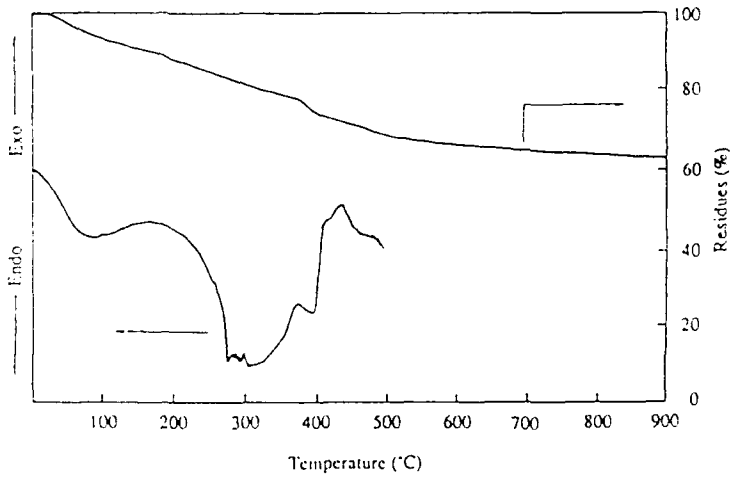

Fig. 1 DTA and TGA curves of MAB in nitrogen

3.3 Pyrolysis of the MAB condensate

The MAB condensate obtained at 240°C was directly pyrolyzed up to 600, 1000, 1400 and 1800°C. Some characteristics of the pyrolysates are shown in Table II. The density increased with increasing the sintering temperature and reached 2.05g/cm^3 at 1800°C , which is slightly lower than the theoretical density of 2.26g/cm^3 for h-BN. Their WAXS are shown in Fig. 2. As noted in the sharpening of the peak of (002) planes and its shift toward the value 3.33Å, the crystal lattice of h-BN grew gradually with increasing temperature.

3.4 Melt spinning

The spinnability of the LA-containing condensates was excellent in spite of their low molecular weight. The best melt-flow of the extrudate was obtained for the condensate obtained at 240°C (Run No.3). The good spinnability is attributed to the planar structure of the oligomeric condensate, in which several borazine rings are connected with each other. This structure is comparable to that of amorphous carbon pitch[7] which is utilized as the precursor of carbon fiber. The latter, having molecular weight of 800-1000, consists of aromatic fused rings in place of borazine networks. In these structures intermolecular aggregation force is so large that the spinnability is much improved. Fig.3 shows a typical SEM micrograph of the precursor fiber. The cross-section of the fiber was circular, and the inner phase was homogeneous.

3.5 Sintering of fiber

During the spinning the fiber surface was slightly hydrolyzed to become infusible. Therefore, the fiber was directly sintered up to 1000°C in an ammonia gas flow without annealing of the fiber. In this stage the sintered fiber was black due to the carbonization of the organic residue. The fiber was further sintered up to 1800°C in a nitrogen flow. The color of the fiber turned brownish at 1200°C and became white above 1400°C. When the sintering up to 1000°C had been done in a nitrogen flow, the color of the fiber remained black even though it was pyrolyzed up to 1800°C. This finding suggests that the pyrolysis in ammonia flow is effective for removing organic residue and carbon contaminants. The fibers sintered at 1000 and 1400°C comprised homogeneous phases, while the one sintered at 1800°C exhibited a slight grain growth in its cross-section.

Table II Thermal conversion to ceramics

Temp. (°C)	Time (hr)	density (g/cm^3)	d(002) (Å)	color
600	1	1.73	3.72	yellow
1000	1	1.78	3.64	pale yellow
1400	1	1.91	3.50	grey
1800	1	2.05	3.39	white

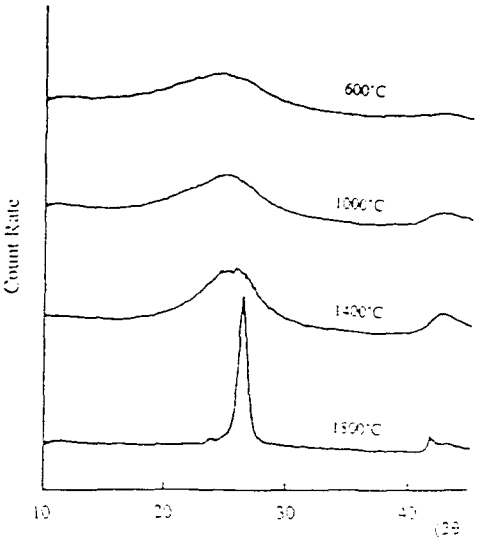

Fig. 2 WAXS of the MAB pyrolysates

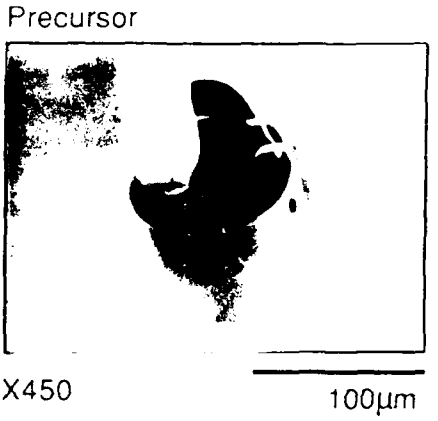

Fig.3 SEM of precursor

3.6 Mechanical properties

Fig. 4 shows the changes in tensile strength and modulus of the fibers as a function of sintering temperature. The modulus was increased with increasing temperature, while the tensile strength decreased at 1400°C and increased again at the higher temperature. The highest tensile strength and modulus were 0.98 GPa and 78 GPa, respectively, which are even higher than those of BN fiber reported before[1]. Most ceramic fibers prepared thus far are known to occur serious deterioration above 1400°C because of the abrupt crystallization and coarse grain growth. The present BN fiber is characterized by the exceptional increase in strength at temperature higher than 1400°C.

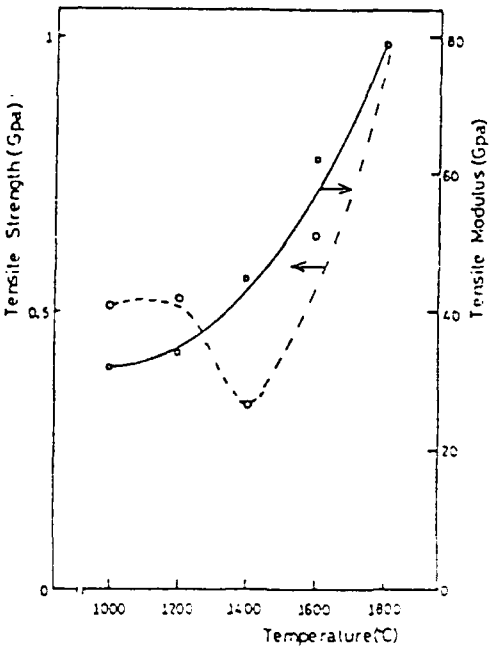

Fig.4 Changes in mechanical properties with sintering temperature

References

(1) J. Economy and R. V. Anderson, J. Polym. Sci., C19, 283 (1967)
(2) K. J. L. Paciorek, D. H. Harris, and R. H. Kratzer, J. Polym. Sci., Polym. Chem. Ed. 24, 173 (1986)
(3) C. K. Narula, R. Schaeffer, and R. T. Pain, J. Am. Chem. Soc., 109, 55, 56 (1987)
(4) P. J. Fazen, J. S. Beck, A. T. Lynch, E. E. Remsen, and L. G. Sneddon, Chem. Meter. 2, 96 (1990)
(5) Inorg. Synth., 13, 41 (1972)
(6) Y.Kimura, N.Hayashi, H.Yamane and T.Kitao Proc. 1st Japan International SAMPE Symposium, Nov. 28-Dec., p906, 1 (1989)
(7) L. S. Singer, Carbon 16, 408 (1978)

SIMPLIFIED DYNAMIC FINITE ELEMENT PROCESSING MODEL FOR THE CVD OF TiB_2 FIBERS

R. J. Diefendorf
Ceramic Engineering Department
Clemson University
Clemson, SC 29634-0907, USA

and

L. Mazlout
Advanced Innovative Technologies, Inc.
Troy, NY 12180, USA

Abstract

Titanium diboride appears to be an attractive candidate for a high temperature reinforcing fiber for intermetallic matrix composites. Titanium diboride has high modulus, reasonably low density, a moderate thermal expansion coefficient and is thermodynamically compatible with a number of potential intermetallic matrices. However, there is considerable disagreement in the literature about its high temperature creep behavior. This work was performed to prepare TiB_2 fibers for evaluation of mechanical behavior using chemical vapor deposition. A simplified finite element, dynamic analysis model is used to describe the chemical vapor deposition of titanium diboride fibers in a cold wall reactor at atmospheric pressure. The gas mixture considered is titanium tetrachloride, boron trichloride, hydrogen, and hydrochloride. A description of the model and the computer program algorithm and subroutines are described. The application of this model to study the effect of deposition parameters on TiB_2 growth and the mechanism of rate limiting processes is discussed. For the mass transport rate limited process, the rate limiting mechanism changes from exhaustion of BCl_3 and $TiCl_4$ at high dilution, to slow BCl_3 and $TiCl_4$ diffusion at moderate concentrations, to slow HCl diffusion away from the fiber surface at high reaction concentrations.

CREEP-RELATED LIMITATIONS OF CURRENT POLYCRYSTALLINE CERAMIC FIBERS

JAMES A. DiCARLO
NASA LEWIS RESEARCH CENTER
CLEVELAND, OH 44135

ABSTRACT

For a thermostructural composite, it is desirable that the reinforcing fibers display high stiffness (modulus) and high strength relative to the matrix, and maintain these properties to as high a temperature as possible. Among other benefits, this allows the composite to operate in the elastic range to high stresses over a wide temperature range. For polymer and metal matrix composites reinforced by currently available ceramic fibers, this condition is generally achieved up to the maximum use temperatures of these composites. This is the case because use-limiting effects are typically related to the matrix (e.g., oxidation, plasticity) and occur at temperatures lower than ~800°C, where current ceramic fibers first begin to show significant creep-related stiffness and strength degradation(1). For ceramic matrix composites (CMC), however, this loss in fiber structural properties can occur in the use temperature ranges projected for a variety of high performance structural applications. Indeed, in some cases, current ceramic fibers show stiffness and strength losses at temperatures well below those where similar effects occur in potential ceramic matrices. At the present time, the structural implications for these effects have not been fully comprehended, either experimentally or theoretically. Clearly, critical questions arise as to whether for any application above ~800°C, the creep-related change in

structural properties displayed by current ceramic fibers can be tolerated and, if not, what minimum properties should be displayed.

The purpose of this paper is to present a status overview of the creep properties, current limitations, and possible improvement approaches for those polycrystalline ceramic fibers with current potential as reinforcement in high temperature structural composites. This is accomplished first by a discussion of how fiber creep influences the thermostructural service lives of composites through such important engineering properties as dimensional stability, strength stability, and failure behavior. Special emphasis is placed on CMC and the key fiber properties that affect their high temperature reliability (2,3). Because service life requirements vary widely from application to application, generic property limitations are assumed for purposes of fiber comparison. For example, for a dimensional stability requirement, a fiber tensile creep strain of less than 1% is assumed for a constant service stress of 100 Mpa. For a typical fiber Young's modulus of 200 Gpa, this imposes an upper limit of 50 for NCS = ϵ_c/ϵ_e = normalized creep strain. Here ϵ_c and ϵ_e are fiber tensile creep and elastic strains, respectively. However, arguments are presented that suggest that when composite lives are limited by maintenance of specific strength levels or avoidance of catastrophic failure, NCS values much less than 50 will probably be required.

With this background in property requirements, the status and performance issues for currently available fibers are then reviewed in terms of their creep-related properties, such as creep, stress relaxation, and stress rupture. Because of the general technical need for long-term performance in oxidizing environments, focus is placed on two general compositional classes: Si-based (e.g., SiC and Si_3N_4) and Al_2O_3-based fibers. In order to better elucidate creep issues and underlying mechanisms for these

fiber classes, they are further subdivided into generic types based on the fiber fabrication approach, for example, chemical vapor deposition, polymer pyrolysis, sintering, sol gel, etc.

To evaluate and compare the creep performance of each fiber type, some recent advances in creep testing and modeling of polycrystalline ceramic fibers are discussed (4,5,6). These advances center on a simple bend stress relaxation (BSR) test (Fig.1). This test was developed at NASA because literature data on fiber creep are scarce and because NCS values below 50 require accurate data in the primary creep stage, a region best evaluated by stress relaxation measurements. It is shown that BSR data on both commercial and developmental fibers can be used not only to indicate the time-temperature conditions for the onset of strength degradation effects in each fiber type, but also to compare and rank fibers in terms of their resistance to stress relaxation (Figs. 2, 3). Also, using some simple basic assumptions, it is shown that the BSR data can be converted to accurate predictions of tensile creep strain as a function of time, temperature, and stress when the fibers are subjected to constant stress and constant temperature conditions. This tensile creep modeling in turn permits estimates to be made of upper use temperatures for each fiber type for a given service stress and life requirement. Assuming a service life of 300 hours and an optimistic requirement of NCS = 50, it is shown that currently available commercial Si-based and Al_2O_3-based fibers can only attain upper use temperatures of about 1200 and 1000°C, respectively (cf. Fig. 4). On the other hand, some developmental fibers are shown to be approaching temperatures more desirable for use in advanced CMC applications (Fig. 3).

Using basic materials engineering theory, suggestions are then offered regarding microstructural alteration approaches that might be taken by each

fabrication method in order to produce polycrystalline fibers with optimum creep resistance. These approaches are based on eliminating or minimizing the underlying creep mechanisms operating in the various types of currently available commercial fibers. Insight into these mechanisms is gained by examining such factors as the creep activation energy which is directly measured in the BSR test. The fact that some of the developmental fibers are already taking microstructural steps in the right direction is discussed. Finally, the paper is concluded with a brief discussion of the potential temperature benefits to be gained if these improvements can be fully implemented in polycrystalline ceramic fibers or if processing methods can be developed for fabrication of more creep-resistant single crystal fibers (cf. Fig. 4).

REFERENCES

1. DiCarlo, J. A.; "High Temperature Structural Fibers-Status and Needs," presented at Fiber Producer Conference, Greenville, SC, May 6-9, 1991, NASA TM 105174.

2. DiCarlo, J. A.; "Fibers for Structurally Reliable Metal and Ceramic Composites," J. of Metals, Vol. 37, No. 6, 1985, pp. 44-49.

3. DiCarlo, J. A.; "CMC's for the Long Run," Advanced Materials and Processes, No. 6, 1989, pp. 41-44.

4. Morscher, G. N. and DiCarlo, J. A.; "A Simple Test for Thermomechanical Evaluation of Ceramic Fibers," J. Am. Ceram. Soc., Vol. 75, No. 1, 1992, pp. 136-140.

5. Morscher, G. N. DiCarlo, J. A., and Wagner, T.; "Fiber Creep Evaluation by Stress Relaxation Measurements," Ceram. Eng. Sci. Proc., Vol. 12, No. 7-8, 1991, pp. 1032-1038.

6. DiCarlo, J. A. and Morscher, G. N.; "Creep and Stress Relaxation Modeling of Polycrystalline Ceramic Fibers," in Failure Mechanisms in High Temperature Composite Materials, ASME, AD-Vol. 22, AMD-Vol. 122, 1991, pp. 15-22.

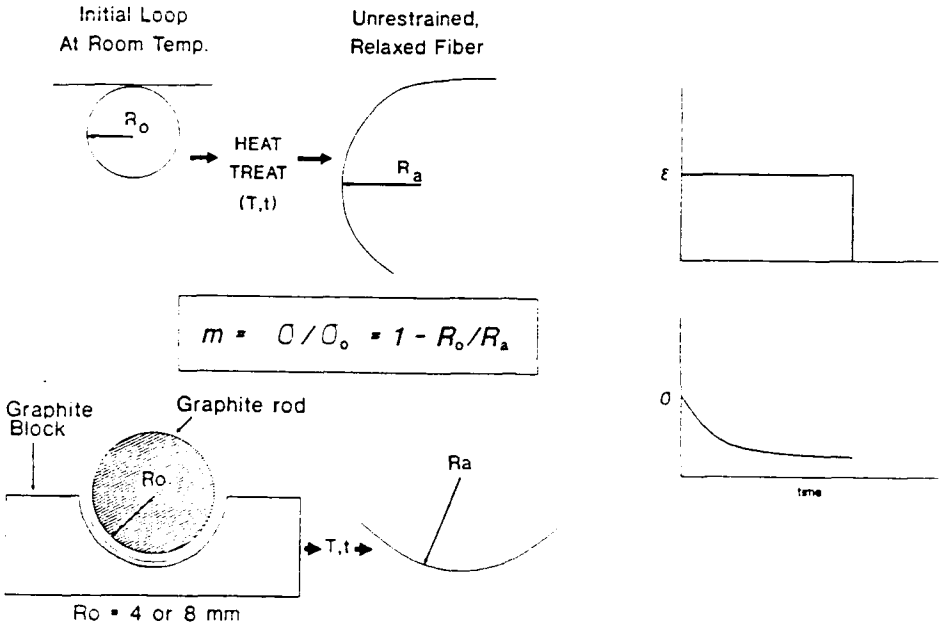

FIGURE 1. BEND STRESS RELAXATION TEST

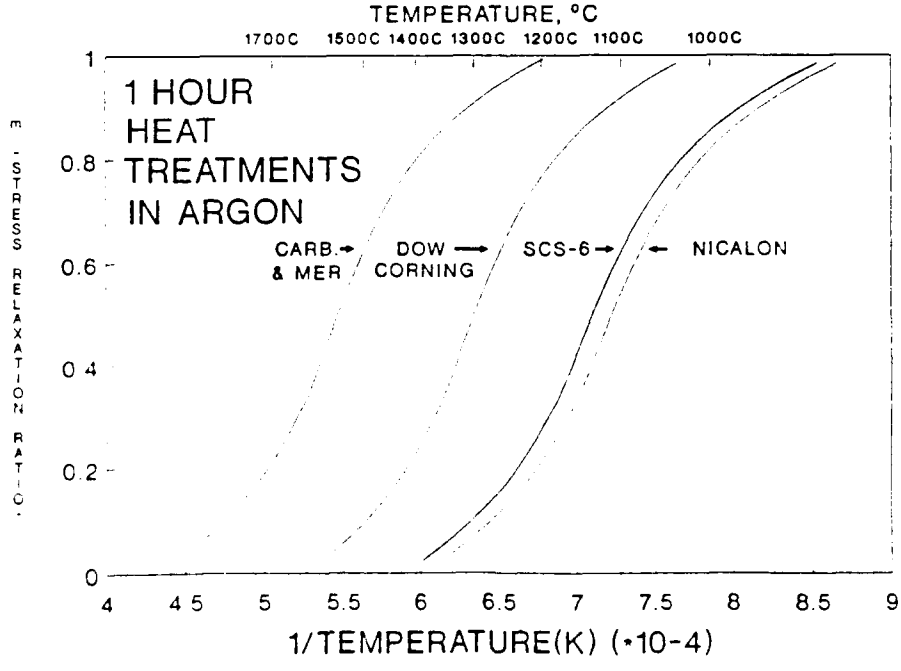

FIGURE 2. TEMPERATURE - DEPENDENCE OF STRESS RELAXATION RATIO FOR SOME Si-BASED FIBERS

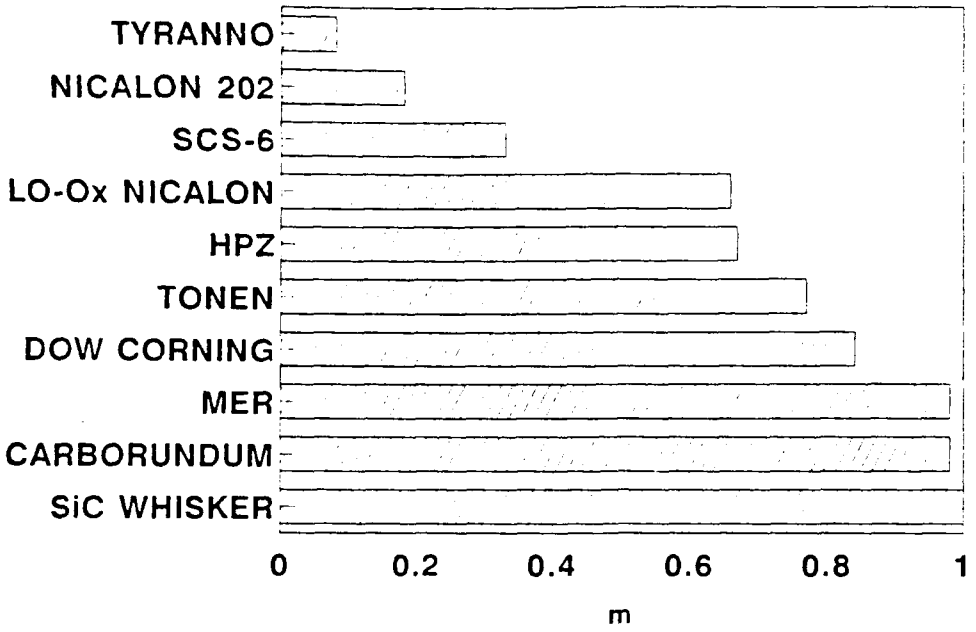

FIGURE 3. COMPARISON AND RANKING OF SOME Si-BASED FIBERS IN TERMS OF RESISTANCE TO CREEP-CONTROLLED STRESS RELAXATION

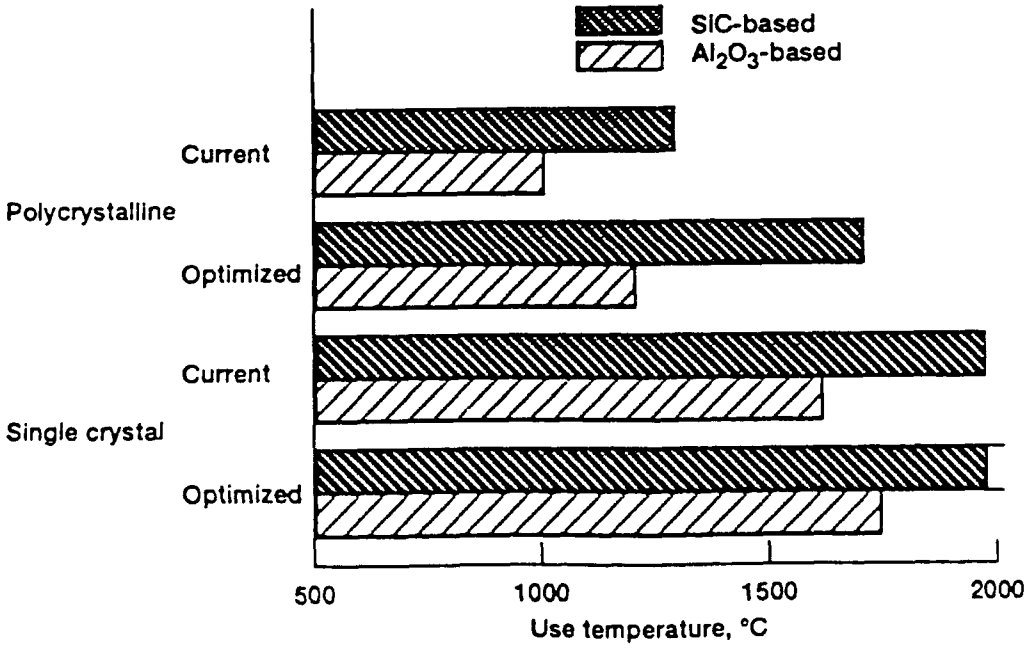

FIGURE 4. ESTIMATES OF CREEP-LIMITED USE TEMPERATURES OF CURRENT FIBERS AND NEW FIBERS WITH OPTIMIZED MICROSTRUCTURES. A DIMENSIONAL STABILITY LIMIT IS ASSUMED OF LESS THAN 1% CREEP STRAIN FOR 300 HOURS AT 100 MPa.

ADVANCES IN THE DEVELOPMENT OF HIGH PERFORMANCE CARBON FIBRES FROM PAN FIBRES

C.P. Bhl

CARBON FIBRES & COMPOSITES GROUP
NATIONAL PHISICAL LABORATORY
NEW DELHI - 110012 (INDIA)

1. Introduction

Advanced composites have acquired the position of "Prime Materials" for most of the critical applications in aero-space, Defence as well as Industrial sectors. The reinforcement fibres for such advanced composites mainly are:

a) Glass fibres
b) Polyarmide fibres, and
c) Carbon Fibres

Out of these, carbon fibres, being light and most refractory, dominate the scenario specially when the product application is at elevated temperatures.

Historically, first patent on carbon fibres development was infact filed on November 1st, 1879. These carbon fibres of Edison were prepared by pyrolysis of Cellulose and were structurally weak. They served well as filaments in electric light bulbs until tungsten filaments came into vogue. The carbon fibre was used in electrical bulbs as late as 1960 in US Navy Ships because they withstood ship vibrations better than tungsten. The (structurally strong) carbon fibres were infact reinvented during later half of 1950. Since then there have been numerous efforts to make carbon fibres with better and better mechanical properties.

2. Raw Materials for Carbon Fibres

From out of the long list of candidate raw materials, today PAN is one of the most popular and promising precursor for the variety of well qualified reasons like high carbon yield, exhibition of plasticity at around 180°C, a very strong carbon back-bone etc. etc.

The first break through in the development of carbon fibres was brought out simultaneously by Shindo in Japan and Watt et al in Royal Aircraft Establishment in U.K. It was soon established that quality of PAN precursor and low temperature thermal stabilisation conditions are two controlling factors for developing high performance carbon fibres from PAN precursor.

By all standards, Japanese PAN fibre industry has excelled in developing far superior precursors required for carbon fibres. This explains the domination of Japanese carbon fibre production the world over (70% of total world production of carbon fibres comes from Japan alone).

3. Development of Carbon Fibres:

Following flow diagram summarises the main steps involved in the manufacture of carbon fibres from PAN:

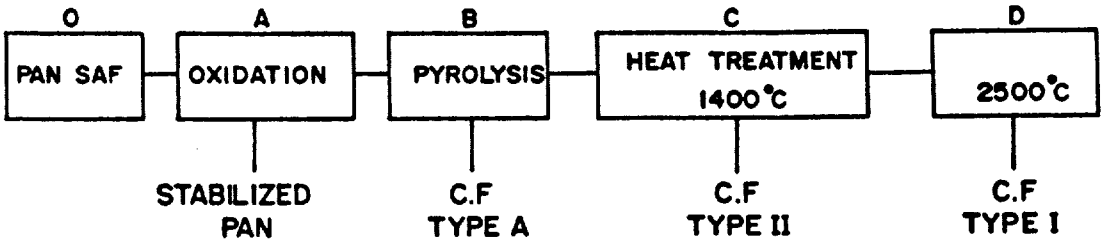

MAIN STEPS IN THE MANUFACTURE OF CARBON FIBER FROM PAN

The second most critical step, after special precursor, is the low temperature stabilisation wherein the open chain structure of PAN is converted into ladder polymer which is associated with a large exotherm as shown in following reactions:

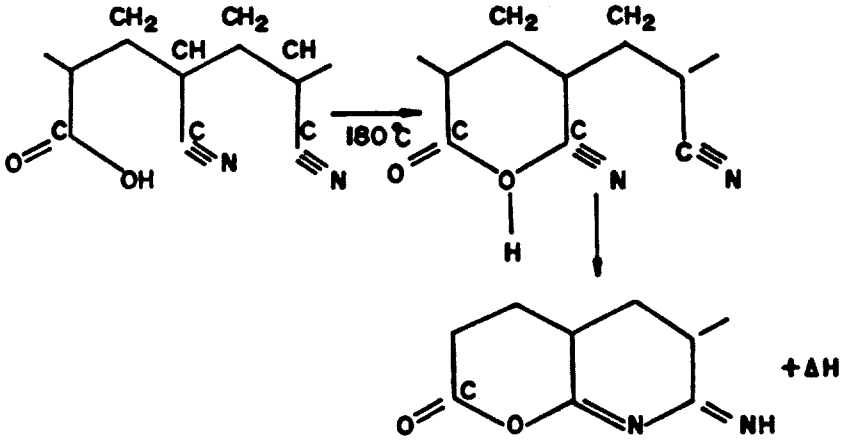

CYCLIZATION REACTION OF POLYACRYLONITRILE.

If this exotherm is not controlled it is liable to cause damage to the original PAN structure and hence will result in deterioration of carbon fibre properties. Additionally the quality of the stabilised PAN fibre depends on atleast following factors:

1. Temperature of oxidation.
2. Tension given to the fibre tow
3. Time of oxidation
4. Ambient used
5. Rate of heating

All these above parameters are function of the quality of the precursor itself. A judicious choice of the processing parameters during stabilisation has to be made therefore. Detailed results will be presented. During heat treatment of PAN in the presence of air, there are two main reactions which take place. These are cyclization of the open chain and the dehydrogenation of the CH_2 groups at the back bone of the chain. For obvious reasons, we would like to have 100% cyclization, if possible, and only 50% dehydrogenation of the back bone for proper cross linking reaction to occur during pyrolysis as depicted below:

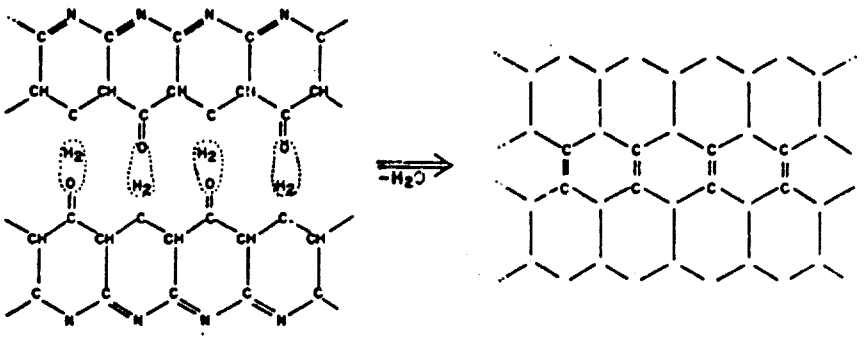

INTERMOLECULAR CROSS-LINKING OF OXIDIZED FIBERS THROUGH DEHYDROGENATION
[FROM MANOCHA. L.M. AND BAHL. O.P (1980). FIB. SCI. TECHNOL. 13, 199]

This alone demonstrates how complicated the stablization step is. It is only through proper knowledge of this step that high performance carbon fibre development can be understood.

Figure 1 shows heat flow behaviour of PAN when heated in air since the cyclisation reaction is exothermic in nature. The exotherm starts around 200°C with a maxima around 265°C. Most of the authors have therefore carried out oxidation at temperatures below 265°C.

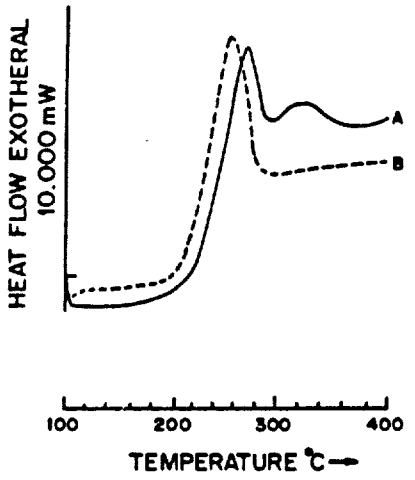

FIG.1. DSC CURVES OF PAN FIBERS
A. IN PRESENCE OF AIR
B. IN PRESENCE OF NITROGEN HEATING RATE 5°C/MIN

We notice from this figure that there is a small shoulder maxima around 320°C to which no importance has reportedly been given by any earlier investigators. We have, for the first time established that this maxima plays an important role during thermal stabilisation of PAN. Following two reactions take place when PAN stabilisation is carried upto second maxima.

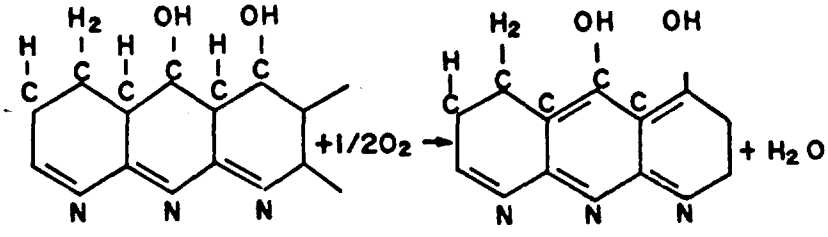

REACTION - 1

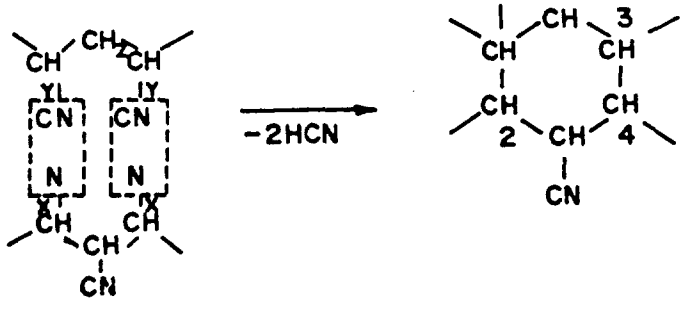

REACTION - 2

The intermolecular cross linking reactions introduces rigidness in the structure whereas the dehydrogination reactions introduces additional aromaticity in the basic structure.

PAN fibre stabilised upto second maxima show entirely different structure and a model has been proposed to explain the structure development. It is pertinent to mention here that such stabilised fibres can be carbonised in a matter of 1-2 minutes only as compared to 50-60 minutes employed for normal stabilised PAN fibres. We have established that the fibre stabilisation by following new approach gives carbon fibres with improved mechanical properties.

4. Post-spinning modification of PAN precursor

The superior grades of PAN precursor developed by Japan are not available to others who wish to develop carbon fibre. The precursor available to other European countries and developed countries could lead to carbon fibres with certain mechanical properties beyond which it was not possible to improve them further because of the precursor quality. Additionally, direct linear dependence of carbon fibre stiffness (HTT 1000°C) on the precursor

Young's modulus, has already been established (Fig. 2).

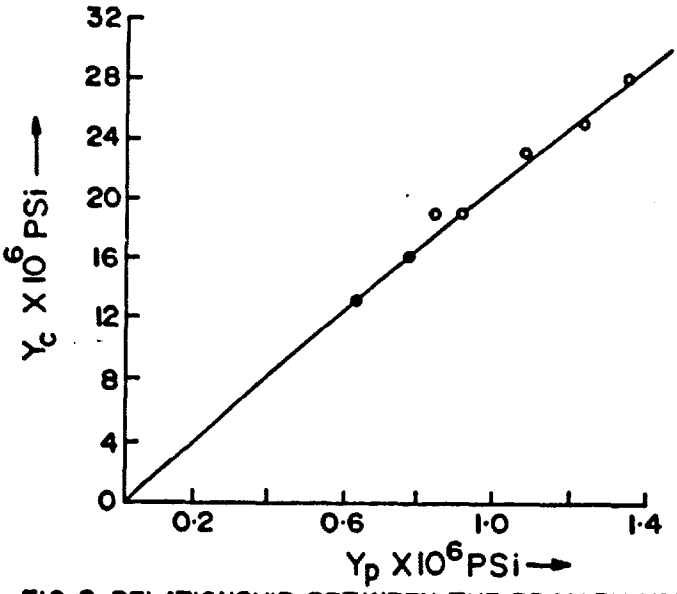

FIG. 2 RELATIONSHIP BETWEEN THE PRIMARY YOUNG'S MODULUS OF THE PRECURSOR, Y_p, AND THE YOUNG'S MODULUS OF THE RESULTING CARBON FIBRE, Y_c

Studies have therefore been undertaken to carry out the post-spinning modifications of such available precursor to improve the carbon fibre quality.

In NPL we have carried out extensive studies on the precursor modification like

i) Stretching in presence of CuCl, Benozic acid, DMF, Acetic Acid, Phtalic acid, nitrogen, air, etc.

It has been possible to lower the activation energy of cyclization from normal 130 KJ/Mole to about 100 K J/mole. This subsequently affects the kinetics of stabilization substantially. The Young's Modulus of the modified precursor has registered two-to four fold improvement. This is tremendous improvement in the precursor quality. However translation of this precursor improvement into carbon fibre properties is quite limited. Details will be presented.

ii) Treatment with aqueous solution of $KMnO_4$

$KMnO_4$ has been found to be very exciting plasticizer/catalyst. MnO_4 - C^4= N conjugation has been confirmed through FTIR analysis. This type of conjugation helps are easy flow of the fibre without registering bond breakage etc. The activation energy of cyclization goes down to 90 KJ/mole. 80-100% improvement in the tensile strength of carbon fibres has been achieved as compared to the strength of unmodified precursor. Strain to failure of the carbon fibres goes upto 1.7 to 1.8%. This study clearly demonstrates that not only

the original precursor quality is important, but at the same time processing parameters during stabilisation and carbonization can play vital role in getting high performance carbon fibres.

iii) A new technique of modification using two different chemical species playing two different roles namely plasticizing and promoting catalytic cyclisation has been employed. The unmodified as well as bi modified precursors have been characterized for their mechanical, physical and thermal behaviour during various stages of processing to carbon fibres. Details will be presented.

Broadly speaking there are three main objectives to be fulfilled through precursor modification. These are:

a) Thinning of the PAN fibres and

b) Stabilization uniformity

c) Improvement in the basic structure.

These factors are vital for achieving high performance carbon fibres.

Histogram below gives the relative values of the carbon fibres derived from modified precursor and unmodified precursor respectively.

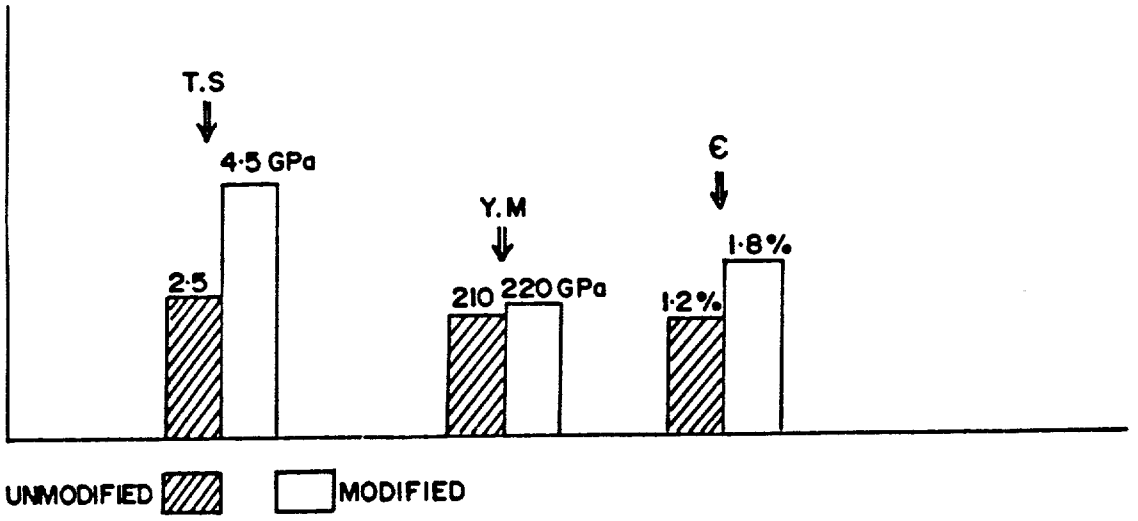

IMPROVEMENT IN THE CARBON FIBRE PROPERTIES OBTAINED THROUGH MODIFICATION OF THE PRECURSOR.

5. World Scenario

Figures 3 and 4 below describe graphically the various grades of ex PAN carbon fibres available commercially and consumption forecast for advanced composites. Details will be presented.

5. World Scenario

Figures 3 and 4 below describe graphically the various grades of PAN carbon fibres available commercially and consumption forecast for advanced composites. Details will be presented.

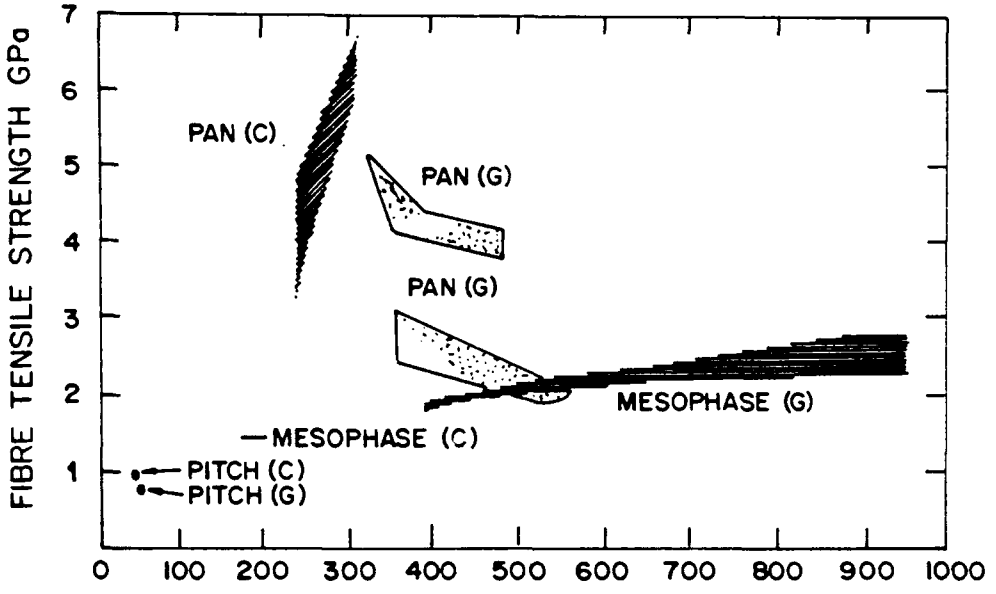

FIG. 3

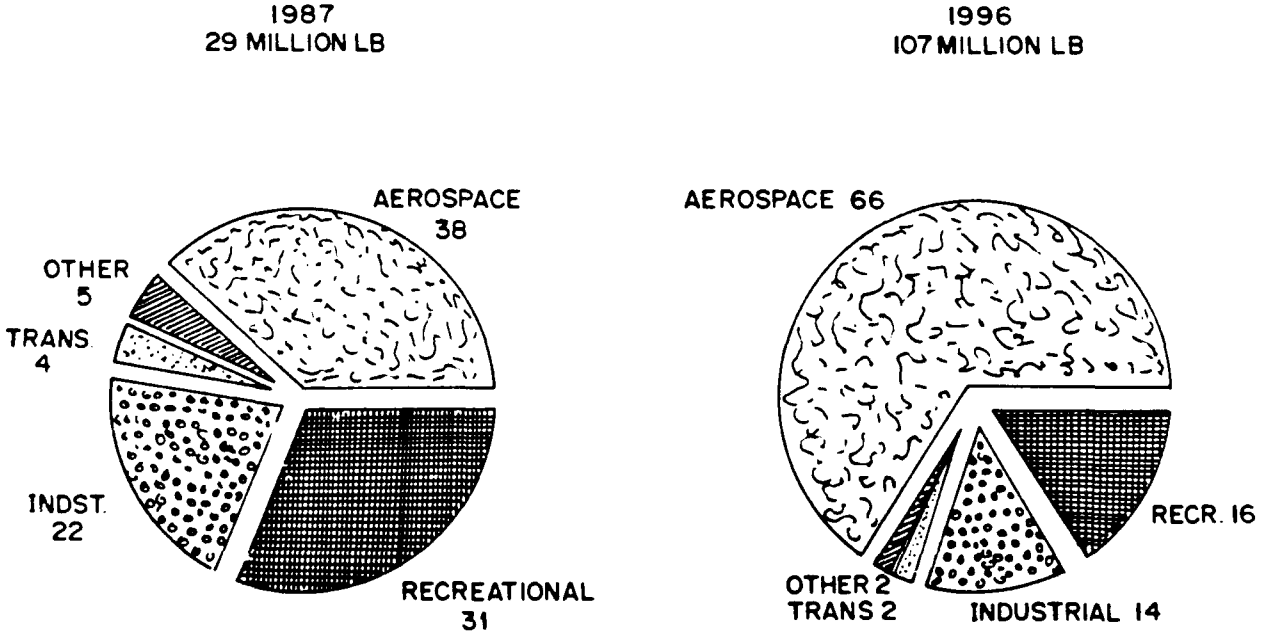

FORCAST CONSUMPTION OF ADVANCED POLYMER COMPOSITES BY APPLICATION.

FIG. 4

SILICONIZING REACTION OF CARBON FIBRES

S.YAMADA, Dept.Mater., Fac.Sci.& Engg., The Nishi Tokyo Univ., Uenohara, Yamanashi 409-01 Japan.
E.YASUDA*, Y.TANABE*, T.AKATSU* and M.SHIBUYA**.
* Res.Inst.Engg.Mater., Tokyo Inst.Tech.
** Dept.Ind.Chem., Fac.Engg., Tokai Univ.

I. Introduction

Recently it has been made clear that high performance carbon fibres(long length) are able to improve the fracture toughness of ceramic matrices basically, through a process of FW(filament winding) by using organic Si compounds, providing as high as over 25 MPa.$m^{1/2}$ of apparent K_{IC} to Si_3N_4. However, the poor resistivity vs. oxidation of carbon fibres limits the range of its application obviously. In order to develop the ceramic composite for higher temperature uses such as ceramic engine being endurable at over 1300°C, the fibres also have to stand the situation. For this purpose, siliconizing reaction of carbon fibres to obtain SiC partially or totally, was investigated.

II. Precursor

Both precursors, a high modulus graphitized fibre(M-40 delivered by Toray, a PAN-derivative) and an air-oxidized PAN, so-called OXYPAN (delivered by Toho Rayon), were employed; while SiO and Si were used as Si-sources. The fibres were put on the SiO or on Si in a graphite crucible and heat-treated in a Tamman-typed graphite oven at 1700°C under reduced pressures of -76, -50 and -20 cmHg(gauge), as well as normal pressure (0 cmHg gauge).

-SiC formed was semi-quantitatively determined by XRD by using calibration curves, corresponding to both precursors. It also means that the siliconized fibres are not amorphous as well-known SiC fibres such as Nicalon and Tirano-fibre but polycrystalline SiC. The reason why such reduced pressures were studied, lay in the fact that the SiC whisker formation was remarkably retarded by pressure, where the thicker whisker formation by a slower crystallization could be realized. In this case, SiC formation should be accelerated on the contrary. The result is as illustrated in Figure 1.

A variety of SEM observations showed that all of the OXYPAN-derivatives resulted in cracks in every filament; whereas Si provided no smooth surface of the specimens derived from the both precursors.

III. Condition of the siliconizing reaction

According to above mentioned result, M-40 and SiO were selected as the starting materials. Reaction temperatures were 1500, 1600 and 1700°C and pressures were the same as above. Figure 2 shows an

overview of carbon fibre(M-40) reacted with SiO under these conditions.

Here it can be seen that only the product of reaction under -76 cmHg at every temperature shows very soft fibrous appearance. This fact corresponds with the SEM observations as shown in Figure 3 for example, where only the specimens obtained under -76 cmHg,not only in Fig.3(1600^{o}C x 1h) but also in all the other ones obtained at 1500 and 1700^{o}C,showed " an inclined structure",being obviously different from the others having a definite boundary just like a sword and its sheath.

The formation mechanism of such an inclined structure should be made clear, together with the mechanical strength of thus formed long fibres, as well as the oxidation resistivity of them. It is now being carried on.

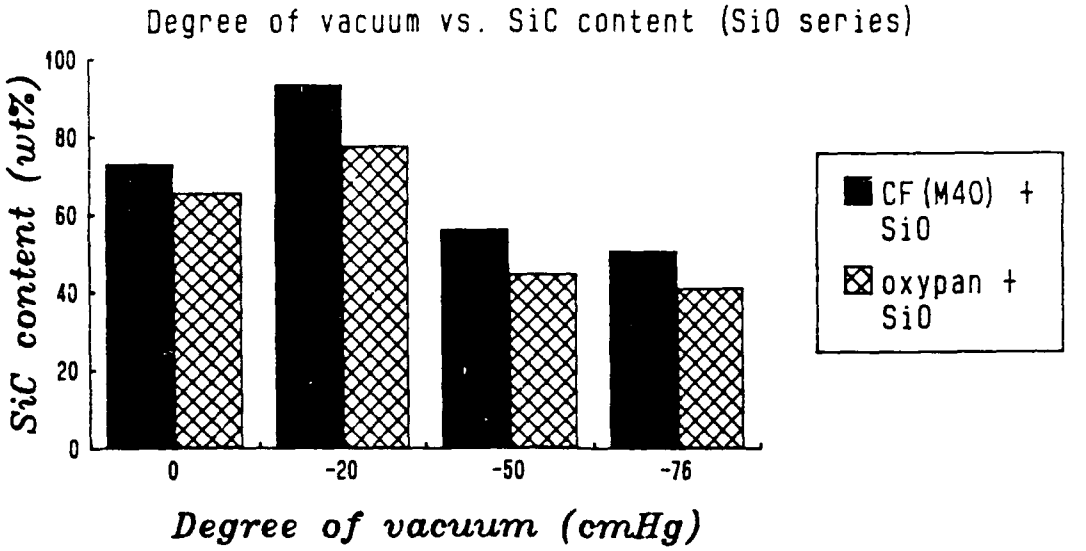

Fig. 1 Degree of vacuum vs. SiC content (SiO series)

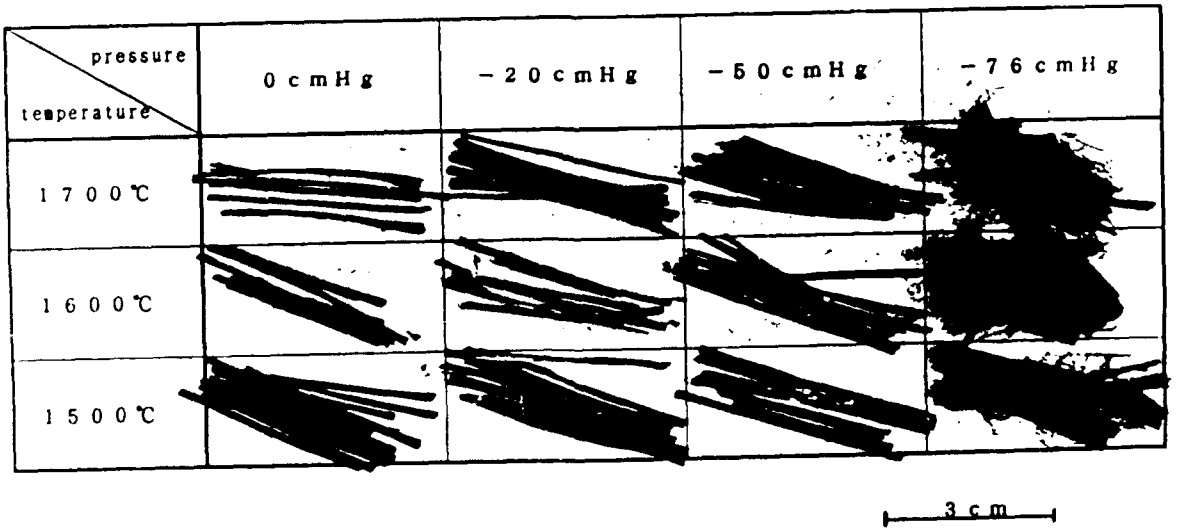

Fig. 2 Overview of carbon fibers (M40) reacted with SiO at various conditions.

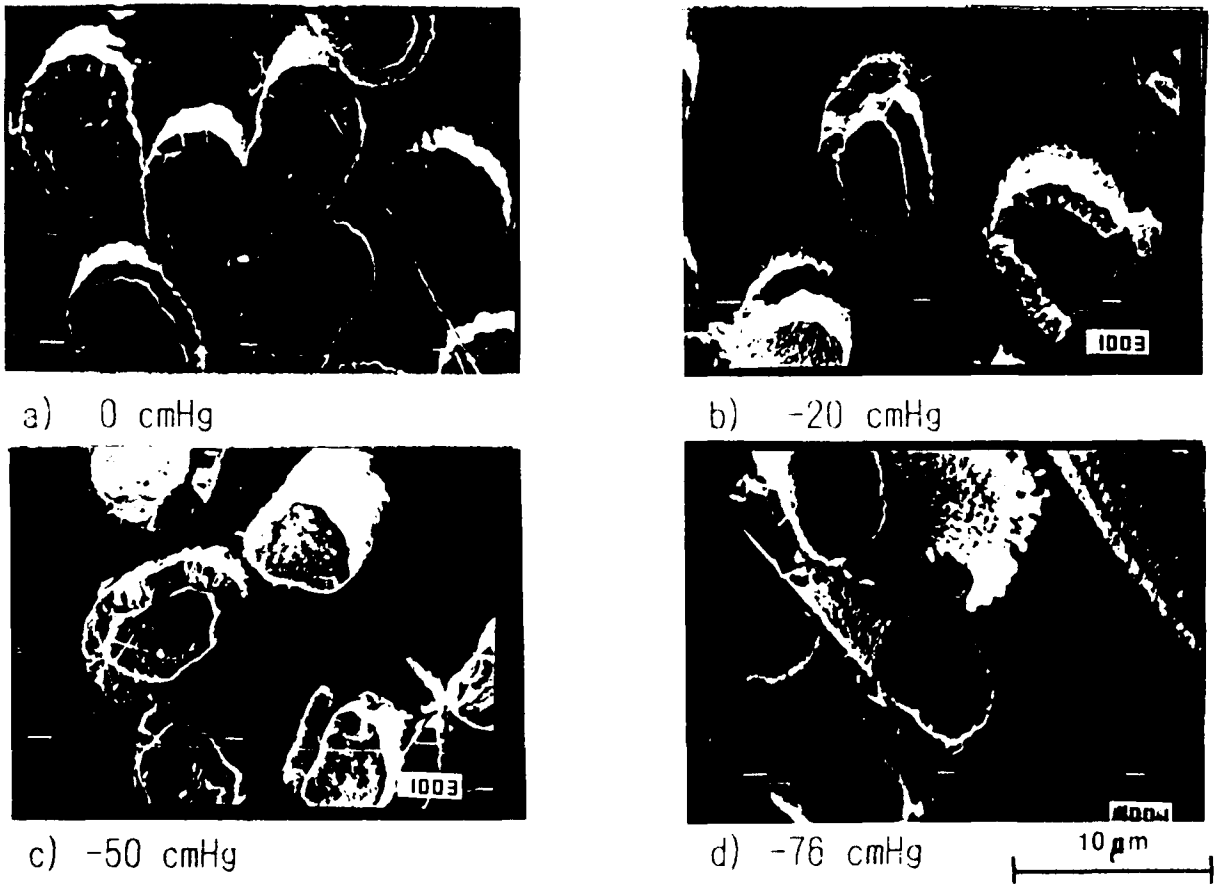

Fig. 3 SEM observations of siliconized samples. heat-treated at 1600°C for 1 hour.

carbon origin : carbon fiber (M40)
silicon origin : SiO

THE DUAL NATURE OF VAPOUR GROWN CARBON FIBRES

Hans Jaeger and Tom Behrsing
CSIRO Division of Materials Science and Technology
Locked Bag 33, CLAYTON, VIC 3168.

INTRODUCTION

Carbon fibres can be readily grown by exposing finely divided metals such as Fe, Co or Ni on a support to hydrogen/ hydrocarbon mixtures at temperatures >=800 °C. This causes a fraction of the metal particles to lift off the support producing behind them, anchored to the substrate, cylindrical, hollow-core filaments with diameters similar to those of the metal particles. These so called primary filaments are progressively thickened to secondary fibres by deposition of carbon resulting from the pyrolysis of the hydrocarbon. Lengthening of the fibres ceases when the metal particle becomes covered with pyrolytic carbon [1,2].

Previously little has been reported about the two stages of growth because under conditions where visible fibres are produced the stages are concomitant though successive for a given part of a fibre. However, it has been observed that near the hollow core of primary filaments 00*l* type planes are straight and parallel to the filament axis[3].

Here we show that the differences between primary filaments and secondary fibres can be studied with electron microscopy when secondary fibres are fractured or when the deposition of pyrolytic carbon is largely prevented. A theoretical analysis of diffraction patterns of primary filaments studied in this work has been reported elsewhere[4].

EXPERIMENTAL

The fibres were grown using A.R. grade ferric nitrate on alumina substrates attached to the end of a ceramic thermocouple sheath located in the centre of an externally heated vertical alumina tube (19 mm i.d.). The reaction mixtures (natural gas, pure methane or A.R. Grade benzene and high purity hydrogen) were introduced at the top of the tube. Benzene/hydrogen mixtures were produced by bubbling the latter through benzene (A.R. grade) at 6 - 25 °C. Other mixtures were established using flow meters.

The substrates were wetted with 0.1 M ferric nitrate solution, dried in air at room temperature and introduced into the reactor, which was purged with argon and heated to the reaction temperature (750 - 1150 °C) over a period of about 30 min. For making fibres, which could be detected visually, selected hydrocarbon/hydrogen mixtures were passed through the system for about 1 hour. The hydrogen was turned off and the hydrocarbon feed continued for another 5

minutes (thickening). Finally the system was purged with argon and the heating turned off. For primary filaments the thickening was omitted. At the end of a run the thermocouple and substrate were removed and the overall distribution, length and appearance of fibres examined with optical microscopy.

The samples were examined in a HITACHI S450-LB scanning electron microscope (SEM) fitted with a Traycor Northern energy dispersive X-ray spectrometer. The fibres were either left on the substrate or they were removed and attached to graphite supports.

Transmission electron microscopy (TEM) examination was carried out using a JEOL JEM 100-CX microscope operated at 100 kV. Samples of thickened fibres were ground lightly in ethanol and drops of the suspension placed on holey carbon films supported on Cu-grids.

Primary filaments were not visible with optical microscopy but they could be detected by observing pieces of grit or soot which appeared to be suspended in mid air. The filaments were collected by moving plain copper grids through the space between the thermocouple sheath and the substrate or through gaps in the latter.

RESULTS

The growth and nature of fibres did not depend on the hydrocarbon used (methane, natural gas or benzene). However, the iron particles varied widely in size and became activated throughout an experiment. Therefore fibres varied widely in length, and diameter, for the same temperature regime.

When the metal particles were small (≈10 nm across) and the temperature was in the range 1000 - 1150 °C the morphology of the fibres was similar to that reported generally in the literature. Observations on fibres broken in tension revealed that the fibres had a dual nature. The bulk of a fibre was usually made up of concentric layers and occasionally the primary filament protruded like a "pig's tail" from the fracture face if the primary filament itself was ruptured; but extended as a taut cord if it was still held by some obstacle outside the field of view. Often adjoining filaments appeared to have become fused during thickening.

When the diameter of a fibre exceeded ≈ 1 μm only the outer layers were transparent to the electron beam in the TEM. Diffraction patterns taken from these areas or from fibres which were thin enough to be transparent to the electron beam consisted mainly of two broadened 00*l* type arcs normal to the fibre axis together with very weak diffuse continuous *h*00 and *hk*0 type rings (Fig.1a). The appearance of the patterns did not change if a fibre was rotated about its axis.

In TEM images primary filaments could also be seen to extend from fracture faces of thick fibres. Usually only one but occasionally several primary filaments extended from what appeared to be a circular single thick fibre. When the primary filament itself was fractured, it could be seen curled back, similar to the appearance of broken primary filaments observed in the SEM. This is illustrated in Figure 1b

which also shows that thin fragments of pyrolytic carbon were sometimes left around the primary filament. These observations indicate that, at this point, the strength of vapour-deposited fibres resides entirely in the primary filaments.

The primary filaments had hollow cores (Fig. 2a) and in diffraction patterns (Fig. 2b) the 00*l* type reflections were very sharp and between them and the origin was fine detail which varied with the inner diameters and tube walls of the filaments. In addition the *h*00 and *hk*0 type rings were broken into segments of spots with six-fold symmetry. These spots had distinct equatorial tails (cf. Figs. 1a and 2b). The arrangement of segments around the rings show that in these primary fibres the 00*l* type planes are parallel to the filament axis and that the carbon arrays in successive layers are rotated with respect to each other.

Primary filaments which were not thickened were usually of uniform thickness across an entire TEM grid, 2.3 mm. These filaments were very flexible and were occasionally arranged in bundles which readily separated on bending (Fig. 3a). Diffraction patterns from individual filaments were the same as shown in Figure 2b. Patterns from a bundle (Fig. 3b) revealed that the 00*l*, *h*00 and *hk*0 type reflections were as expected from aligned individual fibres, but the fine detail between the 00*l* type reflections and the origin was usually not resolved.

When the metal particles were large (>≈ 50 nm), intact fibres were indistinguishable in the SEM from those having small leading iron particles. However, orientation of the 00*l* type planes relative to the fibre axis depended on the size as well as on the shape of the leading particle. For spherical particles, diffraction revealed that the 00*l* type planes in primary filaments were inclined to the filament axis. As a result these filaments broke readily. When the iron particles were acicular the 00*l* type planes were aligned parallel to the filament axis. Irrespective of the orientation of 00*l* type planes in primary filaments, the pyrolytic outer material in thickened fibres was mainly aligned parallel to the fibre axis.

REFERENCES

[1] G.G. Tibbetts, Vapour-grown carbon fibers, in J.L. Figueiredo et al. (eds.) Carbon Fibers Filaments and Composites, Kluwer Academic Publishers. Printed in the Netherlands, 1990. pp. 73-94.

[2] R.T.K. Baker, Catalytic growth of carbon filaments, *Carbon*, 27, (1989) pp. 315-323.

[3] A. Oberlin, M. Endo, and T. Koyama, Filamentous growth of carbon through benzene decomposition, *J. Cryst. Growth.*, 32 (1976) pp. 335-349.

[4] H. Jaeger, V.W. Maslen and A. McL. Mathieson, An analysis of electron diffraction patterns of thin vapour-grown carbon filaments, *Carbon*, 30, (1992) pp. 269-284.

Figure 1:

a) TEM diffraction pattern of a thickened fibre (beam normal to fibre axis); b) TEM image of a broken thickened fibre; the primary filament, encircled by a piece of pyrolytic carbon, extends from the fracture face.

a)

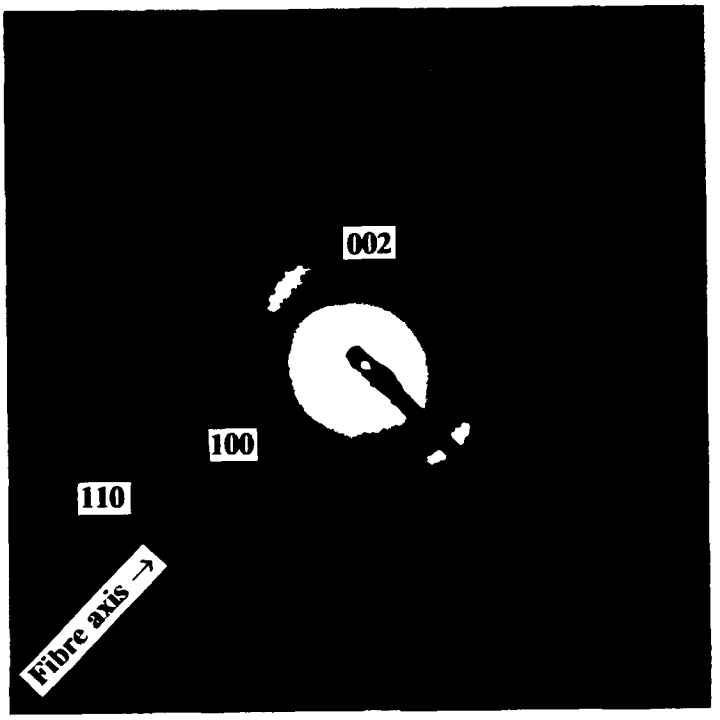

b)

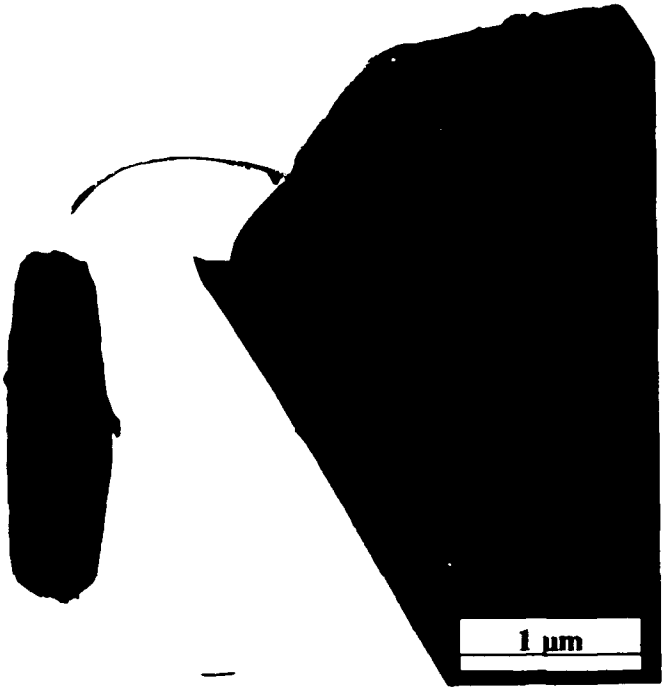

Figure 2:

a) TEM image of a primary filament extending from the fracture face of a thickened fibre; b) TEM diffraction pattern of the primary filament shown in a)(beam normal to fibre axis).

a)

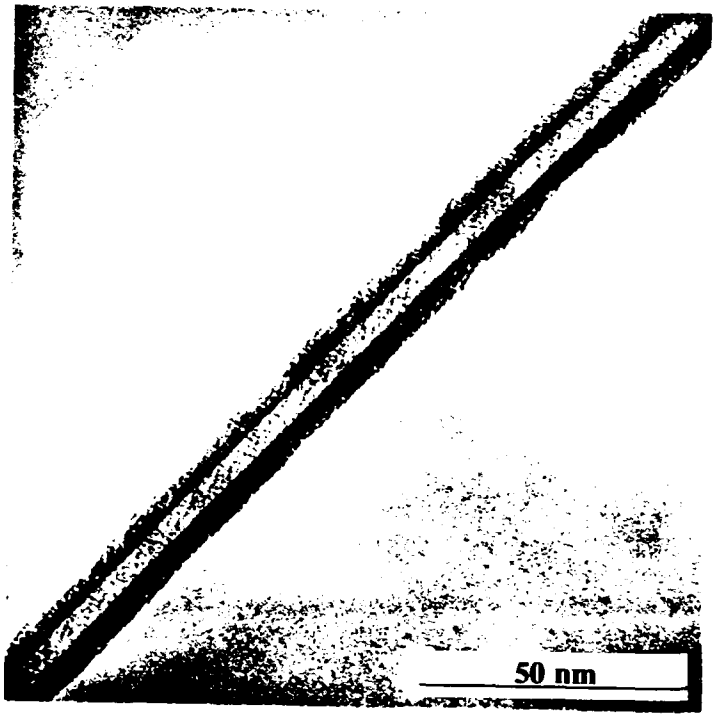

b)

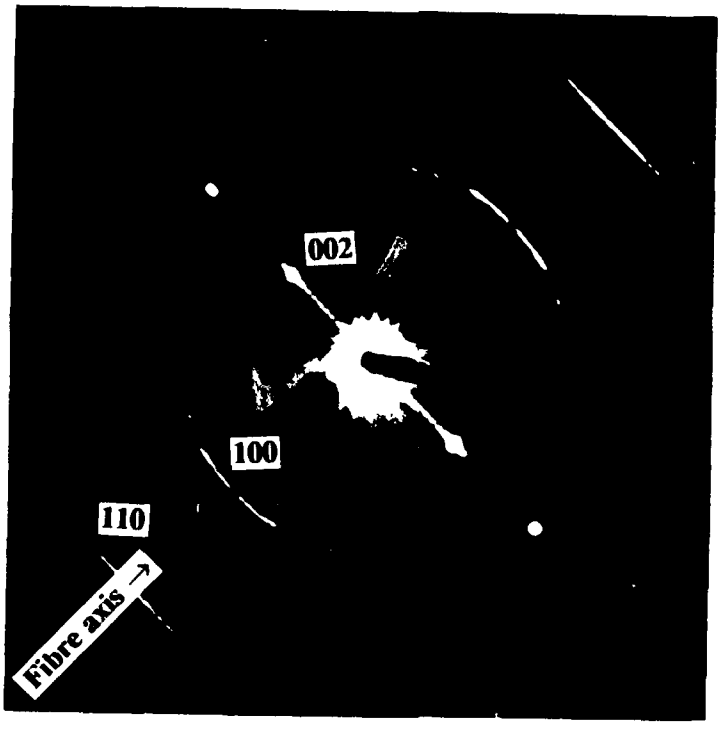

Figure 3:

a) TEM image of a bundle of primary fibres; b) TEM diffraction pattern of the filament bundle; the arrow in a) points to the part of the bundle which contributes to the pattern (beam normal to fibre axis).

a)

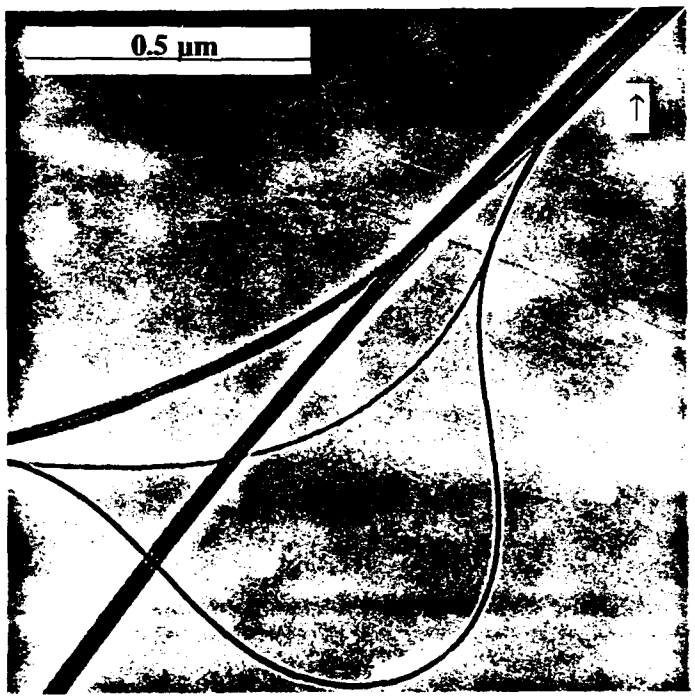

b)

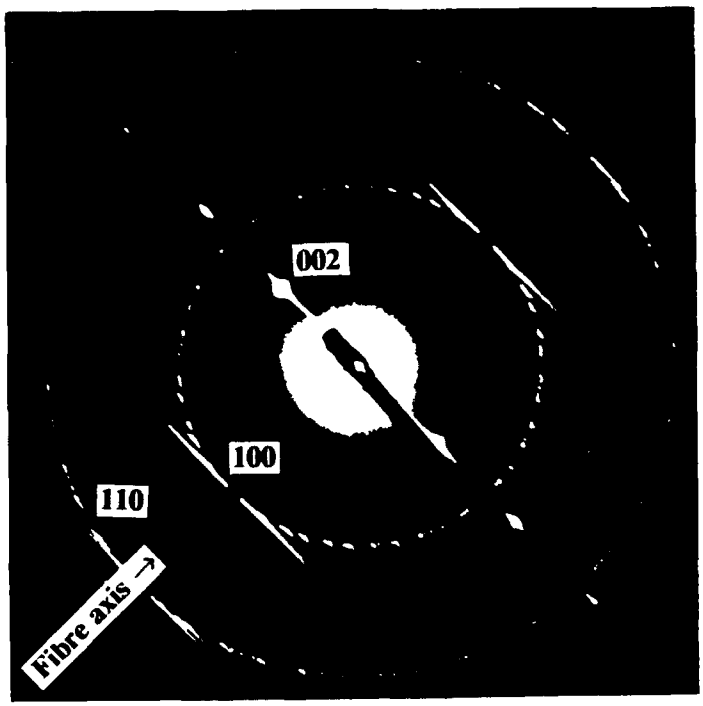

GLASS FIBERS FROM HIGH AND LOW VISCOSITY OXIDE MELTS

FREDERICK T. WALLENBERGER*
Du Pont Fibers, Experimental Station, P. O. Box 80302, Wilmington, Delaware 19880-0302

SHERMAN D. BROWN
University of Illinois, Department of Materials Science and Engineering, Urbana, Illinois 61801

1. Introduction

We wish to report (1) an overview of four generic methods which were known in the literature or de-veloped by us concerning the fabrication on non-silica or low-silica oxide glass fibers from melts having viscosities at the liquidus ranging from <1 to $>10^3$ poise, (2) a mechanism we recently proposed with regard to melt spinning of strong, oxide glass fibers from melts having low viscosities at the liquidus, comparable to those of motor oil at room temperature, and (3) the potential of aluminate and tellurite fibers made by one of these fiber-forming methods as new infrared optical fibers, especially for the infrared range above 3 μm.

2. Background

In the field of alumina-based optical fibers attention has only been paid to single crystal sapphire fibers for special premium applications, but none to optical non- or low-silica glass fibers. Fabrication of sapphire fibers is based on a very slow process, and the cost of the product is very high. However, calcium aluminate bulk glasses are known to have sapphire-like infrared transmission spectra, and if the correspon-ding fibers were made by a modern melt processing method, they might be less costly and still effective.

---

* Present Address: University of Illinois at Urbana-Champaign, Department of Materials Science and Engineering, 204 Ceramics Building, 105 South Goodwin Avenue, Urbana, Illinois 61801

Surprisingly, many calcium aluminate glass fibers with 30-80% alumina were experimentally made and evaluated by several groups before 1970 for structural, but not optical, uses. Research was aimed at identifying compositions of alumina-based fibers having a higher modulus than S-glass, the highest modulus of any silica-based fiber then on record, excluding HM-glass containing toxic beryllia. New high modulus aluminate fibers were identified but none was commercialized.

The excellent work that was done between 1950 and 1970 is accessible, but not readily. It is recorded in a series of unclassified reports to several government agencies. Only one publication appeared in a refereed journal, and deals with fiber formation and glass fiber properties. It is an authoritative source but it is not readily accessible for a different reason; it does not use the word "fibers" in its title or abstract. No theoretical analysis was provided relating composition to viscosity and glass formation, or composition and glass fiber modulus. Interpretations were given for various phenomena, but our analysis shows they are not predictive.

3. Generic Fiber Processes

Onoda and Brown [1970] showed that there is a region ~45% alumina and <5% alumina in the calcia-alumina-silica phase diagram with very high melt viscosities (>10^3 poise), while the remaining compositions have very low melt viscosities (<5 poise). Wallenberger, Brown, et al. [1992] proposed that (1) calcium alu-minate glass fibers are better suited for IR optical, than for structural uses, and can be made by one of four generic melt processes as shown in Figure 1, and (2) selection of a preferred process for a given composition depends only on its viscosity at the operating temperature, where it should be ~10^3 poise as for silicate fibers.

Machlan [1955] was able to identify one out of thousand experimental, quaternary, low silica compositions as having a sufficiently high viscosity above the liquidus to obtain glass fibers by spinning them through an orifice. The melt viscosity was not reported but the melt must have been

10^2 -10^3 poise above the liquidus like a silicate melt. In summary, even the highest viscosities in the alumina system are lower than those in the silica system and it is not likely that this fabrication method will be useful in the alumina system.

Onoda and Brown [1970] were able to identify about sixty out of three hundred experimental, quaternary and ternary, low-silica compositions with 40-50% alumina and <5% alumina having fiber forming viscosities (10^2 -10^3 poise) below the liquidus. The authors did measure the viscosity as a function of tempe-rature. Glass fibers were only obtained from selected compositions by up-drawing from the surface of super-cooled melts, and a continuous process was developed for structural, single component fibers, but not com-mercialized. In summary, a process is available but it is difficult to fabricate clad optical fibers by this route.

Wallenberger, Weston and Brown [1991] reevaluated up-drawing from supercooled melts, and made glass fibers from a quaternary non-silica composition with 46% alumina and a quaternary low silica compo-sition with 42% alumina. They also succeeded in down-drawing both composition from the preforms evident-ly have fiber-forming viscosities (10^2 -10^3 poise) at, but not above, the liquidus. In summary, silica is not required as a viscosity builder (network former) and down-drawing of fibers from a preform might become the method of choice for fibers previously up drawn from supercooled melts. Also, clad optical fibers are more readily made by down-drawing from a preform than by up-drawing process frm a supercooled melt.

The vast majority of glass fibers, especially those with 50-80% alumina have low melt viscosities (<5 poise) and can only be made by inviscid melt spinning, a process whereby a low viscosity jet is ejected into propane, a chemically reactive medium. The pyrolytic decomposition of propane stabilizes the molten jet. The consolidated fiber has a carbon-rich skin. Wallenberger et al [1992] reported that the operative mechanism is rheology-dominated. Incorporation of particulate carbon into the skin of the jet increases its surface viscosity, prevents break-up into Rayleigh waves

and droplets, and facilitates melt spinning of continuous filaments. Carbon may ultimately not be a suitable surface stabilizer for optical fibers; others are being explored.

4. Infrared Optical Fibers

Wallenberger et al. [1991] reported the infrared transmission of calcium aluminate glass fibers to be identical with those of comparable commercial bulk glasses. The new glass fibers, like similar bulk glasses, have sapphire-like infrared transmission (Figure 2), thus potential for becoming a high volume commodity product. Wallenberger, Weston and Brown [1992] also reported the successful fabrication of tellurite (telluria-alumina) glass fibers by up-drawing from supercooled melts. In summary, the exploration of optical non-silica oxide glass fibers by an appropriate generic process is now open to exploration.

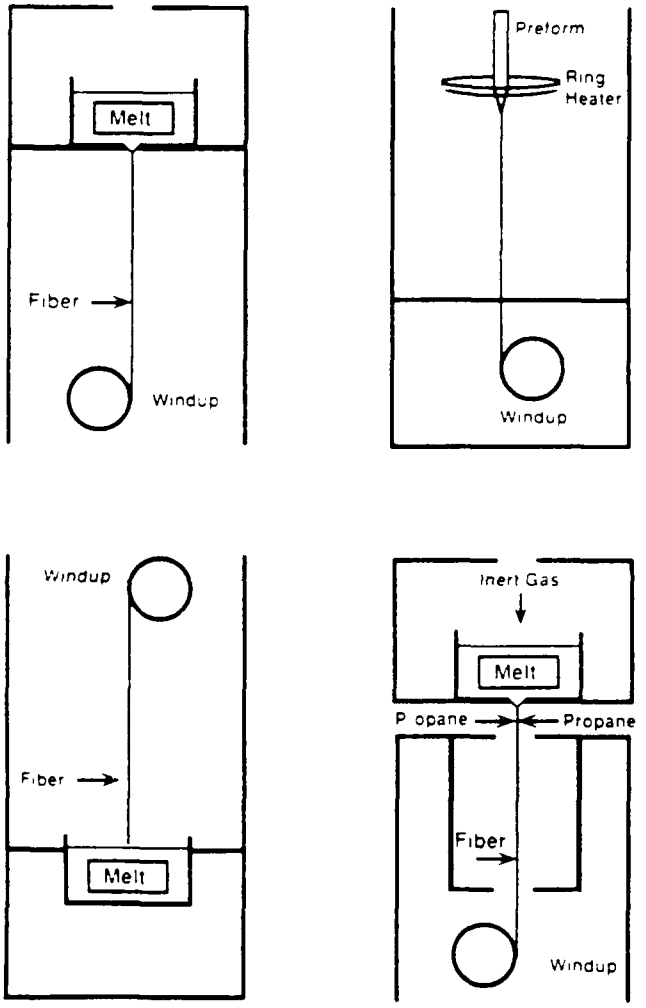

Figure 1. Generic Fiber Processes:
Melt Spinning through an Orifice (top, left), Up-drawing from a Supercooled Melt (bottom, left), Down-drawing from a Preform (top, right),& Melt Spinning from an Inviscid Melt (bottom, right).

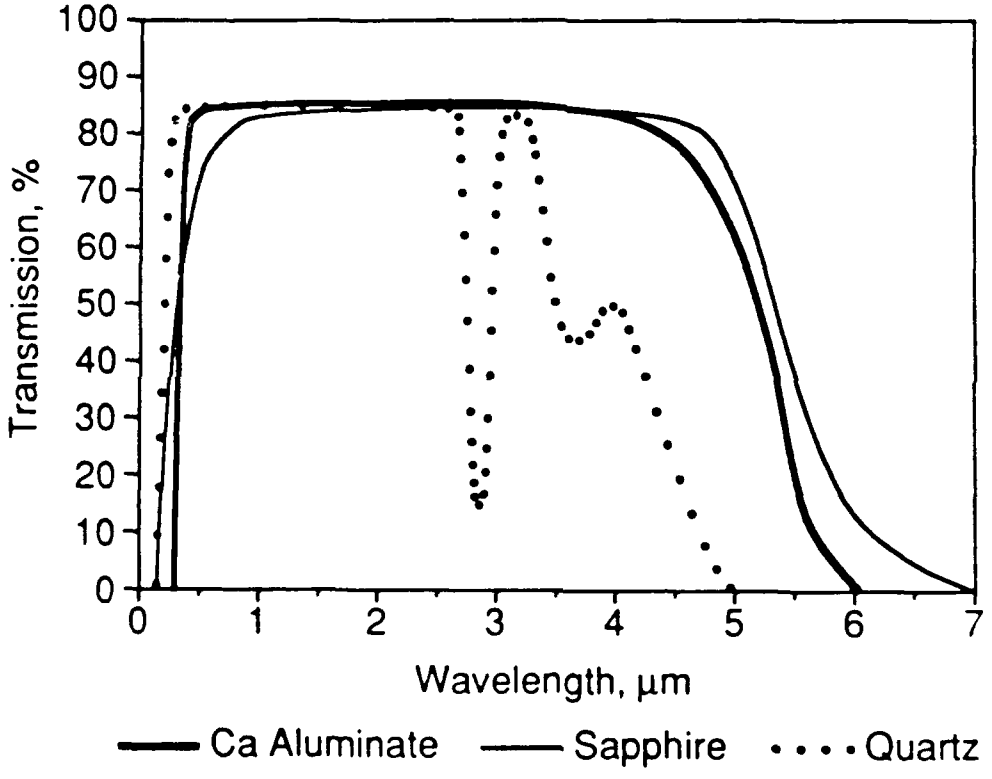

Figure 2. Sapphire and Saphire-like Infrared Transmission